Applying the brakes: Does Prostaglandin Dehydrogenase promote mitotic quiescence in differentiated human urothelium?

Benjamin Jarvis

MSc by Research

University of York

Biology

November 2021

Abstract

The urothelium functions to provide and maintain a tight barrier in the urinary tract whilst retaining the ability to shift phenotype from being mitotically quiescent to rapidly regenerative in the event of injury or infection. Previous observations in the human urothelium have identified bioactive eicosanoids are released upon urothelial damage and can be synthesised within the urothelium itself. However limited studies have been performed to understand the roles, if any, of eicosanoid prostaglandin E_2 in mediating normal urothelial tissue homeostasis. The aim of this study was to investigate the expression of components of the PGE_2 metabolic pathway in human urothelial cells and assess the function in regulating mitotic quiescence and urothelial wound repair.

Prostaglandin dehydrogenase (PGDH), whose function is to inactivate PGE_2, was identified as having a differentiation-associated expression and localisation in normal human urothelial (NHU) cells *in vitro* and *in situ*. Pharmacological inhibition of PGDH activity disrupted mitotic quiescence by releasing urothelial cells into the cell cycle which suggested PGDH may function to retain cells in the G0 quiescent phase. PGDH inhibition also reduced barrier reformation during urothelial wound repair, and this was a cAMP-dependent process illustrating the importance of exogenous cholera toxin (CT) in NHU cell culture.

Taken together, this study presents evidence that PGDH functions in differentiated human urothelium to degrade PGE_2 whose accumulation compromises mitotic quiescence, a characteristic feature of human urothelium *in situ*.

Table of Contents

List of Figures/Tables

Acknowledgements

I cannot express enough thanks to my supervisor, Professor Jenny Southgate, for her guidance and expertise throughout the entirety of the study.

This study took place at the Jack Birch Unit for Molecular Carcinogenesis, University of York and I want to thank every member of the technical staff and students for their encouragement, support, and technical experience throughout the project. I would like to especially thank Dr Jennifer Hinley for her support, mentoring me throughout my time at the JBU and performing immunohistochemical staining. Special thanks also to Rosalind Duke and Zhen Liu for providing lysate and western blotting results, and Dr Andrew Mason for performing differential gene expression RNAseq analysis.

I would also like to thank Dr Gareth Evans for providing useful feedback as the member of my thesis advisory panel.

Declaration

I declare that this thesis is a presentation of original work, and I am the sole author. This work has not previously been presented for an award at this, or any other, University. All sources are acknowledged as References and acknowledgements are made to individuals who provided materials or performed and provided results.

1. Introduction

1.1 The Urothelium

1.1.1 Structure of the Urothelium

The urothelium is the specialised epithelium which lines the urinary tract from the renal pelvis, through the ureters and the bladder, to the proximal urethra and is composed of three distinct cell layers each presenting differing morphologies and cellular phenotypes in accordance with their position within the epithelium (reviewed in Apodaca, 2004). Most luminal are the large, polygonal, occasionally binucleated superficial cells, also known as “umbrella” cells, with diameters of 25-250 μm. Several layers of intermediate cells (10-25 μm in diameter) underlie the superficial cell layer with the number of layers varying dependent on species and degree of bladder distension. The smallest, cuboidal basal cells (~10 μm in diameter) sit adjacent to the basement membrane which separates the urothelium from the sub-urothelial lamina propria, detrusor muscle and fatty connective tissue which along with blood vessel and nerve innervation makes up the ureteric and bladder walls (**Figure 1**) (reviewed in Khandelwal et al, 2009).

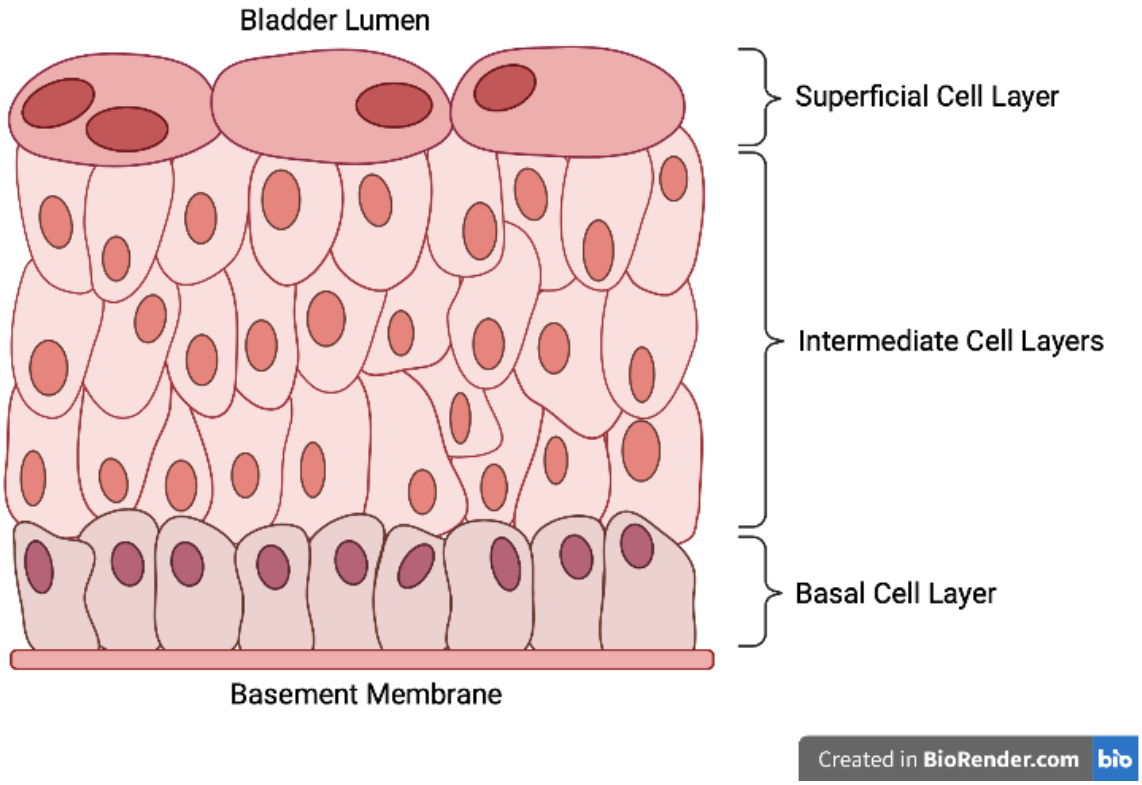

Figure 1.1. Schematic representation of the urothelium.

Adjacent to the lumen of the urinary tract are the large, most-differentiated superficial cells lying above multiple layers of intermediate cells. The basal cell layer lies adjacent to the basement membrane which separates the urothelium from the rest of the bladder structures. Created with BioRender.com.

1.1.2 Function of the Urothelium

The primary function of the urothelium is to provide and maintain a high-resistance barrier between the lumen of the urinary tract and the bloodstream to prevent urine infiltration into underlying tissues (reviewed in Birder and de Groat, 2007). If the urothelial barrier becomes compromised, urine and its toxic components can interact with underlying tissue causing bladder inflammation, known as cystitis. These symptoms manifest in patients with interstitial cystitis (IC) as chronic abdominal discomfort with increased urinary urgency and frequency. This

exemplifies the importance of maintenance of urothelial barrier and therefore the urothelium also possesses a high capacity to repair rapidly in the event of injury for barrier restoration (reviewed in Hicks, 1975). To achieve this, the urothelium shifts from a state of near mitotic quiescence with a very slow turnover rate of cells (~6 months), to one with high levels of proliferation and migration in response to damage. Human urothelial cells have been shown to withdraw from the cell cycle into G_0 phase whilst urothelial cells from other species arrest in G_1 (Chopra et al, 2008). The urothelium must also maintain barrier function whilst accommodating urine within the bladder, stretching, and altering apical surface area as the bladder fills (discussed in Carattino et al, 2013).

The urothelium has also been shown to detect chemical and physical stimuli within the extracellular environment and can respond by release of mediators to signal to underlying cell types (reviewed in Birder, 2010). Molecules including adenosine triphosphate (ATP), acetylcholine and nociceptive stimuli have been identified as having an important sensory role within the urothelium. This demonstrates an importance for the urothelium not only as a barrier but as a site of signal integration.

1.1.3 Urothelial Differentiation

Cellular differentiation can be thought of as cells acquiring characteristics to determine their phenotype to provide the function needed of them at that time (reviewed in DeGraff et al, 2013). In the urothelium, the superficial cells are considered the most differentiated as they contribute to the tight barrier function

through being sealed together by specific tight junction proteins and possession of a urothelium-specific transmembrane protein family, the uroplakins (UPK). Neighbouring superficial cells form intercellular tight junctions to mediate paracellular transport across the urothelium (reviewed in Balda and Matter, 2016). These are formed from both transmembrane and cytosolic proteins which interact to anchor cells to each other (**Figure 1.2**). One constituent of the tight junction is the protein family, the claudins whose expression is important in determining tissue permeability by forming paracellular barrier and pores (reviewed in Krause et al, 2008). Previous studies have identified a differentiation-associated expression profile of several claudin family members in the human urothelium with claudin 3 playing an important assembly role in the terminal tight junction (Varley et al, 2006; Smith et al, 2015). Zonula occludens (ZO) proteins and occludin are other constituents that make up tight junctions.

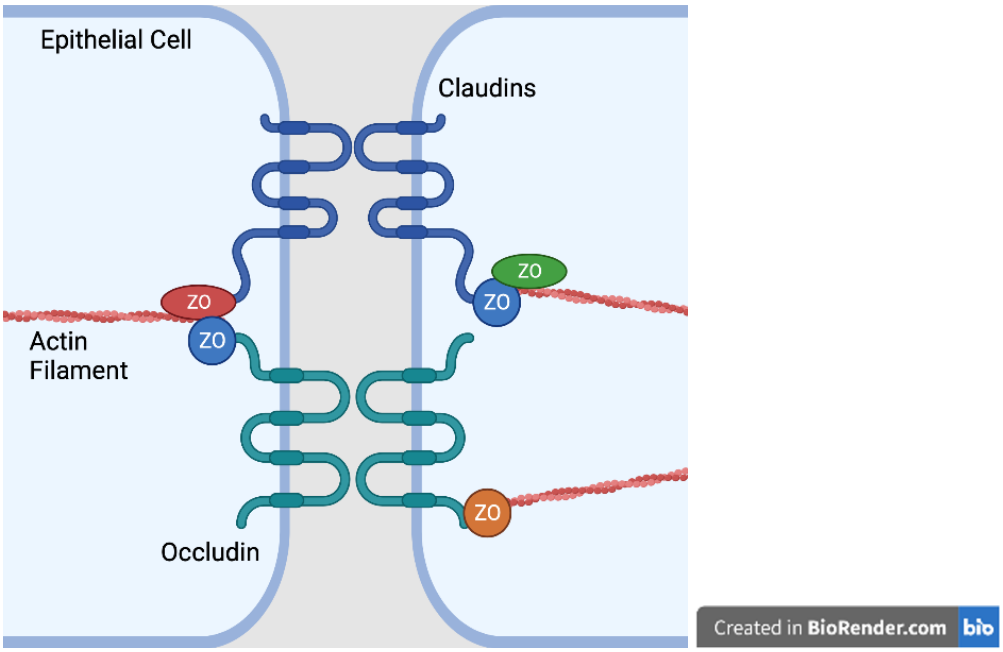

Figure 1.2. Schematic representation of tight junction protein components adapted from Balder and Matter, 2016.

Epithelial cells are sealed together by tight junctions consisting of claudin and zonula occludens family members and occludin which anchor adjacent cells to the cytoskeleton. This limits paracellular transport across epithelia thus providing a functional barrier. Created with BioRender.com.

The UPK family are the protein component of large, hexagonally arranged, apical plaques which cover the luminal surface of the superficial cells, also known as the asymmetric unit membrane (AUM) (reviewed in Sun et al, 1996). Genetic ablation of UPK genes in mice demonstrated a role for AUM in mediating urothelial permeability to water and solutes and contributing to stabilisation of superficial cells during bladder distension (reviewed in Wu et al, 2009). Both UPK and tight junction proteins jointly contribute to maintaining urothelial integrity measurable by trans-epithelial electrical resistance (TER) and provide *in vitro* markers of differentiation due to restrictive localisation to the superficial cells (discussed in Smith et al, 2015).

Both UPK and tight junction protein expression has been shown to be driven by the nuclear receptor peroxisome proliferator-activated receptor γ (PPARγ) identifying PPARγ as an important driver of urothelial differentiation (Varley et al, 2004; Varley et al, 2006). High-affinity, synthetic PPARγ ligands troglitazone (TZ) and rosiglitazone (RZ) upregulated mRNA expression of UPK and claudin family members in human urothelial cells *in vitro.* PPARγ is a ligand-activated transcription factor that heterodimerises with retinoid X receptor α to drive expression of PPARγ target genes and defines the urothelial differentiation programme. Natural ligands for PPARγ include fatty acid metabolites derived from lipoxygenase and cyclooxygenase (COX) metabolism (reviewed in Nosjean and

Boutin, 2002). It was previously suggested that urine-derived compounds may activate PPARγ as superficial cells are constantly bathed in urine however, urothelium from anuric patients, where the kidneys produce little to no urine, demonstrated comparable differentiation markers to control urothelium (Stahlschmidt et al, 2005). Thus, the natural PPARγ-activating ligand in human urothelium is yet to be identified.

1.1.4 Urothelial Repair

As discussed in section 1.1.2, the urothelium has an effective repair response to allow barrier restoration without the need for constant renewal of urothelial cells exemplifying the concept of tissue homeostasis. Epithelial wound repair is a complex, coordinated process involving controlled proliferation and migration of cells adjacent to the wound with the multi-step process achieving restitution of barrier function (Reviewed in Larsson et al, 2016; Kreft et al, 2005).

Like urothelial cells, keratinocytes in the epidermis contribute to both the barrier of the skin and play an important role in wound repair thus providing a well-studied example of epithelial wound repair (reviewed in Pastar et al, 2013). Stem cells residing within the skin provide the regenerative capacity of the epidermis. Whilst it remains a matter of debate whether the urothelium possesses stem cells, studies have suggested a population resides within the basal cell layer and can contribute to all three cell layers of the urothelium upon urothelial injury (Shin et al, 2011). Isolated basal urothelial cells have also been shown to adapt in culture possessing

the capacity to generate differentiated tissue comparable to native urothelium demonstrating plasticity due to environmental factors (Wezel et al, 2014).

Several growth factor and second messenger-mediated signal transduction pathways have been identified as having a role in urothelial wound repair demonstrating a complex, integration of signalling to mediate repair.

1.1.4.1 TGFβ receptor-mediated signalling

Transforming growth factor β (TGFβ) mediated signalling has been identified as being activated by urothelial damage and plays an essential role in migration to restore barrier function (Fleming et al, 2012). Furthermore, infection with Uropathogenic *Escherichia coli* demonstrated the importance of bone morphogenetic protein 4 (BMP4), a TGFβ family protein, in urothelial repair after inflammatory stimuli (Mysorekar et al, 2002).

TGFβ signalling is initiated by the binding of ligand to TGFβ receptor 2 (TGFβRII), a serine/threonine receptor kinase, causing recruitment and phosphorylation of TGFβ receptor 1 (TGFβRI) (reviewed in Haque and Morris, 2017). SMAD2 and SMAD3, members of a receptor-regulated family of SMAD proteins, are phosphorylated downstream of the activated receptor and associate with SMAD4 forming a complex which translocates to the nucleus to regulate target genes involved in cell growth and differentiation. SMURF proteins are ubiquitin ligases which regulate TGFβR signalling through SMAD-targeted degradation. Further regulation of TGFβR signalling is by inhibitory SMAD proteins (I-SMAD) who

inhibit intracellular signalling by competing for SMAD4 binding, down-regulating TGFβR expression and disrupting phosphorylation of SMAD proteins by TGFβ receptors. This process is summarised in Figure 1.3.

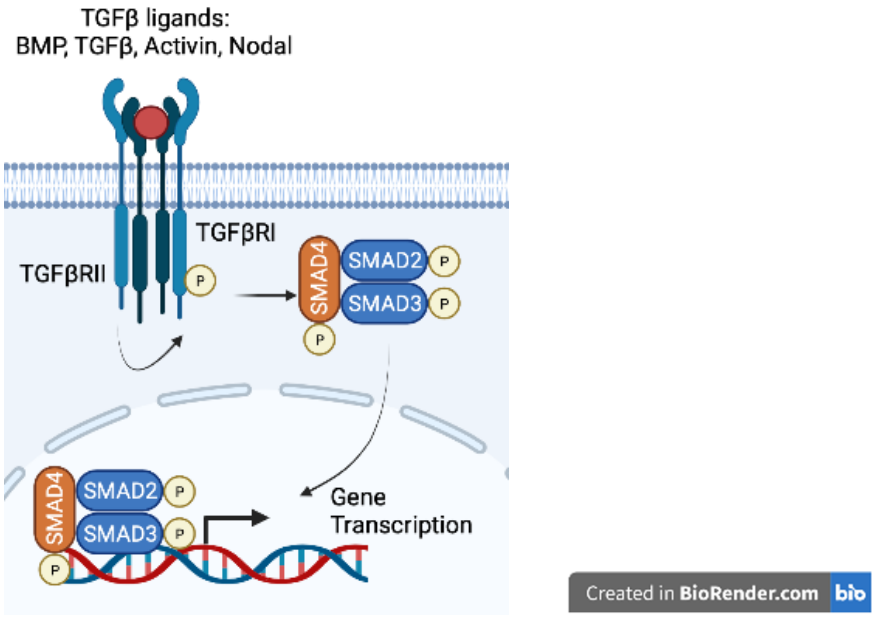

Figure 1.3. Schematic representation of TGFβ signalling

Ligands for TGFβ family members include BMPs, TGFs, activin and nodal which bind to TGFβ receptors causing dimerization and activation of SMAD proteins which translocate to the nucleus to cause changes in gene transcription. Created with BioRender.com.

Urothelial differentiation alters the expression of components of TGFβ signalling; downregulation of TGFβRI and TGFβRII but upregulation of SMAD3 effector protein demonstrating an alteration in activation potential (Fleming et al, 2012). Activation of SMAD3 by phosphorylation occurred in response to wounding stimuli and this was shown to be important in effective wound healing. Cellular responses to TGFβ signalling are governed by the expression of TGFβ ligands, receptors and SMAD proteins determined by the individual cell type as well as by cross-talk with other signal transduction pathways (reviewed in Miyazono, 2000). Together this allows a cell to tailor an appropriate response.

TGFβ-mediated signalling has been shown to be modulated by the eicosanoid prostaglandin E2 (PGE_2) (Lenicov, et al, 2018). TGFβ signalling was antagonised by PGE_2 in monocyte-derived dendritic cells promoting a more tolerogenic phenotype. Furthermore, during myofibroblast differentiation, TGFβ signalling is inhibited by PGE_2 through alterations to adhesion-dependent signalling (Thomas et al, 2007). This exemplifies significant cross-talk between pathways in modulating TGFβ signalling.

1.1.4.2 Fatty Acid Signalling

PGE_2 is a member of a group of lipid modulators produced by the COX enzymes previously shown to be released from urothelial cells damaged *in vitro* (Rastogi et al, 2007) and has been suggested to promote wound repair due to its cytoprotective function in epithelia. Furthermore, urothelial cells isolated from patients with IC showed an impairment of PGE_2 release upon damage (Rastogi et al, 2007). The authors hypothesised that this disrupted the ability for cells to effectively repair and contributed to the pathogenesis of the disease suggesting a role for PGE_2 in urothelial wound repair.

PGE_2 has been shown to be crucial in wound repair in other epithelia. Intestinal epithelial repair requires PGE_2 to promote a wound-associated epithelial phenotype with loss of PGE_2 receptors causing impaired repair (Miyoshi et al, 2017). In pulmonary epithelium PGE_2 promotes early wound repair processes including cell migration with exogenous addition accelerating wound closure (Salva et al, 2001). This highlights PGE_2 as a therapeutic target for treatment of

diseases in which impaired wound repair may play a role in pathogenesis including colitis and asthma and raises the possibility PGE_2 could be beneficial in treating IC patients.

Metabolic products from COX enzymes were previously mentioned in section 1.1.3 due to their ability to act as natural ligands for PPARγ raising the interesting possibility that these metabolites may play a role in both differentiation and proliferation dependent on their biochemistry determined by the stage of degradation. This provides a basis for further exploration into prostaglandin signalling in the urothelium.

1.1.5 Urothelial Cells *in vitro*

To study urothelial cells *in* vitro, normal human urothelial (NHU) cells isolated from surgical samples of ureter or bladder tissue can be propagated in culture providing non-immortalised cell lines with a finite lifespan (Southgate et al, 1994). NHU cells are subsequently grown in low calcium (0.09 mM), serum-free medium where they express the cytokeratin (CK) profile of intermediate/basal urothelium in addition to CK14 and CK16 indicating a more squamous phenotype growing as proliferative monolayers directly contrasting with urothelium *in situ*. Autocrine activation of the epidermal growth factor receptor (EGFR) promotes cell growth in NHU cells with protein amphiregulin as the main endogenous ligand which NHU cells produce themselves (Varley et al, 2005). Keratinocyte serum-free medium for NHU cell culture contains bovine pituitary extract (BPE), recombinant EGF and is supplemented with cholera toxin (CT) which aids in adherence of cells to the

culture substrate. To note, CT also causes constitutive activation adenylyl cyclase (AC) through ADP-ribosylation of G_{α}-stimulatory proteins causing an inactivation of their GTPase activity thus the G protein remains GTP bound and active (reviewed in Bharati and Ganguly, 2011). The downstream effects of this are yet to be defined.

Since NHU cells in culture do not display *in situ* urothelial differentiation markers, urothelial cytodifferentiation can be achieved *in vitro* by incubation of NHU cells with serum and near physiological calcium concentration (2 mM) (Cross et al, 2005). This method induces stratification into a multi-layered, "biomimetic" urothelium which forms barrier of >3000 $\Omega.cm^2$ and provides a model to study urothelial physiology comparable to urothelium *in situ*.

1.2 Prostaglandins in the Urothelium

1.2.1 Prostaglandin Synthesis and Degradation

Prostaglandins are a group of physiologically active fatty acid eicosanoids produced by most cells in the human body functioning predominantly as pro-inflammatory hormones but may also mediate homeostasis mechanisms (reviewed in Park et al, 2006). Prostaglandins are derived from arachidonic acid released from cell membrane phospholipids by the activity of phospholipase A_2. Arachidonic acid is subsequently catabolised to the unstable intermediate prostaglandin H2 (PGH_2) by the activity of the COX enzymes. COX-1 is constitutively present in most human tissues and has a "housekeeping" function in

tissue homeostasis whilst COX-2 is induced by mitogens, hormones, and injury (reviewed in Rouzer and Marnett, 2009). Prostaglandin synthesis continues through the action of specific prostaglandin synthases to produce the primary bioactive eicosanoids prostaglandin D (PGD_2), F2α ($PGF_{2\alpha}$), PGE_2, prostacyclin (PGI_2) and thromboxane (TXA_2). Figure 1.4 illustrates the synthetic pathway of prostaglandin molecules.

PGE_2 synthase (PGES), the enzyme which produces PGE_2 from PGH_2, occurs in several forms with distinct cellular localisation (reviewed in Park et al, 2006). Microsomal prostaglandin E synthase-1 (mPGES-1), sometimes referred to as membrane-associated PGES, is encoded by the *PTGES* gene and is induced by pro-inflammatory stimuli with small contribution to basal PGE_2 levels and is stated to have a marked preference of COX-2 over COX-1. *PTGES2* encodes another PGE_2 synthase distinct to mPGES-1, termed mPGES-2 identified by Tanikawa et al, 2002 and is more ubiquitously expressed than mPGES-1. Cytosolic PGES (cPGES) identified by Tanioka et al, 2000 is a cytosolic enzyme constitutively expressed in most tissues and is coupled to COX-1 and appears to play a role in homeostatic regulation of PGE_2 production. These studies identify a more defined pathway whereby COX-2 and mPGES-1 are linked to inflammation whereas mPGES-2, cPGES and COX-1 are linked to tissue homeostasis thereby determining divergent roles for PGE_2 based on method of synthesis.

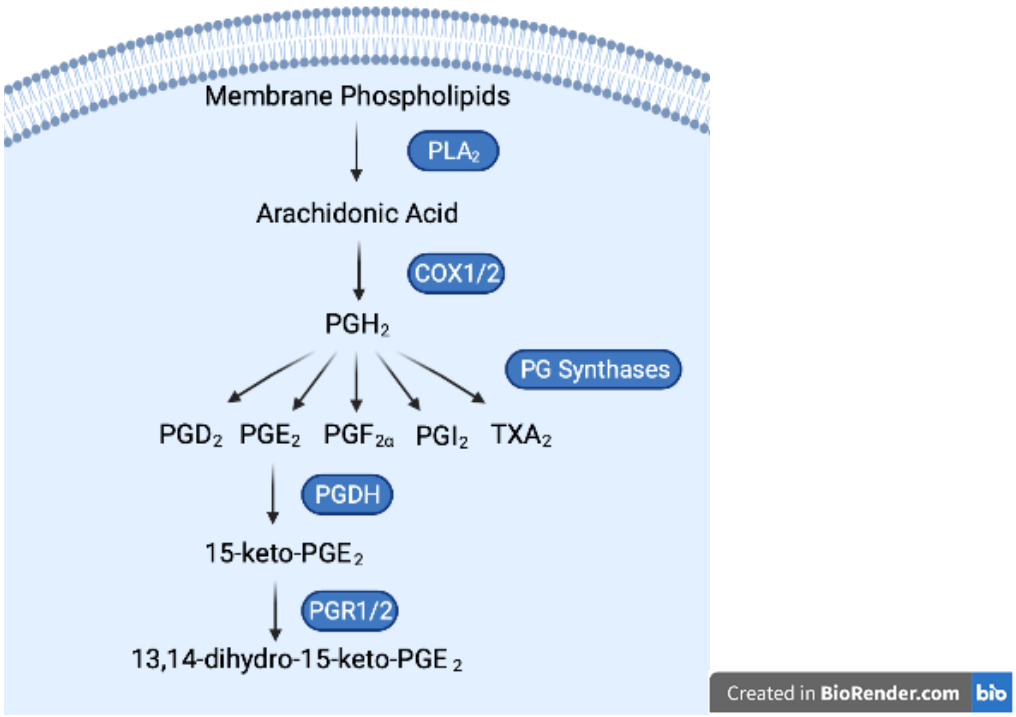

Figure 1.4. Pathway schematic of prostaglandin synthesis and degradation adapted from Kalinski, 2012.

Phospholipase A_2 family members mobilise arachidonic acid from membranous phospholipids which is converted to PGH_2 by the COX enzymes. Specific prostaglandin synthases produce individual prostaglandins including PGE_2. PGDH is responsible for degradation of PGE2 to a 15-keto metabolite which can be further catabolised by PGR enzymes. Created with BioRender.com.

Local concentration of PGE_2 is mediated through degradation by prostaglandin dehydrogenase (PGDH), a member of the short chain nonmetalloenzyme alcohol dehydrogenase family (Zhang et al, 2015). PGDH catalyses the first step in prostaglandin degradation by oxidation of prostaglandins to less active keto forms which have attenuated binding affinities to their receptors. Whilst previously thought as inactive, 15-keto-PGE_2, the degradation product produced by PGDH, has recently been shown to be able to activate the same receptors as PGE_2 (Endo

et al, 2020), discussed further in section 1.2.2. 15-keto-PGE_2 can be further metabolised to 13,14-dihydro-15-keto-PGE_2 by the action of prostaglandin reductase enzymes (reviewed in Tai, 2011) providing further regulation over PGE_2 degradation.

1.2.2 Prostaglandin Signalling

Prostaglandins have been reported to have a wide array of physiological effects with these being cell-type, context, and concentration dependent due to the diversity of prostaglandin receptors available (reviewed in Funk, 2001). Four G protein coupled receptors (GPCR) have been identified which bind PGE_2 ($EP_{1\text{-}4}$ receptors) with these having vast downstream signalling capabilities (reviewed in Reader et al, 2011) illustrated in figure 1.5. The EP_1 receptor is coupled to phospholipase C through $G_{\alpha q}$ which cleaves phosphatidylinositol 4,5-bisphosphate to diacylglycerol and inositol triphosphate. These second messengers mediate intracellular Ca^{2+} mobilisation and protein kinase C activation respectively. The EP_3 receptor inhibits AC activity through $G_{\alpha i}$ thus decreasing cyclic adenosine monophosphate (cAMP) production. Both the EP_2 and EP_4 receptors are coupled to AC through $G_{\alpha s}$ causing increases in cAMP production and both receptors have also been shown to activate T cell-factor/lymphoid enhancer factor (TCF/LEF) signalling in response to PGE_2 (Fujino et al, 2002). Interestingly, PGE_2 has also been shown as capable of trans-activating EGFR in colon epithelium, an important receptor mediating urothelial growth and repair (Pai et al, 2002).

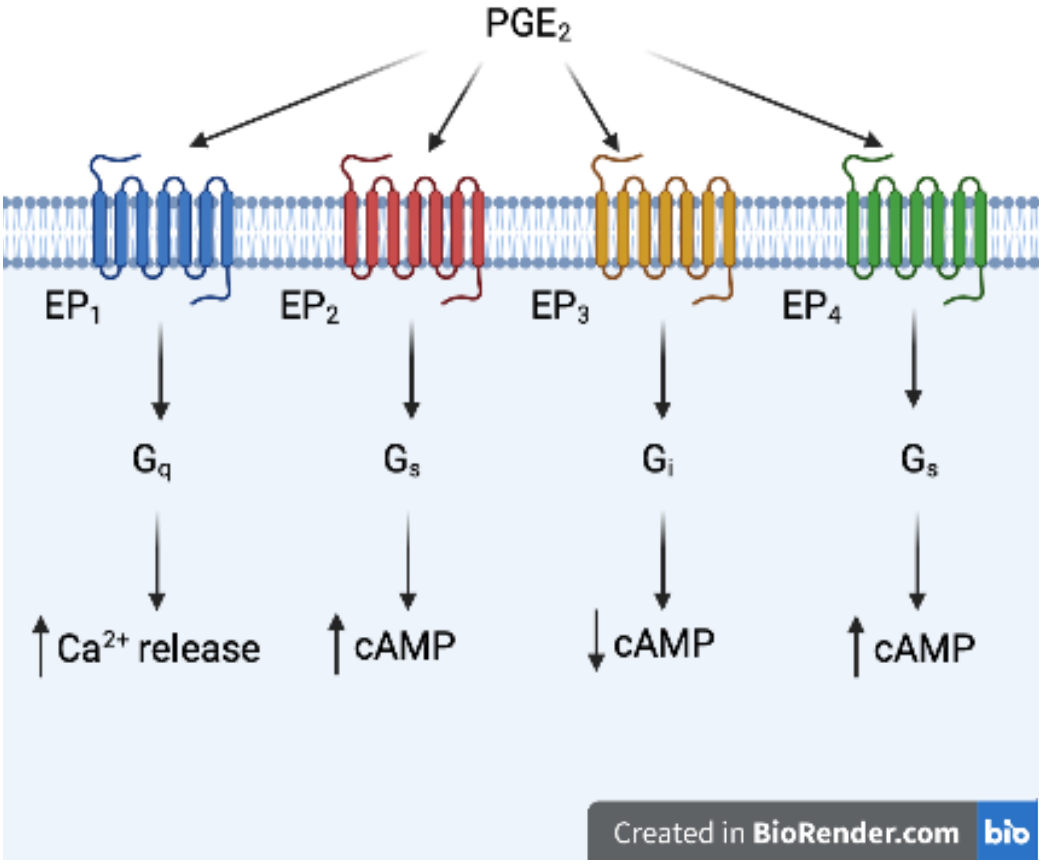

Figure 1.5. Pathway schematic of PGE_2 signalling via the $EP_{1\text{-}4}$ receptors adapted from Reader et al, 2011.

Binding of PGE_2 to: EP_1 causes elevation of intracellular calcium through $G_{\alpha q}$, EP_2 and EP_4 activates adenylyl cyclase and causes increased cAMP production through $G_{\alpha s}$ and EP_3 inhibits cAMP production through $G_{\alpha i}$. Created with BioRender.com.

Downstream of multiple EP receptors, cAMP can bind and activate protein kinase A (PKA), a complex composed of two regulatory and two catalytic subunits, which can alter a multitude of cellular processes with effects being cell-type specific (reviewed in Sassone-Corsi, 2012).

Whilst GPCRs are largely thought to mediate responses to extracellular stimuli by localising to the cell membrane, evidence has also demonstrated EP receptor

nuclear localisation (reviewed in Gobeil et al, 2006). Specific EP receptor expression and localisation therefore determines the cellular response to PGE_2.

1.2.3 Prostaglandins in the Bladder

Human urinary bladder tissue, maintained as isolated bladder strips in a tissue bath experiment, has been previously shown to produce and release PGE_2 *in vitro* (Abrams et al, 1979). Addition of arachidonic acid increased prostaglandin production whilst incubation with indomethacin, a COX inhibitor, reduced prostaglandin release. Release of prostaglandins by the urothelium is induced by stretch and bladder distension (discussed in Sellers et al, 2018). Signalling of urothelial-released prostaglandins to underlying smooth muscle was shown to alter contractile responses in rats and removal of the urothelium abolished this effect (Nakahara et al, 2003). This demonstrates a signalling axis for prostaglandins between the urothelium and underlying detrusor muscle to modulate bladder contraction.

PGE_2 has also been identified as having a cytoprotective role in the urinary bladder through upregulation of glycosaminoglycans which prevent attachment of bacteria to the urothelium (discussed in Khan et al, 1998). PGE_2 synthesis is a proposed defence mechanism against infection with impaired synthesis linked to reoccurrence of bacterial cystitis.

Expression and localisation of several constituents involved in PGE_2 synthesis, signalling and degradation, illustrated in figure 1.4, in the human urothelium have

been previously investigated. Whilst COX-1 protein is expressed in both healthy and diseased bladder smooth muscle tissue, COX-2 has only been reported as being strongly expressed in cancerous urothelial tissue (Shirahama, 2000). COX-1 was reported to be only expressed in the bladder smooth muscle not in the epithelial lining. Previous studies utilising immunohistochemical staining for the EP receptors in different parts of the human ureter identified EP_1 as being highly expressed in urothelial cells but EP_{2-4} staining was weaker or absent (Oll et al, 2012). Strong EP_1 expression was also detected at the mRNA level in both urothelial and smooth muscle cells. However, limitations include the tissue samples being taken from patients with malignant kidney tumours or undergoing nephroureterectomy for hydronephrotic kidney which raises doubt over how 'normal' the samples were. PGDH expression has been reported to localise to the superficial cell layer of human urothelium (Tseng-Rogenski et al, 2008). Whilst these components begin to illustrate a role for PGE_2 signalling in the urothelium, a more thorough investigation into their expression is warranted.

1.2.4 Prostaglandins and Cancer

Bladder cancer is the 11th most incident cancer in the UK with over 10,000 diagnoses per annum (Cancer Research UK, 2017). Successful early diagnosis is important for survival of bladder cancer due to the poor survival statistics associated with metastatic spread (discussed in Saginala et al, 2020). A review by Cheung et al, 2013 reports approximately 75 to 85% of bladder cancer patients have a non-muscle invasive bladder cancer (NMIBC) whereby the cancer is restricted to the mucosa (Ta) or submuscosa (T1). Carcinoma *in situ* (Tis) is a flat,

urothelial lesion but is high risk for muscle invasion. Muscle-invasive bladder cancer (MIBC) (>T2) are cancers that invade into the detrusor muscle layer. Treatment for bladder cancer is heavily dependent on the type and stage thus many investigations have gone into advancing diagnosis and identifying markers to tailor therapeutic strategies on a per patient basis (reviewed in Tran et al, 2021).

PGE_2 has been extensively studied for its pro-tumorigenic effects and thus has been identified as a potential therapeutic target in patients with bladder cancer (reviewed in Woolbright et al, 2020). Chronic inflammation has been suggested as a risk for cancer progression and with COX-2 (induced by inflammatory stimuli) upregulated in cancerous urothelial tissue (Shirahama, 2000), COX-2 inhibitors were studied for their potential in reducing the incidence of bladder cancer (Daugherty et al, 2011). Non-steroidal anti-inflammatory drugs (NSAID) inhibit COX-2, and results indicate regular use of NSAIDs reduce bladder cancer risk especially for non-smokers. However, COX inhibitors have been linked to higher risk of cardiovascular comorbidities (reviewed in Woolbright et al, 2020) so safer alternatives need to be investigated including blockade of PGE_2 synthesis, increasing its breakdown, or disrupting its signalling pathways. EP_2 and EP_4 receptor activation has been identified as correlating with urothelial tumorigenesis (Kashiwagi et al, 2018) and further, cytotoxic chemotherapy-induced release of PGE_2 has been shown to promote bladder cancer chemoresistance (Kurtova et al, 2015). Celecoxib, a COX-2 inhibitor, and a PGE_2-neutralising antibody both attenuated repopulation of cancer stem cells derived from a patient with chemoresistance after cytotoxic chemotherapy in a xenograft model. This

illustrates a mechanism in which PGE_2 promotes carcinogenesis with enzymes involved in PGE_2 synthesis considered oncogenes.

Enzymes involved in the catabolism of PGE_2, shown in figure 1.4, have been identified as potential tumour suppressors. Losses in PGDH expression have been reported in high-grade bladder tumours and correlate with grade of atypia and bladder cancer stage (Celis et al, 1996). PGDH expression has also been reported as having tumour suppressive functions in both lung and breast cancers by promoting apoptosis and inhibiting proliferation associated pathways (Wolf et al, 2006; Ding et al, 2005). Overexpression of PGDH in A549 lung cancer cells induced apoptosis evidenced by activation of pro-caspase 3 (Ding et al, 2005). Often however, the relationship between PGDH expression and cancer is more complicated than first thought. In breast cancer, contradictory studies have reported both up- and down-regulation of *HPGD,* the gene which encodes PGDH, gene expression dependent on classification, staging and metastasis (discussed in Volpato et al, 2020). This makes predicting patient outcomes dependent on *HPGD* expression incredibly difficult.

Silencing of *HPGD* in RT4 bladder cancer cells causes increases in motility and anchorage-independent growth suggesting PGDH plays a metastasis-suppressive role in bladder cancer (Tseng-Rogenski et al, 2010). Prostaglandin reductase enzymes have also been identified as having a novel oncogenic role in pancreatic cancer (Chang et al, 2016). Metabolite 15-keto-PGE_2, an endogenous PPARγ ligand, promoted reactive oxygen species mediated cell death and inhibited pancreatic cell growth. Since PPARγ is a driver of urothelial differentiation, it is

interesting that the enzyme which produces a potential ligand for PPARγ appears important as a bladder tumour suppressor.

1.2.5 PGDH and Urothelial Differentiation

A differentiation-associated role for PGDH has previously been proposed since it localises to the superficial cells of normal human urothelium and RT4 bladder cancer cells, which are considered a more luminal, differentiated cell line, display high levels of PGDH comparable to normal tissue (Tseng-Rogenski et al, 2008). Knockdown of *HPGD* expression by siRNA causes reduction in E-cadherin membrane localisation suggestive of cell-to-cell contact disruption and loss of barrier integrity. E-cadherin is a well-defined tumour suppressor in bladder cancer, which shows a similar correlation between losses in expression and tumour grade to that of *HPGD* in line with disruption to differentiation (reviewed in Bryan, 2015). Whilst these studies provide circumstantial evidence for a role for PGDH in urothelial differentiation and tumour suppression, using RT4 bladder cancer cells does not mimic *in situ* human urothelium so questions remain over how translational this evidence is to normal human urothelium. Therefore, the defined role in normal urothelium for PGDH and PGE_2 signalling is yet to be defined and understanding its function in normal urothelial physiology is important to hypothesise the implications of changes to its expression in bladder cancer.

1.3 Thesis Aims

Urothelial tissue homeostasis can be thought of as a balance between differentiation to maintain the characteristic tight barrier mitotic quiescence whilst retaining the capacity to respond to damage rapidly and efficiently through controlled migration and re-entry into the cell cycle. Lipid signalling pathways are starting to be explored but are far less characterised than other signal transduction pathways in involvement of tissue homeostasis.

The PGE_2 synthesis, response and degradation cascade provides an interesting candidate to be involved in mediating this homeostasis due to it having identified roles in the bladder but several components identified as altered in bladder cancer as discussed in section 1.2.4. It has been proposed that PGE_2 is released during urothelial damage, and this may act to promote restitution of urothelial barrier. With PPARγ identified as a crucial driver of urothelial differentiation, it is interesting that PGDH, the enzyme which produce 15-keto-PGE_2 (a natural PPARγ ligand), from pro-inflammatory mediator PGE_2, appears differentiation-associated in the urothelium. The aim of this thesis was therefore to explore the expression of PGE_2 signalling components in human urothelium by utilising an established *in vitro* differentiation model and to determe the extent PGDH plays in maintenance of urothelial phenotype by analysing differentiation and wound repair.

Specific experimental objectives, explored in chapters 3 and 4 were:

- To investigate expression of prostaglandin synthesis, receptor, and degradation proteins in normal human urothelium using RNAseq datasets produced by the Jack Birch Unit.

- To study whether regulation of local PGE_2 concentration functions in maintenance of urothelial tissue homeostasis and response to damage during wound repair.

2. Materials and Methods

2.1 General

All practical experiments were carried out at the Jack Birch Unit of Molecular Carcinogenesis, Department of Biology, University of York, York, United Kingdom.

2.1.1 Materials

Table 2.1 details the chemical agonists and antagonists used in this study. Compounds were solubilised in dimethyl sulfoxide (DMSO) and frozen at either -20ºC or -80ºC. A 0.1% DMSO control was used in all experiments. All reagents were initially titrated in NHU cells to determine the optimum concentration for use.

Name	Target	Mode of Action	Vehicle	Supplier
SW033291	PGDH	Antagonist	DMSO	Tocris
15-PGDH Inhibitor	PGDH	Antagonist	DMSO	Merck
PGE_2	EP Receptors	Agonist	DMSO	Cayman
16, 16-dimethyl-PGE_2	EP Receptors	Agonist	DMSO	Cayman
Recombinant TGFβ1	TGFβ receptor	Agonist	4mM HCl + 1mg/mL BSA	R&D Systems

Table 2.1. List of agonists and antagonists used.

2.1.2 Suppliers

A full list of suppliers for all reagents is detailed in Appendix 1.

2.1.3 Stock Solutions

Recipes for all stock solutions are detailed in Appendix 2. Sterilisation for heat stable solutions involved an autoclave run at 121ºC for 20 minutes.

2.2 Water

Throughout the study and for all stock solutions, de-ionised water ($d H_2O$) was used. Sterilisation of water involved an autoclave run at 121ºC for 20 minutes.

2.3 Cell Culture

2.3.1 General

All tissue culture experiments took place in an aseptic environment using a microbiological safety cabinet cleaned with 70% (v/v) ethanol solution before and after cell culture work.

2.3.2 Isolation of NHU Cells

Normal human urothelial (NHU) cells were provided and established as finite cell lines *in vitro*. NHS Research Ethics Committee approval was obtained: Leeds (East) REC 99/095 and REC 16/YH/0396 (URoBank). Cells were originally isolated from normal human urothelial tissue obtained from anonymous surgical samples from patients with no history of urothelial cancer and with informed patient consent. NHU cells were maintained in complete keratinocyte serum-free medium (KSFMc, Invitrogen) as previously described (Southgate et al, 2002), unless stated otherwise. KSFMc contains recombinant epidermal growth factor (Invitrogen), bovine pituitary extract (BPE, Invitrogen) and 30 ng/ml cholera toxin (CT, Sigma) to aid in plating efficacy. Cells were incubated at 37ºC and 5% CO_2 in air. NHU cells were grown on Cell$^+$ culture plasticware (Sarstedt).

2.3.3 Maintenance of NHU Cells

At visual confluence, NHU cells were passaged by removing medium from cell cultures and incubating with 10ml 0.1% ethylenediaminetetraacetic acid (EDTA) in phosphate buffered saline (PBS) at 37ºC until cells are rounded and separated when viewed under a microscope. This is followed by trypsinising until cells have lifted from the flask base and resuspending in KSFMc + trypsin inhibitor and centrifuged for 4 minutes. The supernatant was removed, and the pellet resuspended in fresh KSFMc to remove the trypsin. NHU cells can then be counted using a haemocytometer and reseeded at an appropriated density. For all

experiments in this thesis, cells were used between passages 3 and 5. Experiments were carried out using one independent NHU cell line unless stated otherwise. Each NHU cell line used is outlined in table 2.2.

NHU Cell Line	Origin	Donor Sex	Donor Age
Y929A	Ureter	Unknown	Paediatric
Y1151	Ureter	Female	31
Y1887	Ureter	Male	72
Y2089	Renal Pelvis	Male	50
Y2471	Ureter	Female	68
Y2797	Ureter	Female	57
Y2860	Ureter	Male	65

Table 2.2 List of NHU cell lines used.

2.3.4 Induction of Differentiation

NHU cells grown in KSFMc initially propagate due to an EGFR-mediated autocrine loop but fail to express markers of terminal differentiation. Urothelial cytodifferentiation is therefore induced as previously described (Cross et al, 2005). Confluent cultures were treated with medium supplemented with 5% adult bovine serum (ABS) for 4-5 days with media replaced every 2-3 days. Subsequently, exogenous calcium was increased from a concentration of 0.09mM to 2mM and maintained for a further 7 days with media replaced every 2-3 days. This method has been shown to promote contact-induced quiescence and expression of differentiation-associated genes characteristic of *in situ* urothelium.

2.3.5 Measurement of TER

TER is used to quantify barrier function of epithelial cells *in vitro* (discussed in Rubenwolf and Southgate, 2011). NHU cells maintained in ABS for 4-5 days are passaged and seeded into Greiner membranes at 5 x 10^5 cells per membrane where the calcium concentration is increased to 2 mM 24 hours after seeding. TER could then be monitored subsequently manually using an EVOM™ Voltohmmeter (World Precision Instruments) or automatically using cellZscope® equipment. The number of Greiner membranes in each experiment is outlined in the corresponding figure legend. Data is expressed as the mean TER of the replicate cultures ± standard deviation (SD).

2.4 Gene Expression Analysis

An “in house” mRNAseq dataset was provided by the Jack Birch Unit to assess gene expression in ABS/Ca^{2+} differentiated NHU cells. This dataset was generated from RNA sequencing performed on RNA taken from NHU cells from three donors which were either actively proliferating or at late-stage differentiation (ABS/Ca^{2+} method). Expression was reported as transcripts per million (TPM). Differential gene expression analysis was carried out by Dr. Andrew Mason involving a donor-matched comparison of undifferentiated vs. differentiated NHU cells. Log2 fold change for each individual gene was calculated as well as an adjusted p value (q value) by the Benjamini-Hochberg method. A fold change of ≥ 1 or ≤ -1 and a q value ≤ 0.05 were the criteria for a gene to be statistically and biologically significant.

2.5 Immunoblotting

2.5.1 Cell Lysis

Cell cultures for lysis and immunoblotting were grown in 6-well plates (2.5mL media per well) where media was aspirated off and cultures washed twice with ice cold PBS. Cultures were lysed *in situ* with 100µl complete SDS sample buffer, scraped from the well and collected into chilled microfuge tubes. Lysates were sonicated twice for 10 seconds at 25W with cooling on ice between. After a further 30 minutes on ice, lysates were microcentrifuged at 14,000rpm for 30 minutes at 4ºC and the supernatant aliquoted into a fresh microfuge tube.

2.5.2 Protein Quantification

Protein concentration was measured by a Coomassie assay in which lysates were compared to a standard curve produced from known dilutions of bovine serum albumin (BSA, Pierce) and read using a Multiskan Ascent® microplate reader.

2.5.3 Western Blotting

Lysates were diluted in *d*H_2O to attain required protein concentration then LDS sample buffer and reducing agent were added. Cell lysates were incubated for 10 minutes at 70ºC and briefly microcentrifuged before 30 µg of protein was resolved for 80-90 minutes on NuPage™ 4-12% Bis-Tris gels (Invitrogen) using either MOPS or MES running buffer. Protein was then transferred wet onto polyvinylidene difluoride membranes (Merck) for 90 minutes.

2.5.4 Membrane Labelling

Membranes were blocked in either 5% milk or Odyssey™ blocking buffer (Li-Cor Biosciences) for 1 hour then probed with primary antibody overnight at 4ºC (primary antibodies listed in table 2.3). Bound primary antibody was detected using goat anti-mouse antibody conjugated with Alexa Fluor 800 and goat anti-rabbit antibody conjugated with Alexa Fluor 680 (secondary antibodies listed in table 2.4) and visualised using Odyssey™ imaging system (Li-Cor Biosciences). β-actin was used as an additional loading control.

2.5.5 Immunoblotting Antibodies

Antigen	Host	Class	Dilution	Block	Supplier
β-actin	Mouse	mAb	1:10000	Both	Sigma
Keratin 13	Mouse	mAb	1:1000	Odyssey	Origene
Claudin 4	Mouse	mAb	1:1000	Odyssey	Invitrogen
MCM2	Rabbit	mAb	1:1000	Odyssey	Cell Signalling
PGDH	Rabbit	mAb	1:10000	Odyssey	Abcam
Phospho-Akt (S473)	Rabbit	pAb	1:1000	Odyssey	Cell Signalling
Phospho-ERK1/2	Rabbit	pAb	1:1000	Odyssey	Cell Signalling
Phospho-GSK3β (S9)	Rabbit	pAb	1:1000	Milk	Abcam

Phospho-Smad3 (S423+S425)	Rabbit	mAb	3:5000	Odyssey	Abcam
PPARγ	Rabbit	pAb	1:500	Odyssey	Cell Signalling
Total Smad3	Rabbit	mAb	1:5000	Odyssey	Abcam
Zonula occludens-3	Rabbit	mAb	1:1000	Both	Cell Signalling

Table 2.3. List of primary antibodies used for immunoblotting.

Antigen	Host	Class	Dilution	Block	Supplier
Mouse IgG (Alexa 800)	Goat	pAb	1:10000	Both	Molecular Probes
Rabbit IgG (Alexa 680)	Goat	pAb	1:15000	Both	Rockland

Table 2.4. List of secondary antibodies used for immunoblotting.

2.6 Indirect Immunofluorescence Microscopy

2.6.1 Slide preparation

NHU cells were seeded onto sterile 12-well glass slides at 7 x 10^5 cells/mL with 50µL of media per well. Cells were left to attach for a minimum of 4 hours at 37ºC before being flooded with 5mL KSFMc 5% ABS per slide. Cultures were treated as described in Section 2.3.4 to induce cellular quiescence and urothelial

differentiation. Cells were briefly washed in PBS before being fixed for 30 seconds in a 1:1 fresh solution of methanol and acetone before being air dried and stored at -20ºC.

2.6.2 Immunocytochemistry

To prevent antibodies spreading between wells, a grease pen was used to outline each well. Primary antibodies were diluted in tris buffered saline (TBS) containing 0.1% BSA and 0.1% NaN_3 and 15-20µL was added to each well and incubated overnight at 4ºC. Primary antibodies (detailed in table 2.5) were removed carefully by pipetting to avoid cross-contamination between wells and slides were washed 3 times with PBS for 5 minutes. Alexa 488- and Alexa 555-conjugated secondary antibodies (detailed in table 2.6) diluted in TBS containing 0.1% BSA and 0.1% NaN_3 were applied to wells at room temperature for 1 hour with slides protected from light. Slides were washed in PBST (PBS containing 0.25% (w/v) Tween-20) and incubated with PBS containing 0.1µg/mL Hoechst 33258 to visualise nuclei. After further washes with PBST and *d*H_2O for 5 minutes each and drying at room temperature, slides were mounted in ProLong Gold ^{TM} antifade, coverslips applied and sealed with clear nail varnish. Slides were stored in the dark either at 4ºC or frozen at -20ºC for longer term storage. Slides were observed and imaged on an Olympus BX60 epifluorescence microscope using selected filters. No primary antibody control was included in all experiments.

2.6.3 EdU Incorporation Assay

To investigate proliferation in NHU cells, DNA replication was measured by incubating cells with 5-ethynyl-2'-deoxyuridine (EdU), a thymidine analogue incorporated into newly synthesised DNA allowing monitoring of cells entering S phase. NHU cells were grown as described in Section 2.5.1 and upon reaching correct time point, pulsed with 2μM EdU for 16 hours to capture cells entering the cell cycle. Slides were then fixed with formalin or methanol:acetone as described in Section 2.5.1 before being stained with a solution containing Alexa-488-azide which cross-links to EdU in a 'click' chemistry reaction. From this point, slides are protected from light and additional immunostaining with primary antibodies as described in Section 2.5.2 is carried out.

2.6.4 Image Analysis

Programme ImageJ (v1.50g Java 1.8.0_60) was used to analyse images by highlighting individual Hoechst 33258 stained nuclei as regions of interest allowing for nuclei counts per image. Antibody labelled images could then be overlaid with a particle analysis cut off to exclude all but NHU cell nuclei determined at 430-3000 particles (Figure 2.1). Four fields of view were analysed using ImageJ to provide technical replicates. For nuclear labelling, positive cells were counted and expressed as mean ± SD. For cytoplasmic and membrane labelling, representative images are shown.

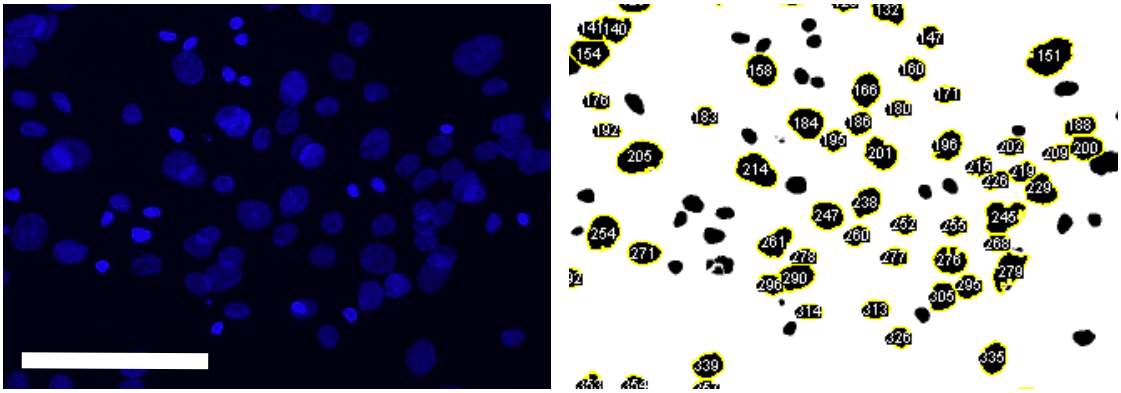

Figure 2.1. Determination of NHU cell nuclei ImageJ analysis cut off

Hoechst 33258 stained nuclei (*left)* were analysed in ImageJ to count only nuclei visually determined to be NHU cell nuclei involving a particle cut off (*right*). Scale bar = 50 μm.

2.6.5 Immunofluorescence Antibodies

Antigen	Host	Dilution	Supplier
MCM2	Rabbit	1:500	Cell Signalling
Phospho-Smad3 (S423+S425)	Rabbit	1:500	Abcam
Total Smad3	Rabbit	1:50	Abcam
Zonula occludens-3	Rabbit	1:800	Cell Signalling

Table 2.5. List of primary antibodies used for immunocytochemistry.

Antigen	Host	Dilution	Supplier
Alexa Fluor 488 Goat-anti rabbit	Goat	1:500	Invitrogen

Alexa Fluor 488 Goat anti-mouse	Goat	1:500	Invitrogen
Alexa Fluor 594 Goat anti-rabbit	Goat	1:500	Invitrogen
Alexa Fluor 594 Goat anti-mouse	Goat	1:500	Invitrogen

Table 2.6. List of secondary antibodies used for immunocytochemistry.

2.7 Time-Lapse Microscopy

NHU cells were seeded onto 24-well plates at 1.6 x 10^5 cells per well, grown to visual confluence and treated for 12 days as described in Section 2.3.4 to produce differentiated NHU cell cultures. Cultures were media changed either 12 or 24 hours prior to being scratch wounded, as detailed in the text, using a sterile 200µL pipette tip horizontally and placed into an environmental chamber (Solent Scientific) at 37ºC and 5% CO_2 in air. Six replicate wells were measured for intraexperimental repeats. Cultures were observed using videomicroscopy with individual images programmed to be taken continuously for 48 hours. Wound area could then be quantified at interval time points using programme ImageJ and expressed as percentage wound closure from the initial wound area.

2.8 Statistical Analysis

Graphical representation and statistics were carried out using GraphPad Prism (GraphPad Software, La Jolla California, USA). Where appropriate, data are presented as a mean ± SD with details of the number of technical or intraexperimental replicates, statistical test and appropriate post-tests in the associated text or figure caption.

Replicates in experiments in which the same NHU cell line was used but subsequently maintained in different, replicate cultures are described as “intraexperimental” as opposed to “technical” repeats. This is because even though the cells are derived from the same, initial sample, they may show population variance when cultured separately and these intraexperimental repeats had statistical analysis performed on their results whereas technical replicates did not. Individual Greiner membranes in TER analysis and individual culture wells in time lapse analysis are examples of intraexperimental repeats.

3. Characterisation of PGE_2 signalling in human urothelial cells *in vitro*

3.1 Introduction

Urothelial tissue homeostasis can be thought of as a tightly controlled balance between differentiation to generate and maintain its barrier function whilst retaining the ability to exit mitotic quiescence and regenerate in the event of injury. The bioactive eicosanoid PGE_2 has been implicated in cell regulation in other epithelia. In colonic epithelium, knockout of PGE_2 receptor EP4 disrupts normal tissue homeostasis through increases in apoptosis and enhanced immune cell infiltration (Matsumoto et al, 2019). During the proliferative phase of the menstrual cycle, PGE_2 may induce proliferation of glandular cells of the endometrium (Jabbour and Boddy, 2003). PGE_2 can also promote proliferation of normal bronchial epithelial cells (Fan et al, 2015). This raises the possibility that PGE_2 may play a role in the promotion of proliferation in the human urothelium.

As discussed in section 1.2, PGE_2 is implicated in bladder carcinogenesis with degradation enzymes widely considered as tumour suppressors indicating, like in other epithelia, PGE_2 may be involved in promoting proliferation. PGDH, the enzyme responsible for degradation of PGE_2, has been shown to be expressed in the normal human urothelium (Tseng-Rogenski et al, 2008) but its function remains largely unknown.

3.2 Aims and Hypothesis

The hypothesis is that PGDH functions to degrade PGE_2 whose accumulation would allow release of urothelial cells into the cell cycle. Catabolism of PGE_2 would therefore promote mitotic quiescence but removal of PGDH-expressing cells, such as in the instance of damage, would promote proliferation and repair of the urothelium. To investigate this hypothesis, the aim of this chapter was to characterise the expression and function of the canonical components involved in PGE_2 synthesis, degradation, and response in human urothelial cells. Specific objectives were:

- To evaluate the transcript expression of components of the PGE_2 metabolic pathway in NHU cells and determine whether differentiation status affects their expression.
- To determine the protein expression and localisation of key components of the PGE_2 metabolic pathway *in situ* and *in vitro*.
- To inhibit PGDH, whose activity may modulate PGE_2 availability, and assess the effects on mitotic quiescence and wound repair in NHU cells.

3.3 Experimental Approach

The NHU cell differentiation mRNAseq dataset (section 2.7) was examined to determine if genes associated with PGE_2 catabolism, degradation and response were expressed at the transcript level by human urothelial cells *in vitro*. Differentially- expressed genes were expressed as a $\log_2$ fold change.

To confirm differential expression at the protein level, PGDH protein expression was analysed by immunoblotting in NHU cells harvested sequentially through ABS/Ca^{2+} differentiation and compared to lysate from actively proliferating NHU cells. Claudin 4 was included as a previously reported marker of urothelial differentiation (Varley et al, 2006). Immunohistochemical labelling of PGDH was undertaken in normal human ureter to determine localisation in urothelium *in situ*.

Since PGDH catabolises the degradation of PGE_2, it was of interest to understand the effect of exogenous PGE_2 on differentiated NHU cells. Whilst PGE_2 has been reported to have a short half-life *in vivo*, *in vitro* studies suggest a slightly prolonged half-life (Bygdeman, 2003; Kozak et al, 2001). To overcome the degradation by PGDH, in this study 16,16-dimethyl-PGE_2 ($dmPGE_2$), a PGE_2 derivative with resistance to degradation by PGDH, was used unless stated otherwise (**Figure 3.1**). $dmPGE_2$ has been reported to act similarly to PGE_2 as an agonist for the EP receptor subtypes. To identify if PGE_2 acts by inducing changes to signal transduction pathways within the human urothelium, ABS/Ca^{2+} differentiated NHU cells were exposed to exogenous $dmPGE_2$ for increasing amounts of time ranging from 30 to 120 minutes. Phosphorylation of downstream

targets of the EP_4 receptor and EGFR, mitogen-activated protein kinase (also known as ERK), Akt and glycogen synthase kinase 3β (GSK3β), were chosen since EGFR has been previously shown to be trans-activated by PGE_2 signalling (Pai et al, 2002). Zonula occludens-3 (ZO-3), a urothelial differentiation-associated marker was included to confirm urothelial differentiation.

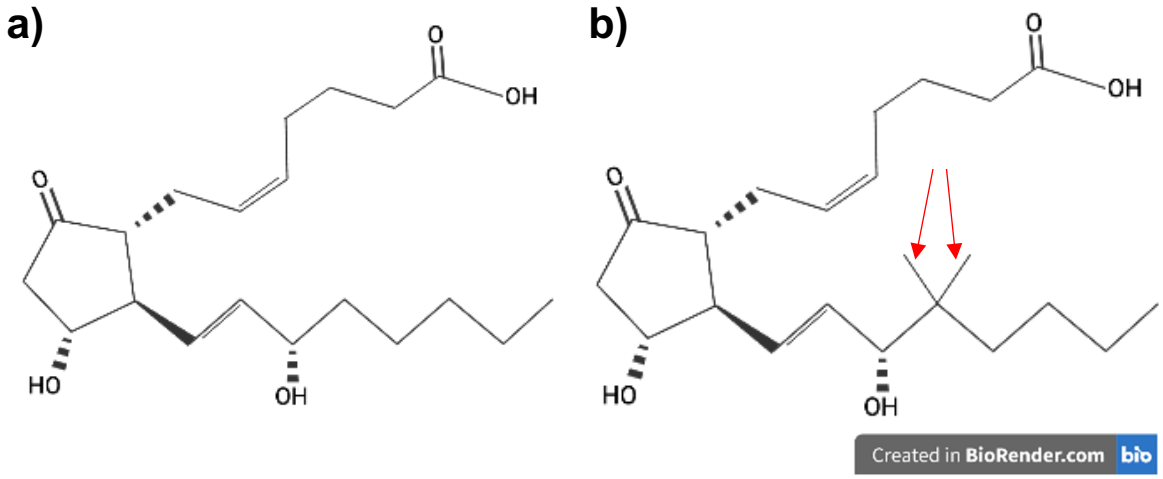

Figure 3.1. Chemical structures of a) prostaglandin E_2 and b) the derivative 16,16-dimethyl-prostaglandin E_2

16,16-dimethyl-PGE_2 has resistance to PGDH-mediated degradation as the two hydrogens at position 16 are replaced by methyl groups (*red arrows*). Created with BioRender.com.

To investigate the function of PGDH in human urothelium, two small-molecule inhibitors of PGDH, 15-PGDH inhibitor (PGDH-i) and SW033291 were used (**Figure 3.2**). PGDH-i is a thiazolidinedione analogue identified as a chemical inhibitor of PGDH with an IC_{50} value of 25 nM (Wu et al, 2011). PGDH-i significantly elevated the levels of PGE_2 in A459 human lung adenocarcinoma cells after a 5-hour incubation. SW033291 is a potent inhibitor of PGDH with an inhibitor dissociation constant *K*i ~ 0.1 nM and promotes tissue regeneration in colon, liver, and haematopoietic injury models (Zhang et al, 2015). Both inhibitors

were initially titrated across a concentration range of 1 to 10 μM for PGDH-i and 0.2 to 5 μM for SW033291. Cytotoxicity and proliferation were assessed by indirect immunofluorescence microscopy in NHU cells treated for 48 and 72 hours ± PGDH-i or SW033291. Proliferation was assessed by expression of mini-chromosome maintenance protein 2 (MCM2), a protein important in recruitment of eukaryotic DNA replication factors. An estimate for cell number was calculated from the total number of Hoechst 33258 stained nuclei per field of view as discussed in section 2.5.4.

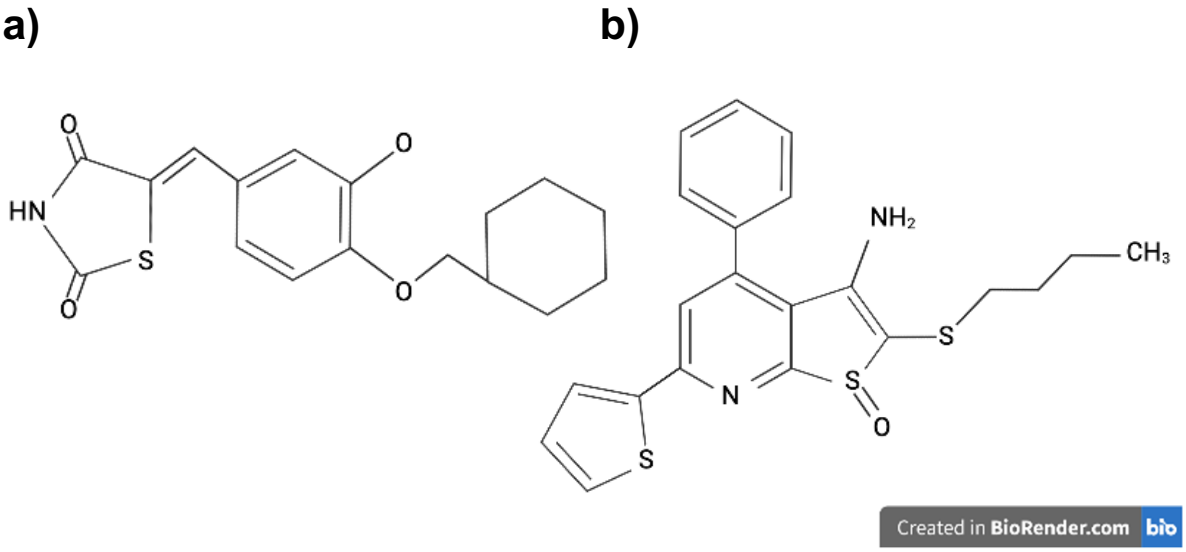

Figure 3.2. Chemical structures of a) PGDH-inhibitor and b) SW033291.
Created with BioRender.com.

Finally, the effect of PGDH inhibition on cellular proliferation and barrier function during wound repair was assessed by pre-treating ABS/Ca^{2+} differentiated NHU cell cultures ± PGDH-i or SW033291 for 12 hours followed by scratch wounding. $dmPGE_2$ was included as a positive control. Proliferation was assessed by EdU incorporation and MCM2 immunolocalisation on NHU cells differentiated on glass slides by epifluorescence microscopy. After wound repair, the original scratch wound location was unable to be identified therefore multiple fields of view were

analysed in the same well to examine proliferation in the entire culture, not relative to the wound location. Barrier function was measured by TER using cellZscope® equipment on NHU cells differentiated on Greiner membranes. As discussed in section 1.2.2, effects of PGE_2 can be mediated by alteration of intracellular cAMP concentration so barrier experiments were conducted in conjunction with cholera toxin (CT), an adenylyl cyclase activator which constitutively produces cAMP, hereafter referred to as +CT and -CT. The broader effects of cAMP signalling in the urothelium are discussed in chapter 4.

3.4 Results

3.4.1 Assessment of transcript expression for PGE_2 metabolic pathway components in urothelial cells

RNAseq analysis identified that genes required for PGE_2 synthesis, degradation, and response were expressed at the transcript level in ABS/Ca^{2+} differentiated NHU cells and many components were differentially-expressed between undifferentiated and ABS/Ca^{2+} differentiated NHU cells (**Figure 3.3** illustrates the components of the canonical pathway and indicates where transcripts were detected in ABS/Ca^{2+} differentiated cells; **Figure 3.4** illustrates the fold change in transcript expression between undifferentiated and ABS/Ca^{2+} differentiated cells). Whilst mRNA for COX1 encoding gene, *PTGS1*, was absent, COX2 encoding gene, *PTGS2*, was expressed. Investigation of the *PTGES* family demonstrated all three synthases are expressed by NHU cells. *PTGES1* was upregulated upon

differentiation (Log_2FC = 4.58, q = 0.00003) whilst *PTGES3* was downregulated (Log_2FC = -0.937, q = 0.0006) (**Figure 3.4**).

PGE_2 receptor genes, *PTGER1, PTGER2* and *PTGER3* had low or absent mRNA expression whilst *PTGER4* was expressed and upregulated upon differentiation (Log_2FC = 1.826, q = 0.001) (**Figure 3.4**).

HPGD had very low transcript expression in undifferentiated NHU cells but increased dramatically upon differentiation (Log_2FC = 6.537, q = 0.00000047). This identified *HPGD* as the most highly upregulated gene of the PGE_2 metabolic cascade. Both prostaglandin reductases *PGR1* and *PGR2* were expressed in NHU cells. A summary of the transcript changes to PGE_2 metabolic pathway components upon ABS/Ca^{2+} differentiation can be found in Table 3.1.

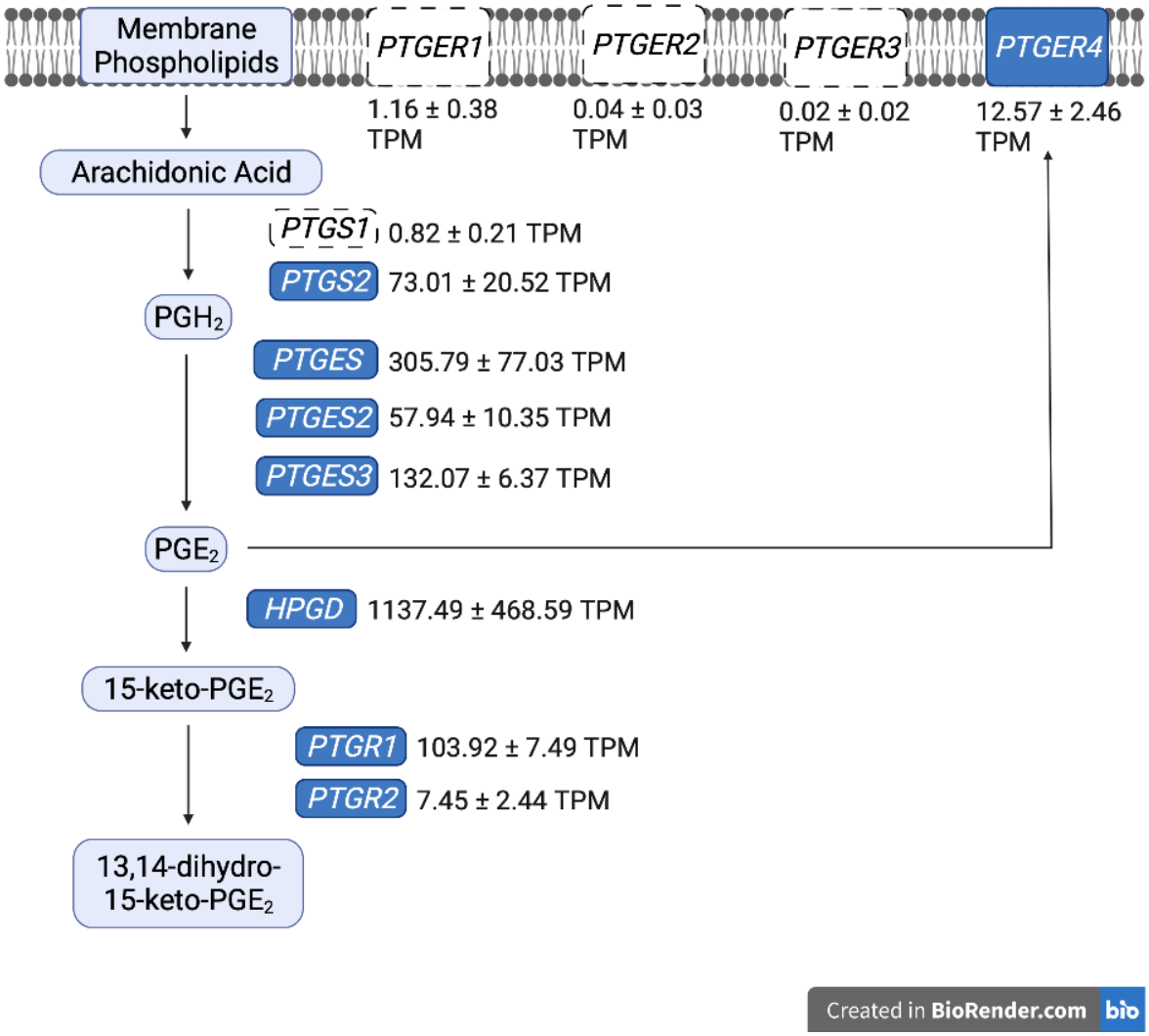

Figure 3.3. Transcript expression of PGE_2 metabolic pathway components in differentiated NHU cells

Analysis of mRNA expression for PGE_2 metabolic pathway component genes in ABS/Ca^{2+} differentiated NHU cells. Gene expression is reported as transcripts per million (TPM) (±SD). Components illustrated in blue are present at the mRNA level, components illustrated as having dashed borders are classed as absent. Created with BioRender.com.

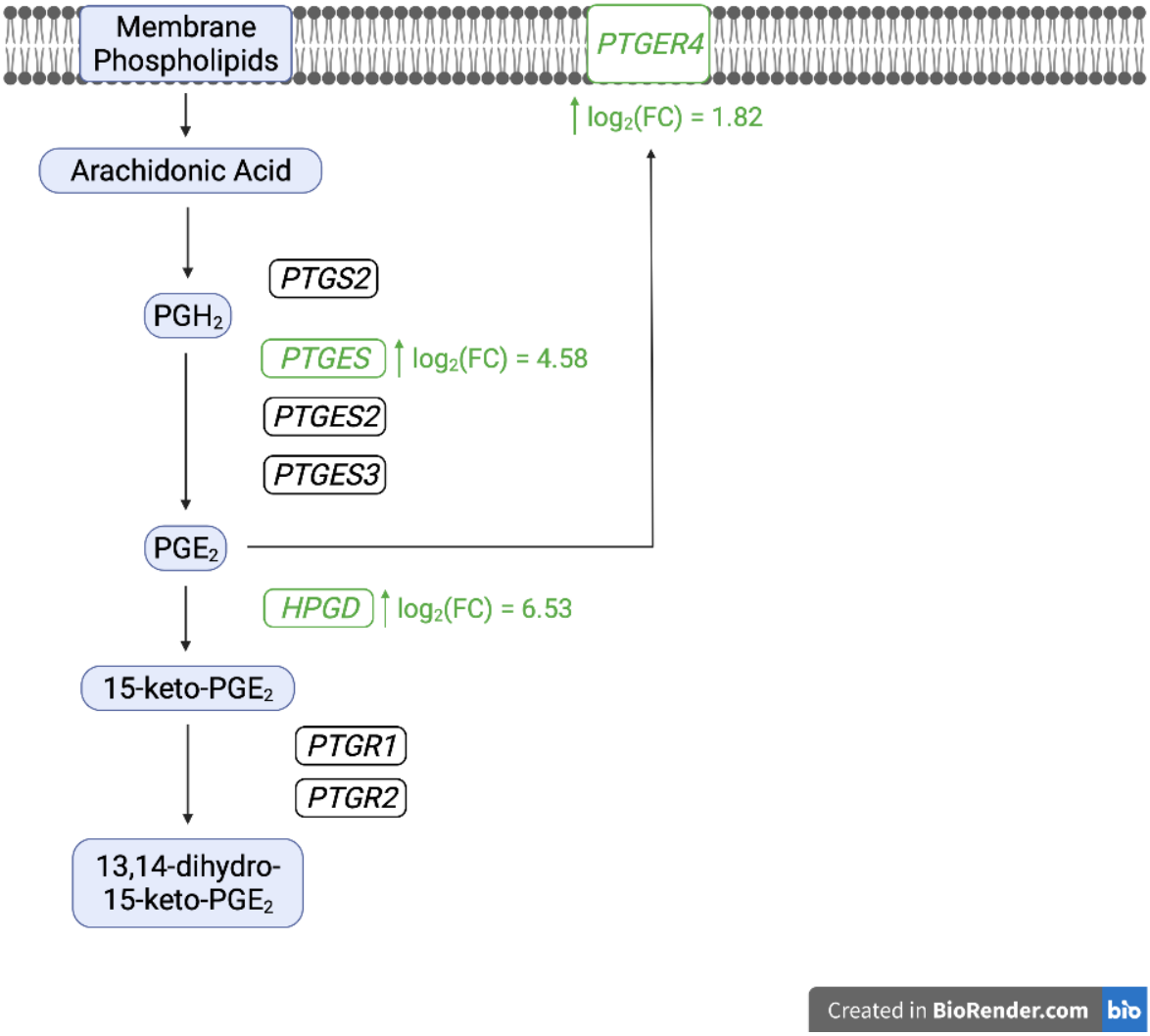

Figure 3.4. Log_2 fold change of transcript expression of PGE_2 metabolic pathway components comparing undifferentiated to ABS/Ca^{2+} differentiated NHU cells

Fold change of mRNA expression between proliferative and ABS/Ca_{2+} differentiated NHU cells for PGE_2 metabolic pathway component genes log_2 transformed. Genes considered statistically and biologically significant which were upregulated are labelled in green. Created with BioRender.com.

Gene	Protein	Fold Change (log_2)
PTGS2	Cyclooxygenase-2	0.279
PTGES	Microsomal prostaglandin E synthase-1	4.580
PTGES2	Microsomal prostaglandin E synthase-2	-0.061
PTGES3	Cytosolic prostaglandin E synthase	-0.937
PTGER4	EP_4 receptor	1.826
HPGD	Prostaglandin dehydrogenase	6.537
PTGR1	Prostaglandin reductase 1	0.303
PTGR2	Prostaglandin reductase 2	-0.195

Table 3.1 Log_2 fold change of transcript expression of PGE_2 signalling components comparing undifferentiated NHU cells to ABS/Ca^{2+} differentiated NHU cells

3.4.2 Characterisation of PGDH expression and localisation in human urothelium *in vitro* and *in situ*

Immunoblotting analysis (blot provided by Rosalind Duke) of NHU cells *in vitro* provided by Zhen Liu supported the transcript findings demonstrating PGDH protein was absent in undifferentiated cells but was induced upon incubation with 5% ABS and increased as differentiation progressed (**Figure 3.5**). However, lack of lysate prevented inclusion of a loading control, so this finding must be taken with caution. Immunohistochemical labelling of PGDH in normal human ureter performed by Dr. Jennifer Hinley demonstrated strong, superficial, cytoplasmic localisation with weaker labelling observed in intermediate cell layers and an absence of PGDH in basal cells (**Figure 3.7**). These results suggest a differentiation-associated role for PGDH in the human urothelium.

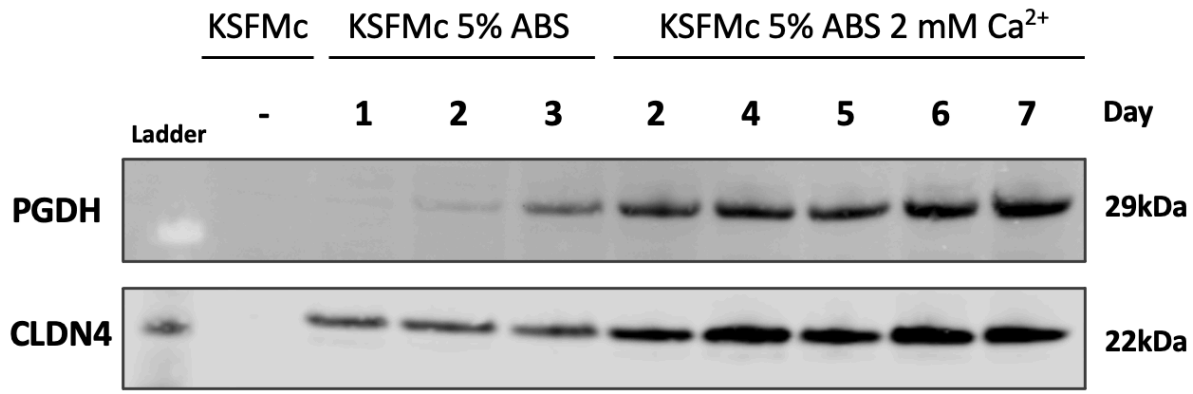

Figure 3.5. PGDH protein expression induction in ABS/Ca^{2+} differentiated NHU cells

Expression of PGDH protein was examined in NHU cells (Y2471) in an undifferentiated state or at sequential time points harvested during ABS/Ca^{2+} differentiation with cultures lysed in SDS sample buffer. PGDH expression was assessed by western blotting using the EPR14332 (Abcam) antibody (n=1). Claudin 4 was included as a known urothelial differentiation marker to act as a positive control. Lysate provided by Zhen Liu and immunoblotted by Rosalind Duke.

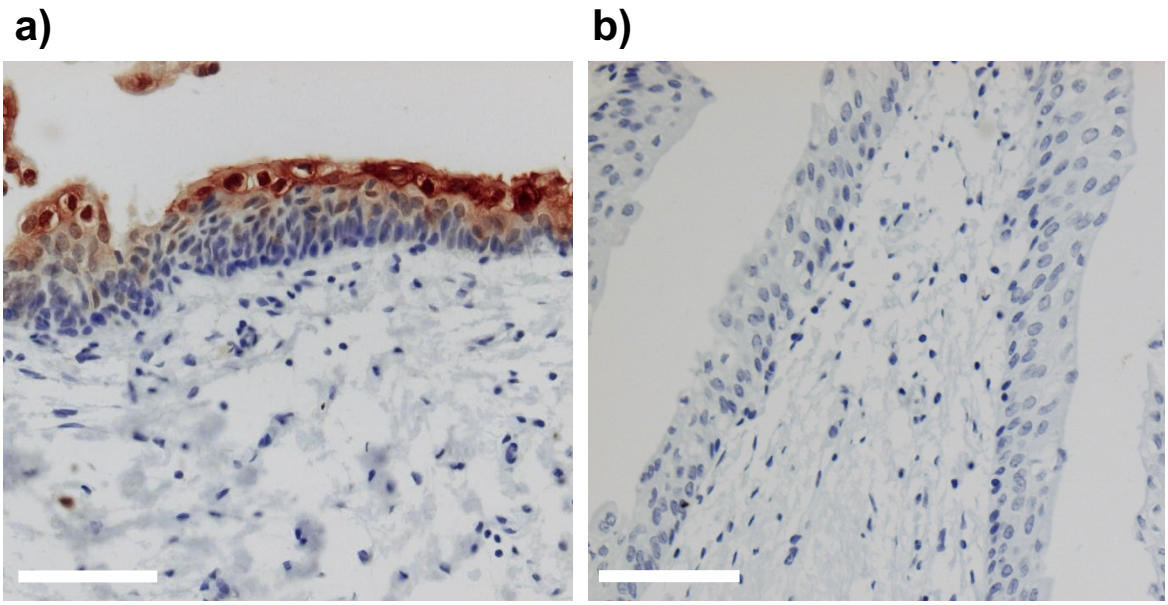

Figure 3.6. PGDH protein localisation in normal human urothelium

Immunohistochemical labelling of a) PGDH protein in normal human ureter (Y1187) using the EPR14332 (Abcam) antibody showing strong, superficial localisation with lower expression in intermediate cells and an absence in the basal cell layer. b) Negative control

with no primary antibody. Scale bar = 100 μM. Immunohistochemistry performed by Dr. Jennifer Hinley.

3.4.3 Analysis of candidate signal transduction pathways by exogenous PGE_2 stimulation

Upregulation of PGDH protein suggested an increase in degradation of PGE_2 in differentiated NHU cells therefore, to understand why elimination of PGE_2 is important in the urothelium, differentiated NHU cells were treated with exogenous $dmPGE_2$. Immunoblotting analysis demonstrated phosphorylation of Akt was weak in both control and $dmPGE_2$ treated cultures at all time points whilst a steady level of GSK3β phosphorylation was observed (**Figure 3.7**). ERK was phosphorylated at 30 minutes after treatment with both DMSO and $dmPGE_2$ but decreased after 2 hours, however as no lysate was taken at time 0 minutes, it is unknown whether treatment with $dmPGE_2$ induced ERK phosphorylation or if this is the basal level. No immediate signal transduction changes by exogenous $dmPGE_2$ treatment were identified but longer-term changes to gene transcription were not examined in this experiment.

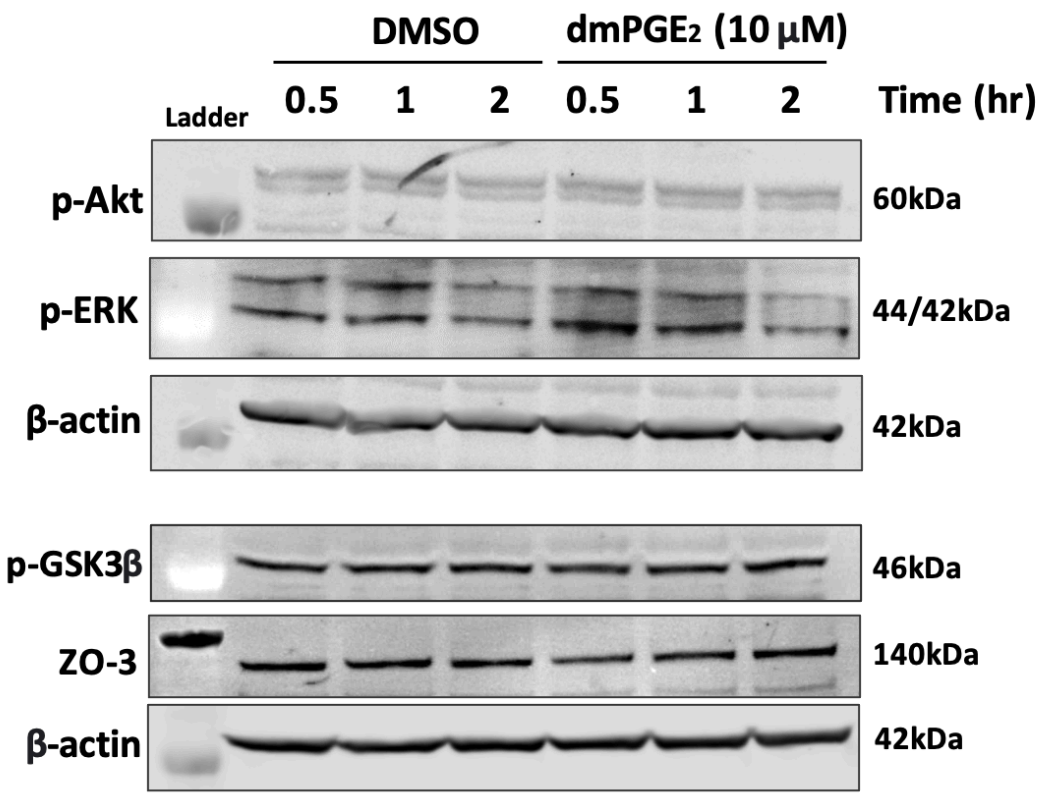

Figure 3.7. Immunoblot assessment of Akt, ERK and GSK3β phosphorylation following exogenous PGE_2 treatment to differentiated NHU cell cultures

NHU cells (Y1151) were differentiated following the ABS/Ca^{2+} method and harvested after treatment with $dmPGE_2$, an analogue of PGE_2 that cannot be catabolised by PGDH, for 30, 60 or 120 mins. Phosphorylation of Akt, ERK and GSK3β were assessed by western blotting and were unaffected when treated with $dmPGE_2$ (n=1). ZO-3 was included as a differentiation marker. β-actin was included as a loading control.

3.4.4 Effect of PGDH inhibition on NHU cell culture density and cellular proliferation

ABS/Ca^{2+} differentiated NHU cell cultures incubated ± PGDH-i or SW033291 for 48 and 72 hours were used to assess the effects of PGDH inhibition in urothelial cells *in vitro* to determine the optimum concentration for subsequent experiments.

When counting NHU nuclei for an estimate for cell number, a distinctive smaller, intensely bright, nuclear staining was identified hereafter referred to as “small nuclei” (**Figure 3.8**). Both larger and smaller nuclei number were quantified individually in four independent fields of view to give total and individual counts (**Figure 3.9-3.10**).

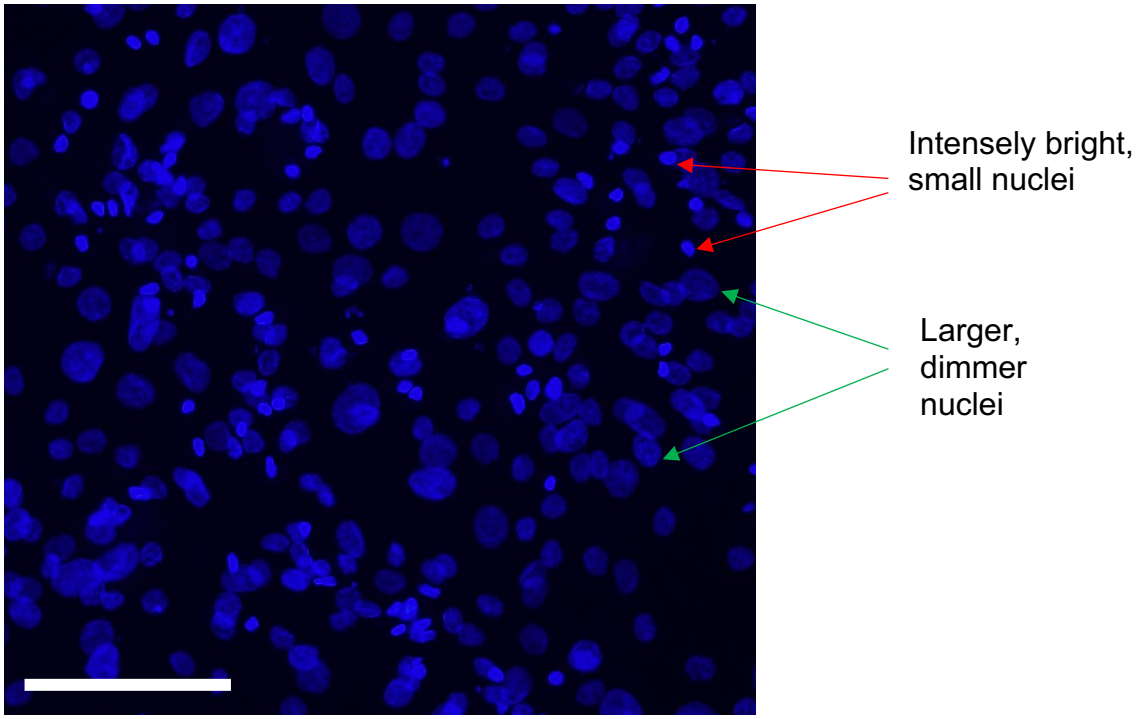

Figure 3.8. Example image displaying smaller, intensely bright nuclei.
Hoechst 33258 stained nuclei were quantified in ImageJ and scattered population of small, intensely bright nuclei were identified (*red arrows*) distinctive from the larger, dimmer NHU cell nuclei (*green arrows*). Scale bar = 100 µm.

Assessment of NHU cells incubated with either of the PGDH-inhibitors for 48 hours revealed a decrease in the total number of nuclei when incubated with 200 nM SW033291 in comparison to the DMSO control (**Figure 3.9a**). No differences were observed in the total number of nuclei in NHU cells incubated with any of the three concentrations of PGDH-i or 1 µM, 5 µM SW033291. After 72 hours, there was no difference in the total number of nuclei in NHU cells incubated with PGDH-i

but similarly to at 48 hours, a potential decrease is seen when incubated with 200 nM SW033291 (**Figure 3.9b**).

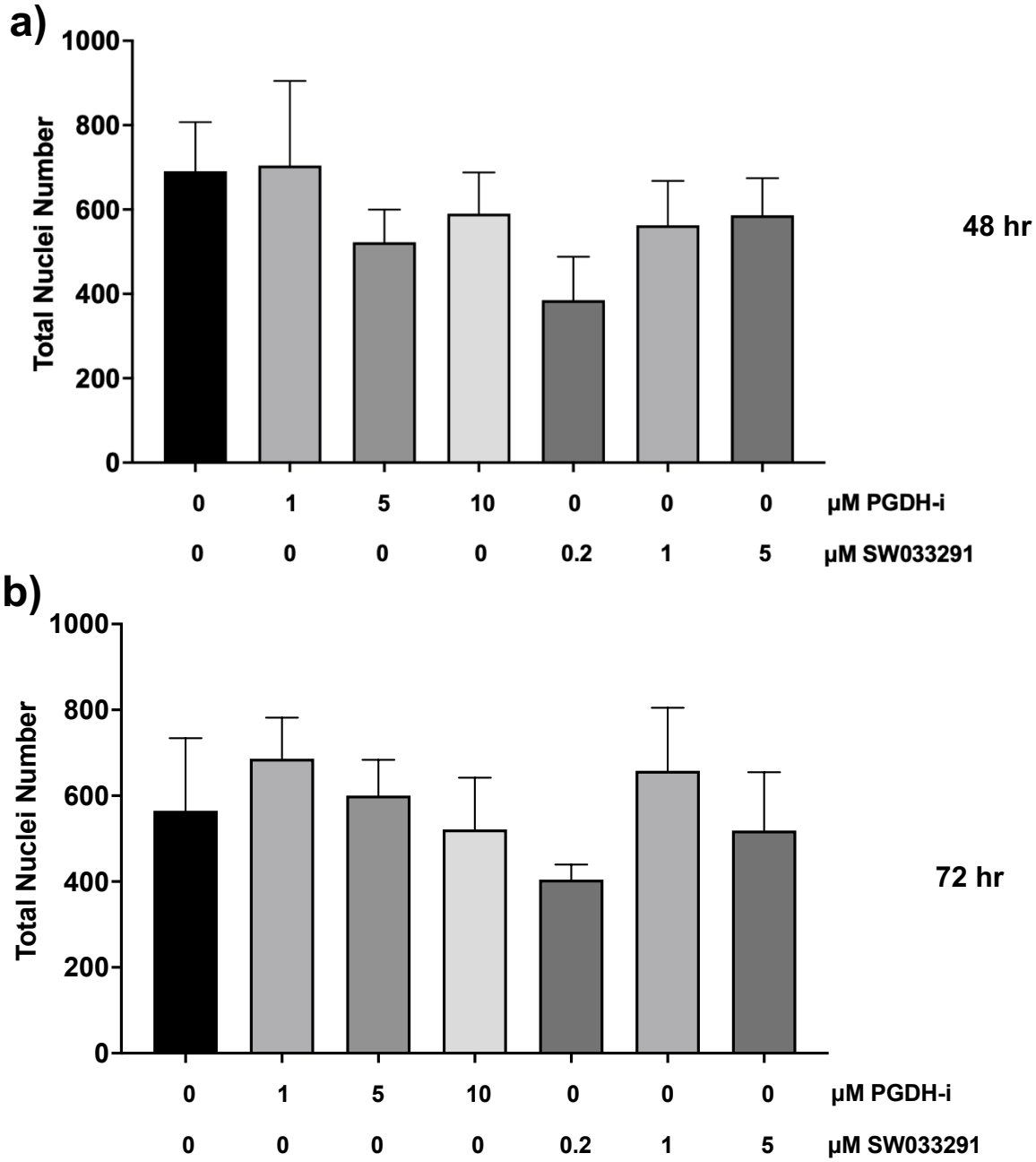

Figure 3.9. Effect of PGDH inhibition on total NHU nuclei number

NHU cells (Y929A) were differentiated following the ABS/Ca^{2+} method on glass slides and fixed a) 48 and b) 72 hours after treatment with 1-10 µM PGDH-inhibitor or 0.2-5 µM SW033291. Total number of Hoechst 33258 stained nuclei (±SD) were counted in 4 fields of view (technical replicates).

Assessment of NHU cells incubated with either of the PGDH-inhibitors for 48 hours revealed a decrease in the number of large nuclei when incubated with 10 or 5 μM PGDH-i or 200 nM SW033291 in comparison to the DMSO control (**Figure 3.10a**). No difference was observed in the number of large nuclei in NHU cells incubated with 10 μM, 1 μM PGDH-i or 5 μM, 1 μM SW033291. After 72 hours, there was no differences observed in the number of large nuclei in NHU cells incubated with either of the PGDH-inhibitors (**Figure 3.10b**).

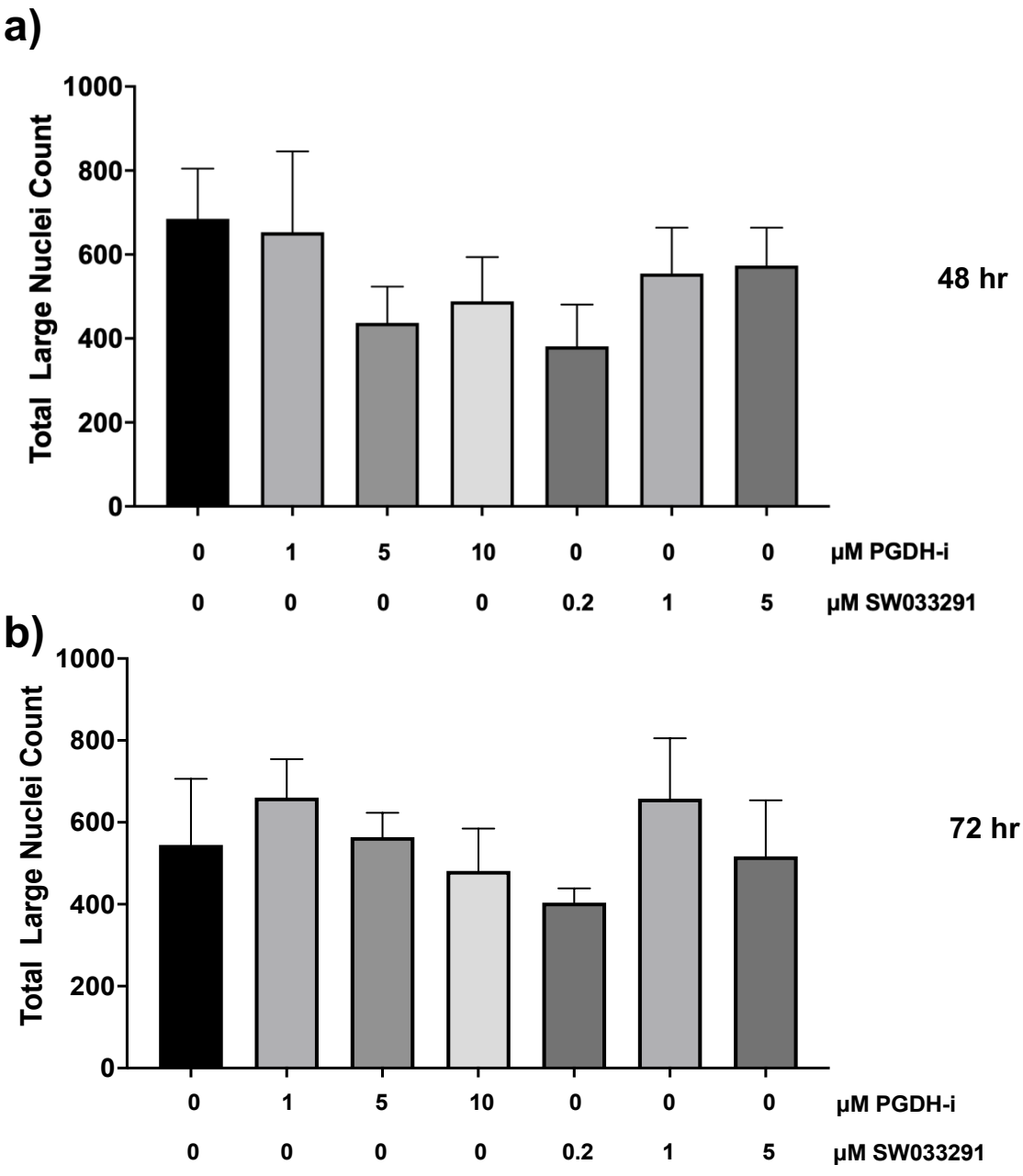

Figure 3.10. Effect of PGDH inhibition on large NHU nuclei number

NHU cells (Y929A) were differentiated following the ABS/Ca^{2+} method on glass slides and fixed a) 48 and b) 72 hours after treatment with 1-10 μM PGDH-inhibitor or 0.2-5 μM SW033291. Total number of large, dimmer, Hoechst 33258 stained nuclei (±SD) were counted in 4 fields of view (technical replicates).

Assessment of NHU cells incubated with either of the PGDH-inhibitors for 48 hours revealed an increase in the number of small nuclei when incubated with PGDH-i at 10, 5 or 1 μM compared to the DMSO control (**Figure 3.11a**). No difference in small nuclei was observed in NHU cells incubated with any concentration of SW033291 when compared to the DMSO control. Similarly at 72 hours, incubation with PGDH-i at 1, 5 or 10 μM increased the number of small nuclei observed but incubation with any concentration of SW033291 did not when compared to the DMSO control (**Figure 3.11b**). Differences in nuclear size may suggest apoptosis within the cultures incubated with PGDH-i which will be discussed further subsequently.

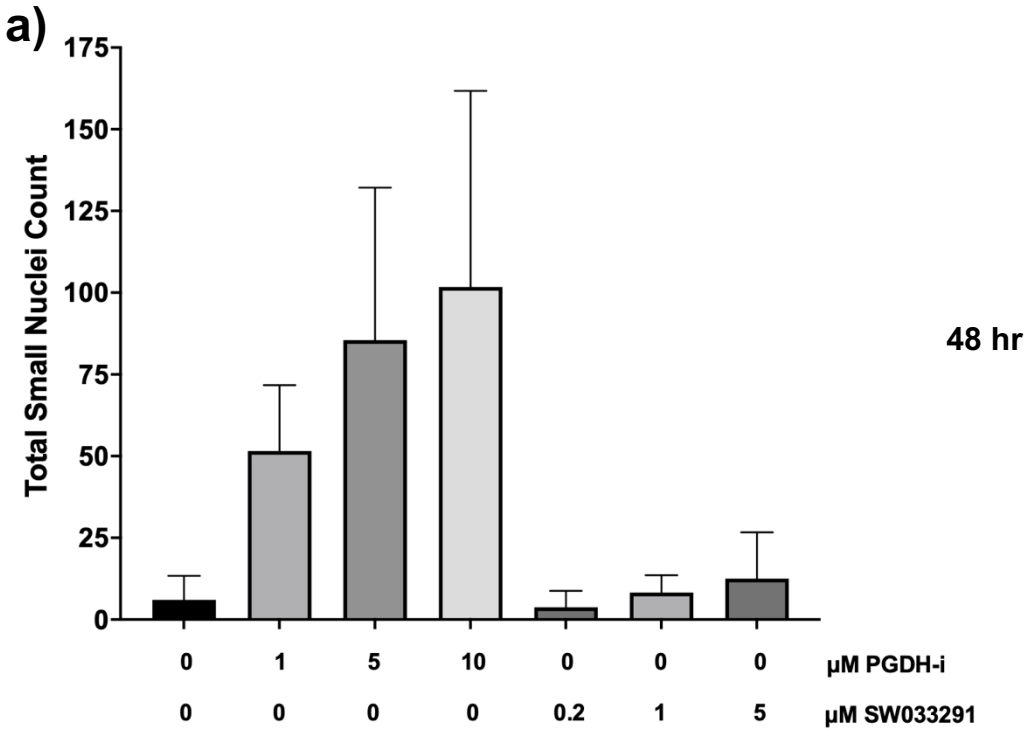
a)
Total Small Nuclei Count
175
150
125
100
75
50
25
0
48 hr
0 1 5 10 0 0 0 µM PGDH-i
0 0 0 0 0.2 1 5 µM SW033291

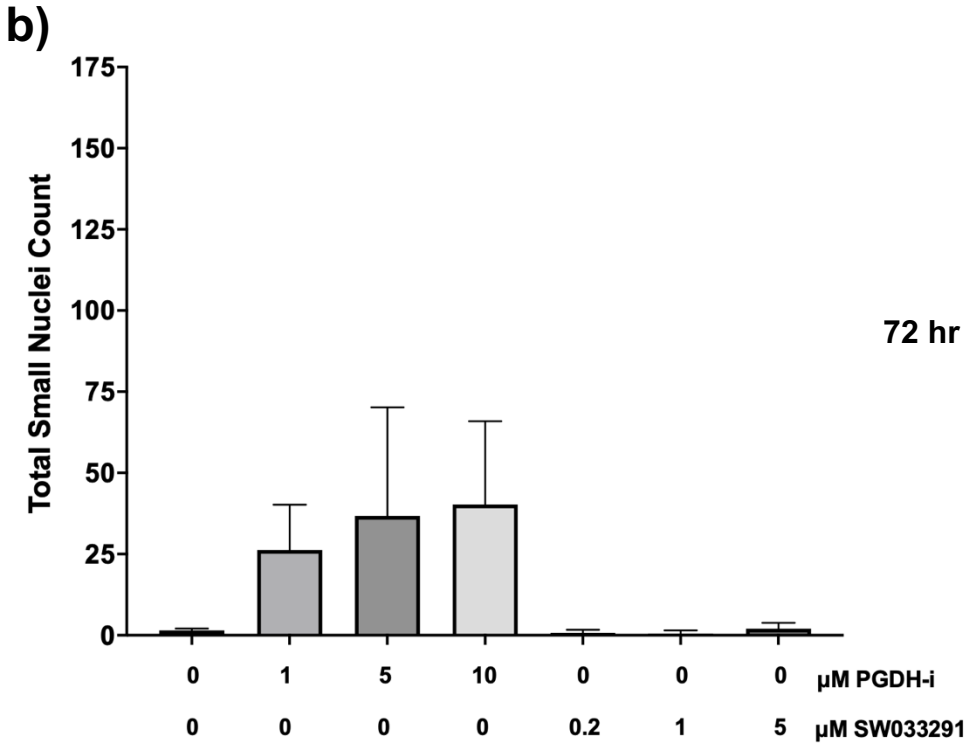
b)
Total Small Nuclei Count
175
150
125
100
75
50
25
0
72 hr
0 1 5 10 0 0 0 µM PGDH-i
0 0 0 0 0.2 1 5 µM SW033291

Figure 3.11. Effect of PGDH inhibition on small nuclei number

NHU cells (Y929A) were differentiated following the ABS/Ca^{2+} method on glass slides and fixed A) 48 and B) 72 hours after treatment with 1-10 μM PGDH-inhibitor or 0.2-5 μM SW033291. Total number of intensely bright, Hoechst 33258 stained, small nuclei (±SD) were counted in 4 fields of view (technical replicates).

MCM2 expression was confined to large NHU nuclei, no expression was observed in the small nuclei population. At 48 hours, incubation with 0.2 and 1 μM SW033291 appeared to increase the MCM2 positivity which persisted at 72 hours with incubation with 10 μM PGDH-i also appearing to increase MCM2 positivity at 72 hours (**Figure 3.12a-b**). However, representative images illustrate the distribution of MCM2 positive cells in inhibitor treated cultures is not randomly distributed, appearing in patches, causing difficulty in reflecting this statistically (**Figure 3.12c**). ZO-3 was included as a marker of urothelial differentiation (**Figure 3.12d**). MCM2 positivity was unchanged by 1 μM PGDH-i at both 48 and 72 hours but an increase to 5 μM visually increased the appearance of clusters of MCM2 positive nuclei and was chosen as the optimum concentration. 0.2 and 1 μM SW033291 increased the appearance of MCM2 positive nuclei clusters, however, as incubation with 0.2 μM reduced the total nuclei count at 48 hours, 1 μM was chosen as the optimum concentration. Representative images of MCM2 and ZO-3 immunolocalisation for chosen optimum concentrations of both PGDH-inhibitors are shown in figure 3.12c-d. Representative images for MCM2 and ZO-3 immunolocalisation for non-optimum concentrations are detailed in Appendix 3.

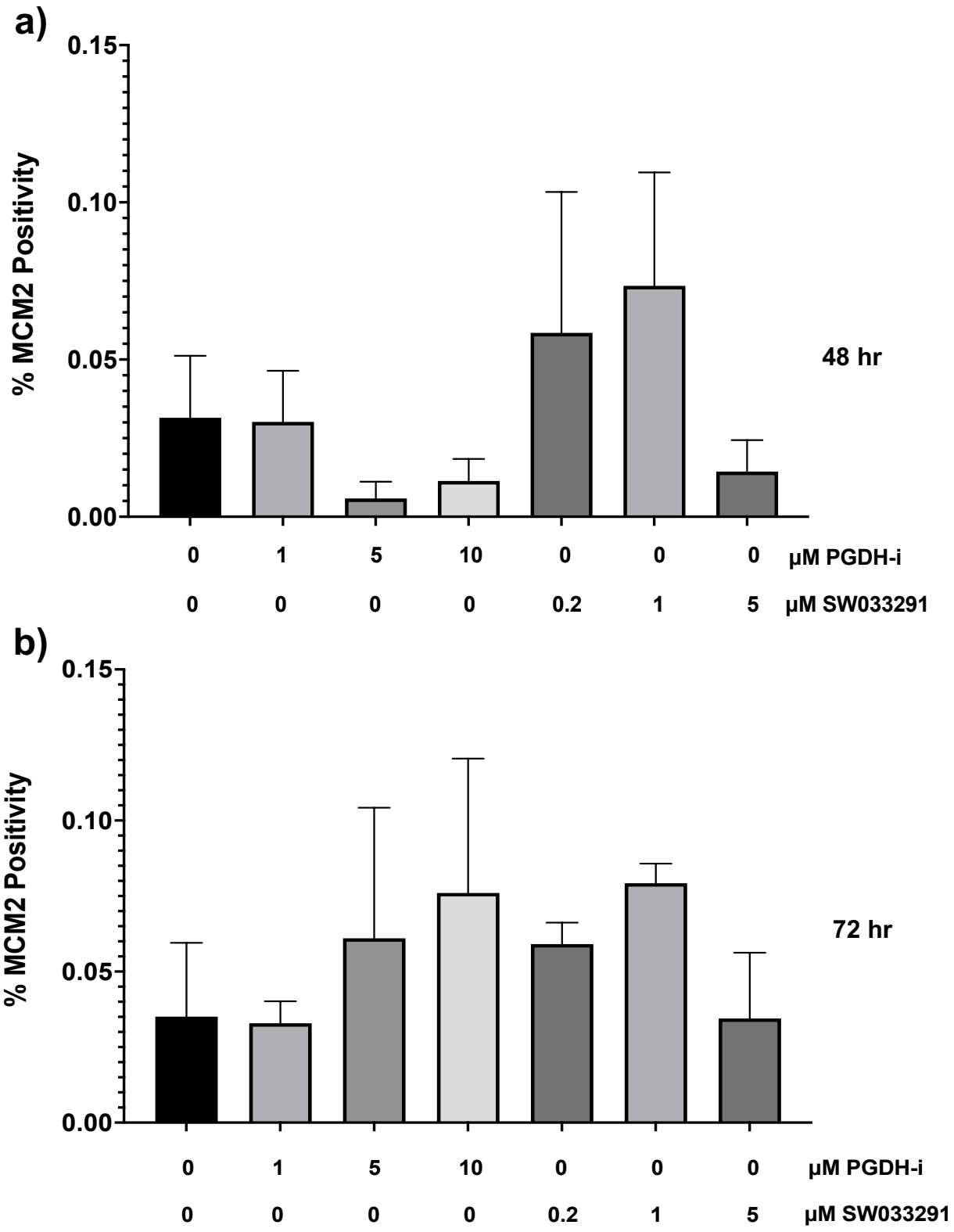
a)
% MCM2 Positivity
0.15
0.10
0.05
0.00
48 hr
0 1 5 10 0 0 0 µM PGDH-i
0 0 0 0 0.2 1 5 µM SW033291
b)
% MCM2 Positivity
0.15
0.10
0.05
0.00
72 hr
0 1 5 10 0 0 0 µM PGDH-i
0 0 0 0 0.2 1 5 µM SW033291

c)

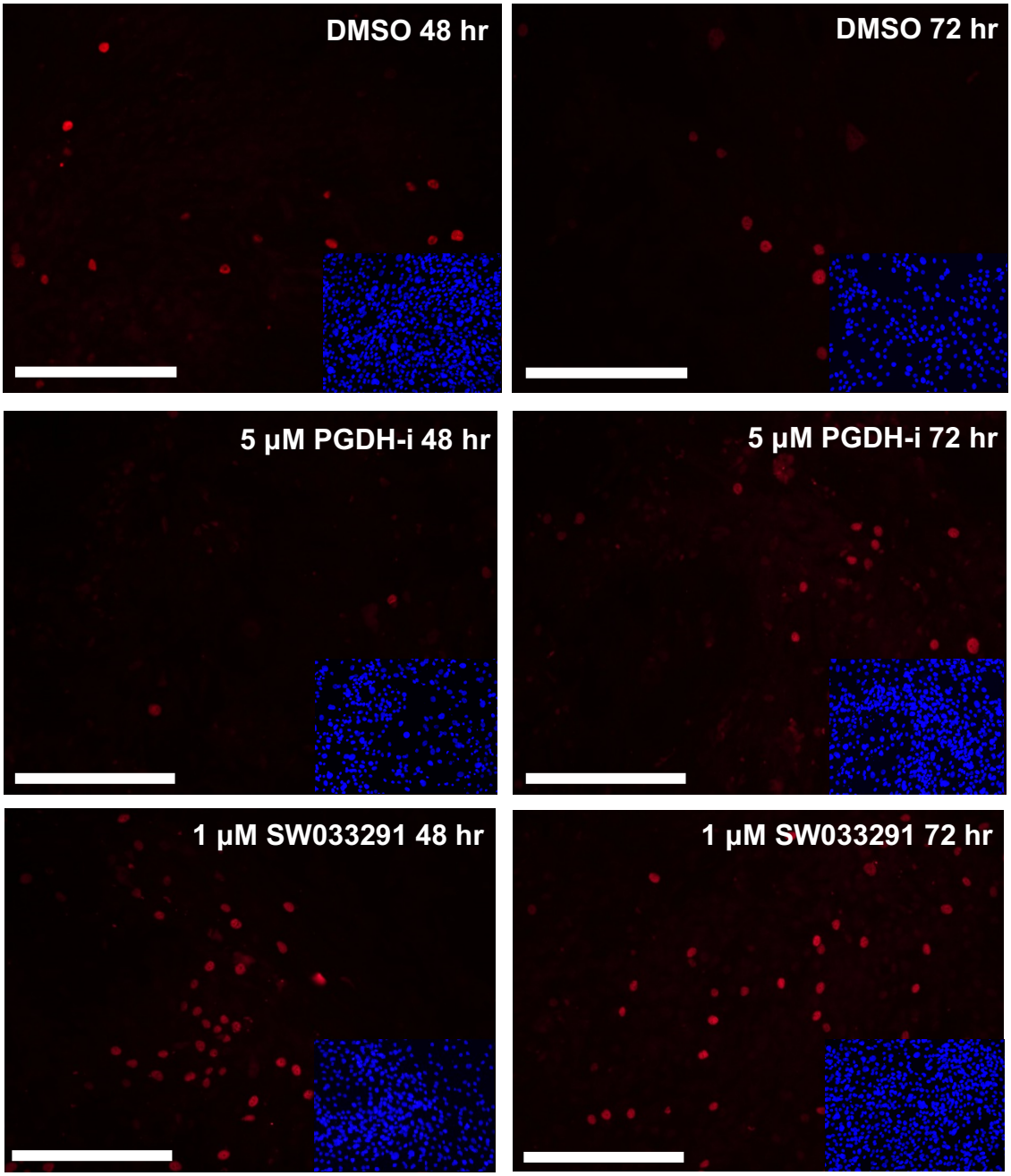
DMSO 48 hr
DMSO 72 hr
5 µM PGDH-i 48 hr
5 µM PGDH-i 72 hr
1 µM SW033291 48 hr
1 µM SW033291 72 hr

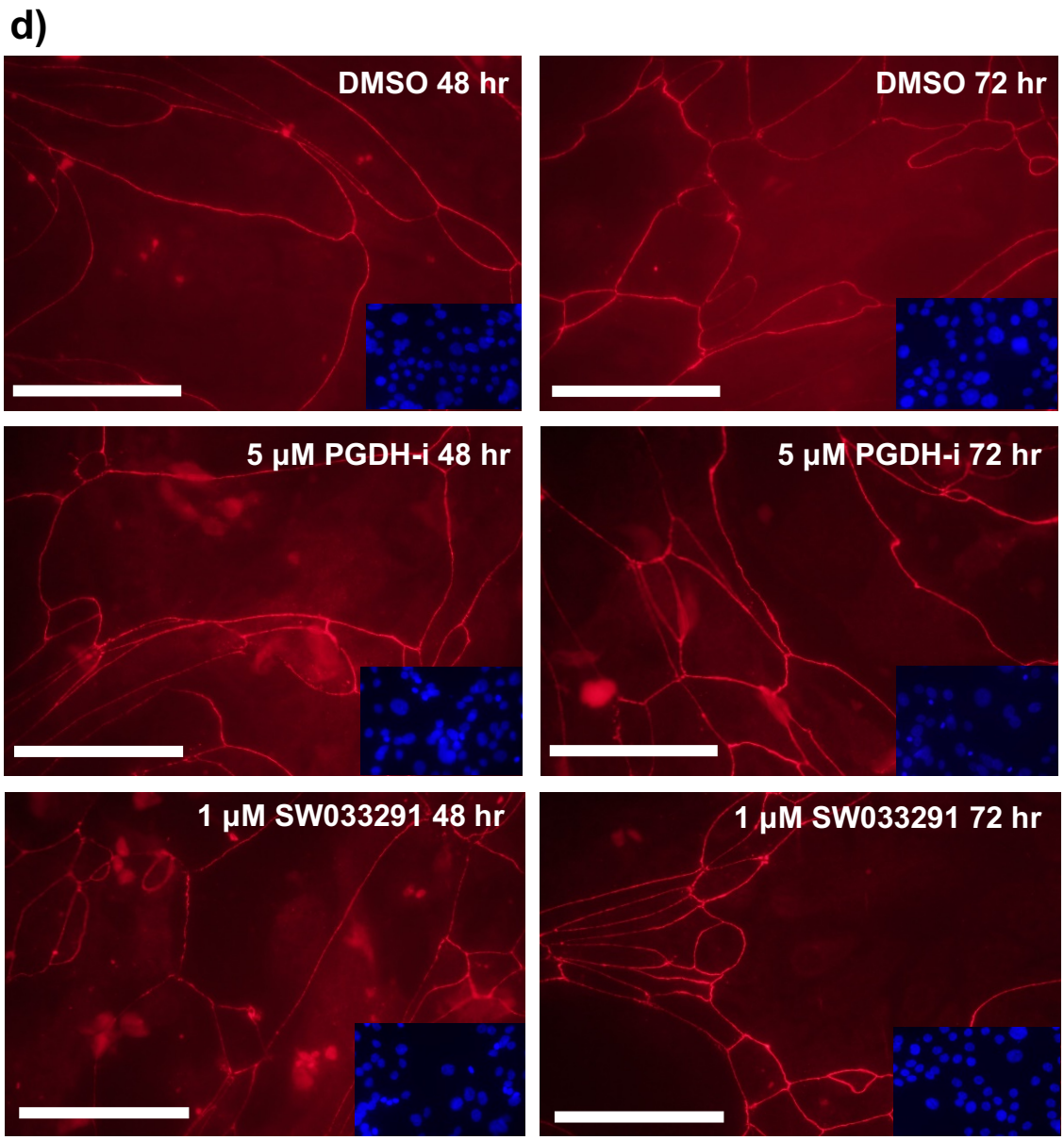

Figure 3.12. Effect of PGDH inhibition on cell cycle entry

NHU cells (Y929A) were differentiated following the ABS/Ca^{2+} method on glass slides and fixed a) 48 and b) 72 hours after treatment with 1-10 µM PGDH-inhibitor or 0.2-5 µM SW033291. Mean percentage of MCM2 positive cells (±SD) was calculated of 4 technical repeats. Representative images of c) MCM2 positive NHU cells and d) ZO-3 staining after treatment with chosen optimum concentration 5 µM PGDH-inhibitor or 1 µM SW033291 after 48 and 72 hours. DNA stained with Hoechst 33258 (*blue*) displayed in bottom left corner. Scale bar = 200 µm for MCM2; Scale bar = 40 µm for ZO-3.

3.4.5 Effect of PGDH inhibition on barrier recovery during urothelial wound repair

NHU cells differentiated by the ABS/Ca^{2+} method on Greiner membranes, as described in section 2.3.5, were used to monitor urothelial barrier recovery post scratch-wounding with TER measurements taken immediately prior to and after wounding with subsequent measurements taken continuously during repair. TER was also measured during the 12-hour incubation with PGDH inhibitors prior to scratching to assess the effect of PGDH inhibition on stable barrier. In NHU cultures differentiated +CT, no effect of PGDH inhibition on stable barrier was observed with no difference in TER after 12 hours compared to the DMSO control ($p = 0.48$) (**Figure 3.13a**). In NHU cultures differentiated -CT, incubation with $dmPGE_2$ ($p = 0.011$) or SW033291 ($p = 0.0014$) significantly reduced the TER compared to DMSO control after 12 hours (**Figure 3.13b**). Incubation with PGDH-i had no effect on TER after 12 hours compared to the DMSO control ($p = 0.87$).

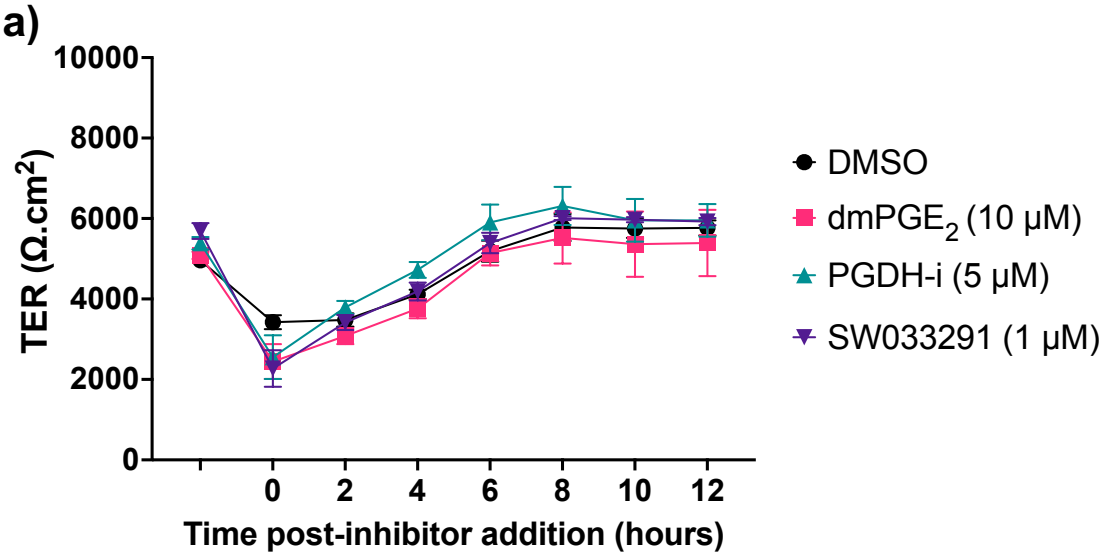

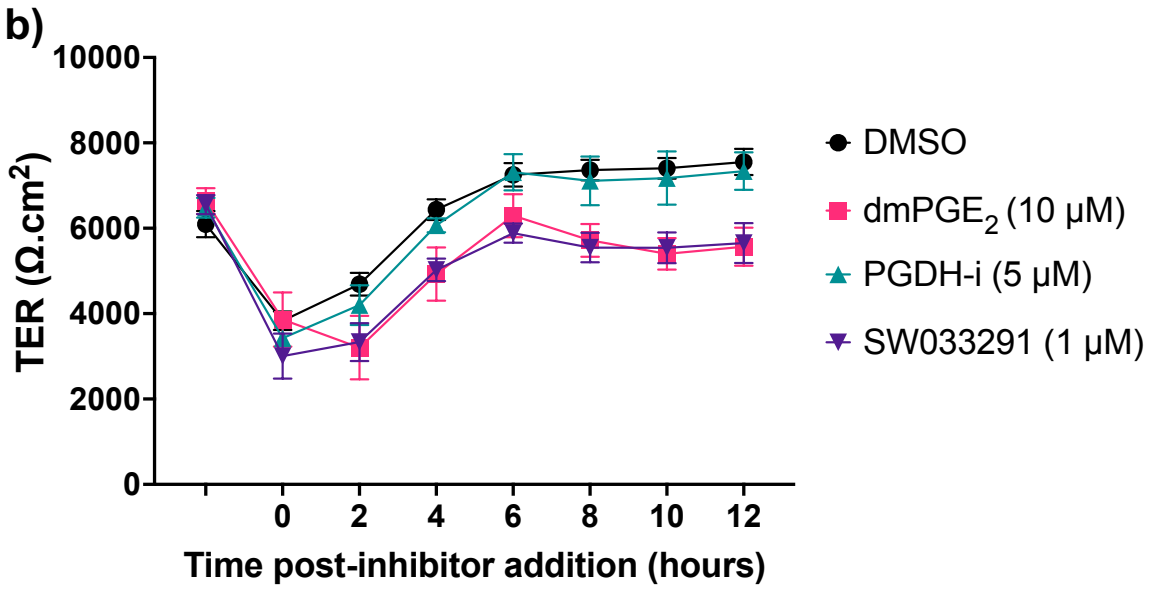

Figure 3.13. Effect of PGDH inhibition on stable barrier in differentiated NHU cultures

NHU cells (Y2860) were differentiated following the ABS/Ca^{2+} method on Greiner membranes to measure the trans-epithelial electrical resistance (TER) by cellZscope® equipment. Cultures were pre-treated for 12 hours with 10 μM $dmPGE_2$, 5 μM PGDH-i or 1 μM SW033291 in a) the presence and b) the absence of cholera toxin. Incubation with $dmPGE_2$ and SW033291 reduced the TER compared to the DMSO control. TER is plotted as mean (± SD) (n=3).

In NHU cultures differentiated +CT, mean TER prior to scratching of DMSO treated cultures was 5679 $\Omega.cm^2$ (± SD = 184), $dmPGE_2$ treated cultures was 5391 $\Omega.cm^2$ (± SD = 823), PGDH-i treated cultures was 5956 $\Omega.cm^2$ (± SD = 405) and SW033291 treated cultures was 5925 $\Omega.cm^2$ (± SD = 89) (**Figure 3.14a**). Barrier recovery in the DMSO control took ~24 hours before plateauing and stabilising. The rate of barrier recovery was calculated between the initial scratch and 24

hours, the point at which the TER begins to plateau and compared between DMSO and PGDH inhibitor treated cultures (**Figure 3.14b**). No significant difference was observed in the rate of barrier recovery between cultures treated with either of the PGDH inhibitors and the DMSO control ($p = 0.80$).

In NHU cultures differentiated -CT, mean TER of DMSO treated cultures was 7552 $\Omega.cm^2$ (± SD = 306), $dmPGE_2$ treated cultures was 5567 $\Omega.cm^2$ (± SD = 444), PGDH-i treated cultures was 7339 $\Omega.cm^2$ (± SD = 439) and SW033291 treated cultures was 5653 $\Omega.cm^2$ (± SD = 466) (**Figure 3.14c**). Barrier recovery in the DMSO control took ~20 hours before plateauing and stabilising. The rate of barrier recovery was calculated between the initial scratch and 20 hours, the point at which the TER begins to plateau and compared between DMSO and PGDH inhibitor treated cultures (**Figure 3.14d**). A significant reduction in barrier recovery post-scratch was observed in NHU cultures treated with PGDH-i ($p = 0.008$) or SW033291 ($p = 0.028$) compared to the DMSO control.

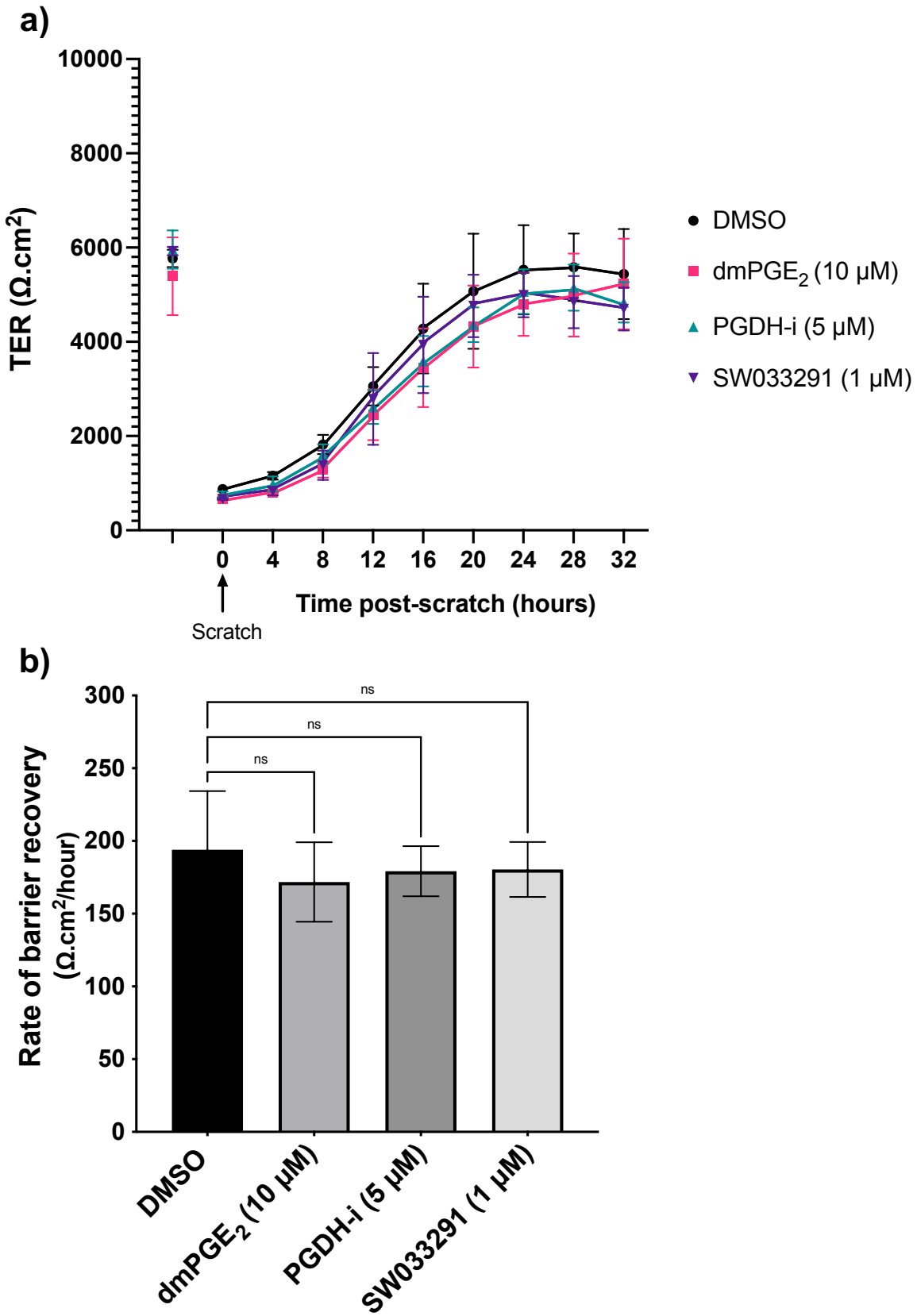
a)
10000
8000
6000
4000
2000
0
TER (Ω.cm²)
0
4
8
12
16
20
24
28
32
Time post-scratch (hours)
Scratch
DMSO
dmPGE2 (10 μM)
PGDH-i (5 μM)
SW033291 (1 μM)
b)
300
250
200
150
100
50
0
Rate of barrier recovery (Ω.cm²/hour)
ns
ns
ns
DMSO
dmPGE2 (10 μM)
PGDH-i (5 μM)
SW033291 (1 μM)

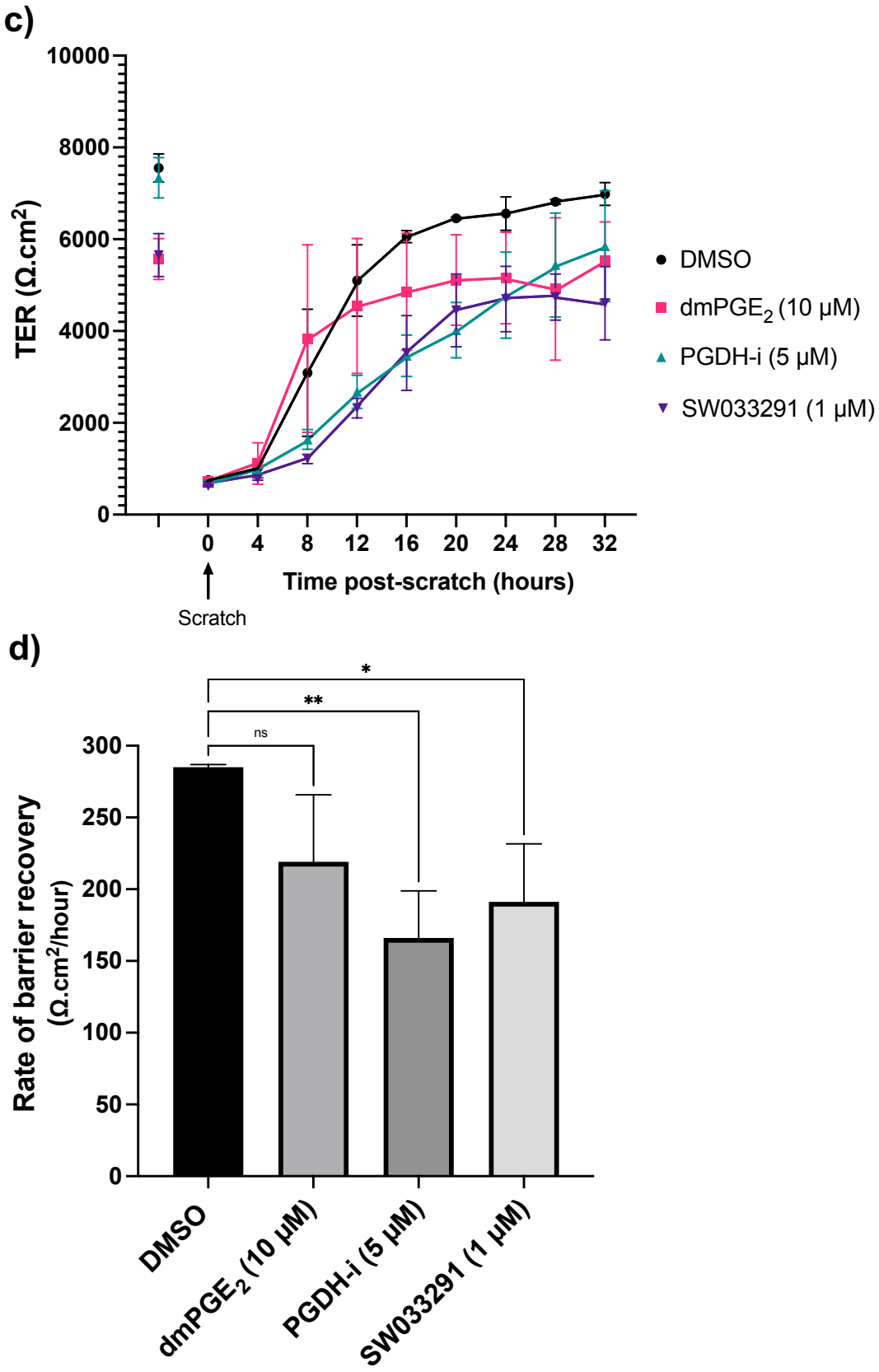
c)
10000
8000
6000
4000
2000
0
TER (Ω.cm²)
0
4
8
12
16
20
24
28
32
Time post-scratch (hours)
Scratch
DMSO
dmPGE2 (10 µM)
PGDH-i (5 µM)
SW033291 (1 µM)
d)
*
**
ns
300
250
200
150
100
50
0
Rate of barrier recovery
(Ω.cm²/hour)
DMSO
dmPGE2 (10 µM)
PGDH-i (5 µM)
SW033291 (1 µM)

Figure 3.14. Effect of PGDH inhibition on barrier recovery during wound repair in NHU cultures

NHU cells (Y2860) were differentiated following the ABS/Ca^{2+} method in a-b) the presence and c-d) the absence of cholera toxin on Greiner membranes to measure the trans-epithelial electrical resistance (TER) by cellZscope® equipment. Cultures were pre-treated for 12 hours with 10 µM $dmPGE_2$, 5 µM PGDH-i or 1 µM SW033291 and scratched with a sterile 200 µl pipette tip. a and c) Barrier recovery is plotted as mean (± SD) (n=3) at interval time points during wound repair. b and d) Rate of barrier recovery to plateau was calculated and expressed as mean (± SD) (n=3). Statistical analysis was by one-way ANOVA followed by Dunnett's post-test. * ≤ 0.05; ** ≤ 0.01.

3.4.6 Effect of PGDH inhibition on cellular proliferation and tight junctions during urothelial wound repair

NHU cells differentiated by the ABS/Ca^{2+} method on glass slides, as described in section 2.5.1, were used to investigate the effects of PGDH inhibition on markers of cell cycle activity and on the composition of tight junction proteins during urothelial wound repair. Analysis of unwounded control cultures demonstrated very few cells incorporated EdU or express MCM2 at 48 or 72 hours suggestive of mitotically quiescent cultures (**Figure 3.15a-b**). Similarly, at 48 hours post-scratch, few to no cells incorporated EdU or expressed MCM2 but at 72 hours this was increased suggesting cells begin to proliferate 72 hours after scratch wounding.

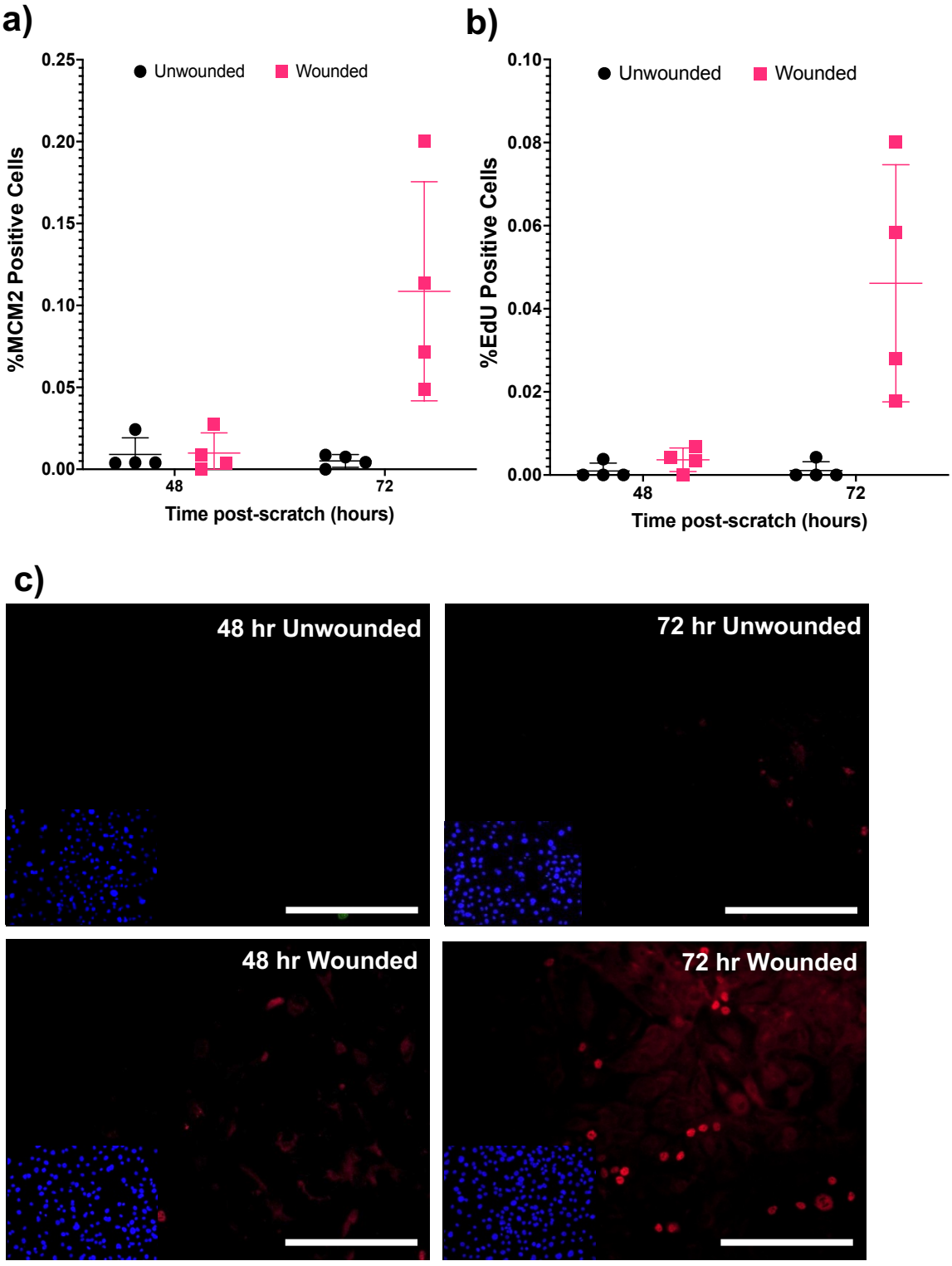
a)
b)
c)
Unwounded
Wounded
%MCM2 Positive Cells
%EdU Positive Cells
Time post-scratch (hours)
0.25
0.20
0.15
0.10
0.05
0.00
0.08
0.06
0.04
0.02
48
72
48 hr Unwounded
72 hr Unwounded
48 hr Wounded
72 hr Wounded

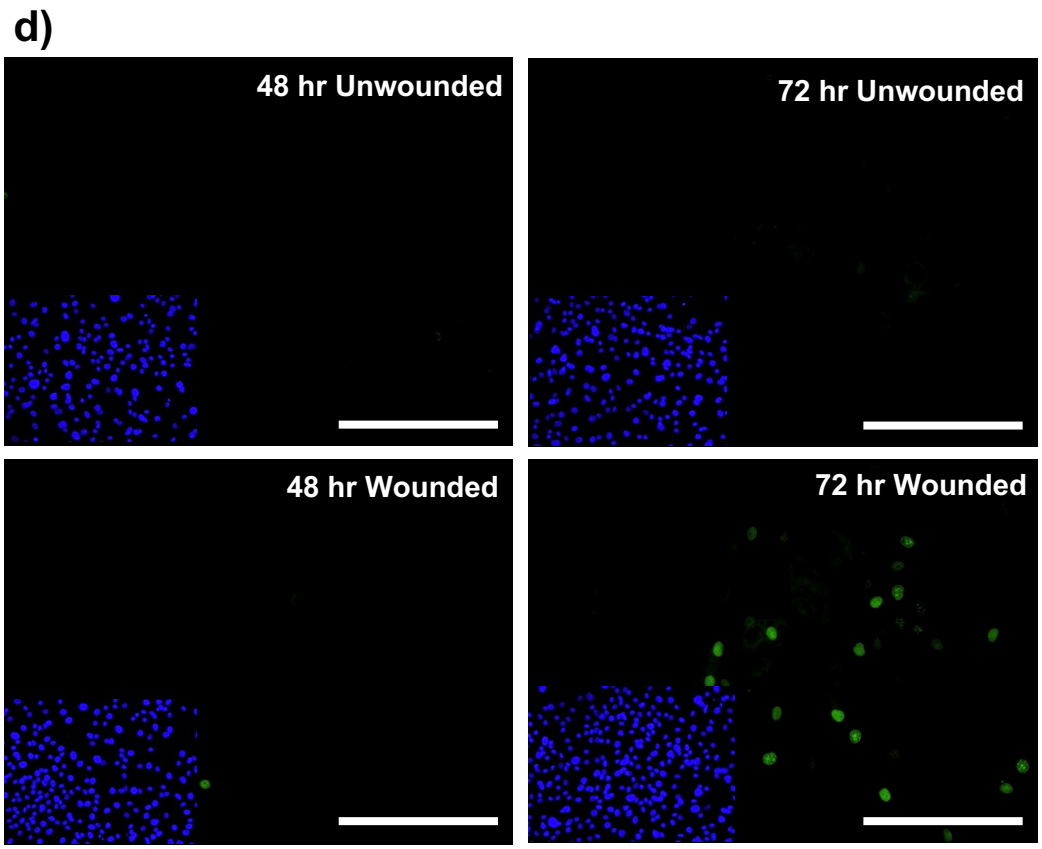

Figure 3.15. Effect of scratch wounding on cell cycle activity

NHU cells (Y2089) were differentiated following the ABS/Ca^{2+} method on glass slides and fixed 48 and 72 hours after scratch wounding with a 200 µl sterile pipette tip. The mean percentage of a) MCM2 positive and b) EdU positive cells (± SD) was calculated for four fields of view (technical replicates). Representative images of c) MCM2 and d) EdU positive nuclei in wounded and unwounded cultures after 48 and 72 hours. DNA stained with Hoechst 33258 (*blue*) displayed in bottom left corner. Scale bar = 200 µm.

Analysis of MCM2 positivity in unwounded cultures after 48 hours demonstrated incubation with $dmPGE_2$, PGDH-i and SW033291 appeared to increase the percentage of cells expressing MCM2 (**Figure 3.16a**). EdU incorporation after 48 hours appeared elevated in cultures incubated with $dmPGE_2$ and PGDH-i compared to the DMSO control, but not in cultures incubated with SW033291 to the same extent (**Figure 3.16b**).

Analysis of MCM2 positivity in unwounded cultures after 72 hours demonstrated incubation with SW033291 or PGDH-i increased the percentage of cells expressing MCM2, but not in cultures incubated with $dmPGE_2$ (**Figure 3.16c**). EdU incorporation after 72 hours was higher in cultures incubated with SW033291, but cultures incubated with dmPGE2 and PGDH-i did not display as large an increase (**Figure 3.16d**).

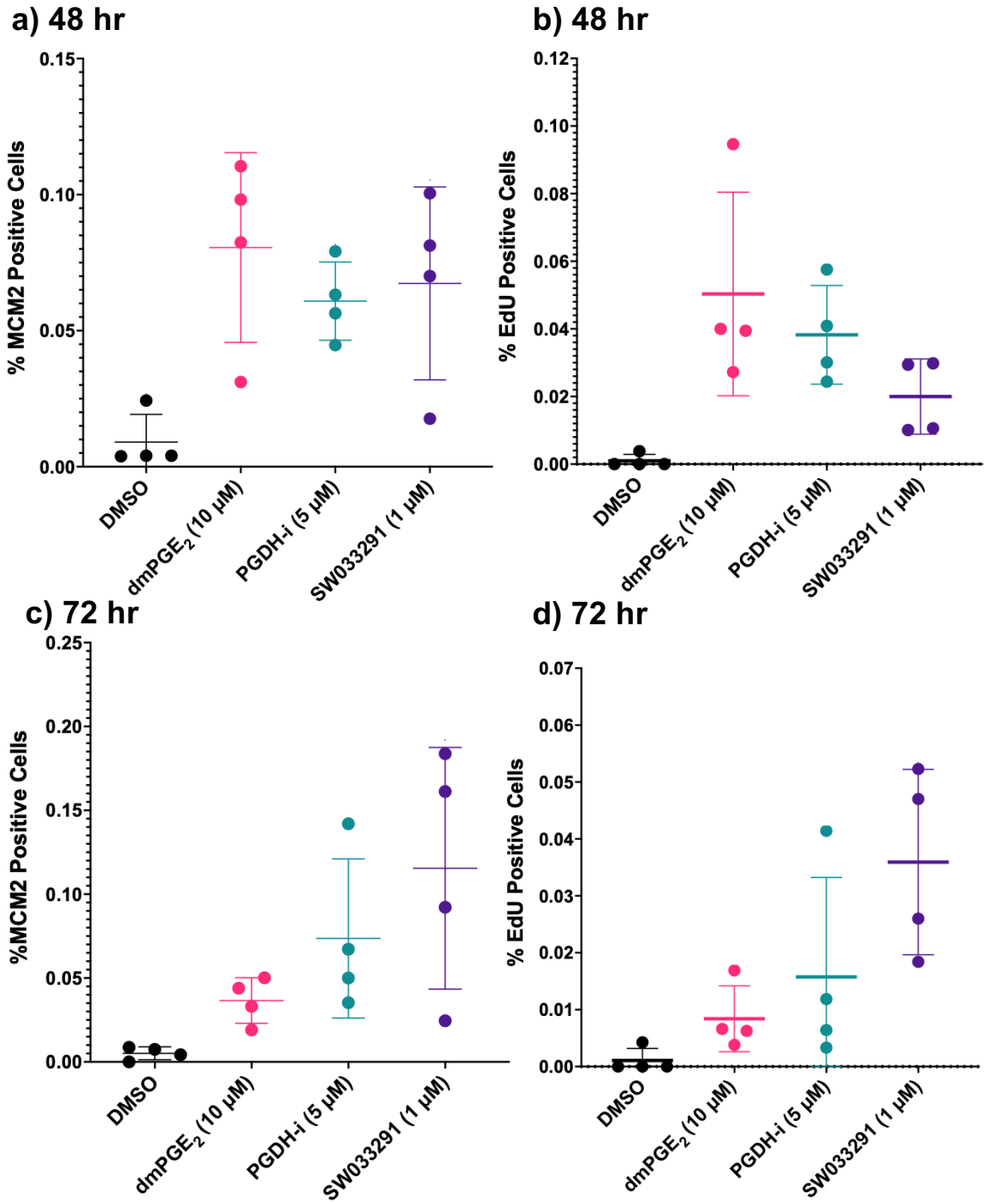

e)

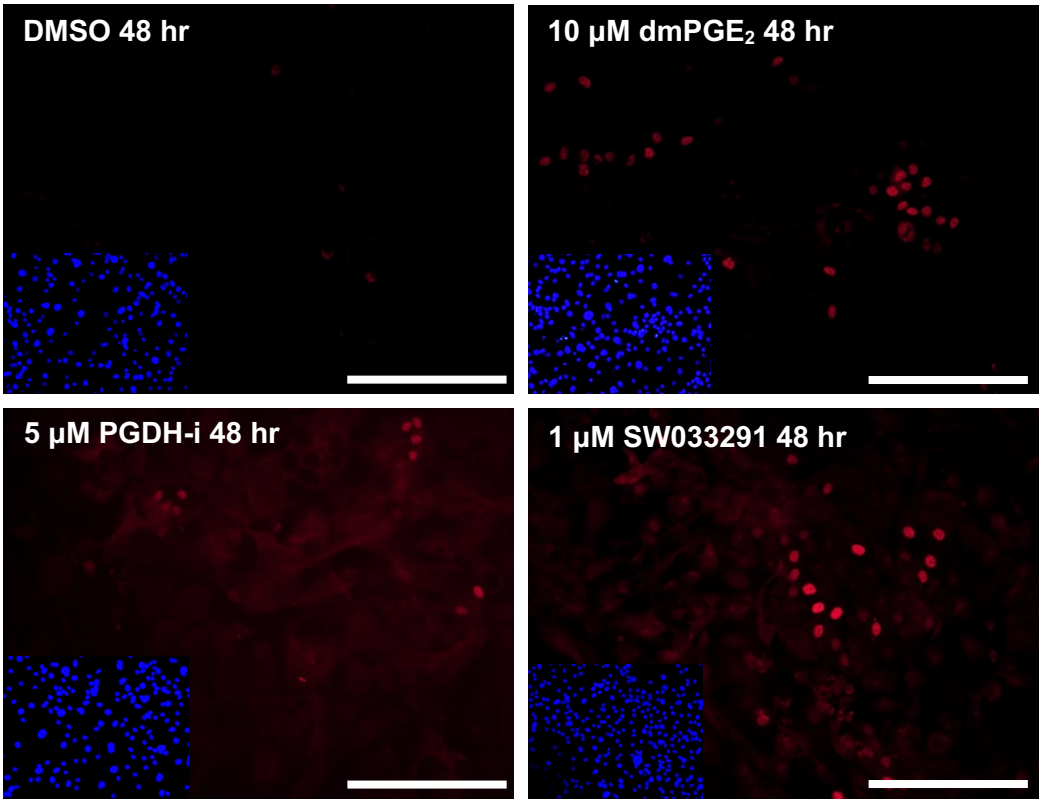
DMSO 48 hr
10 μM dmPGE2 48 hr
5 μM PGDH-i 48 hr
1 μM SW033291 48 hr

f)

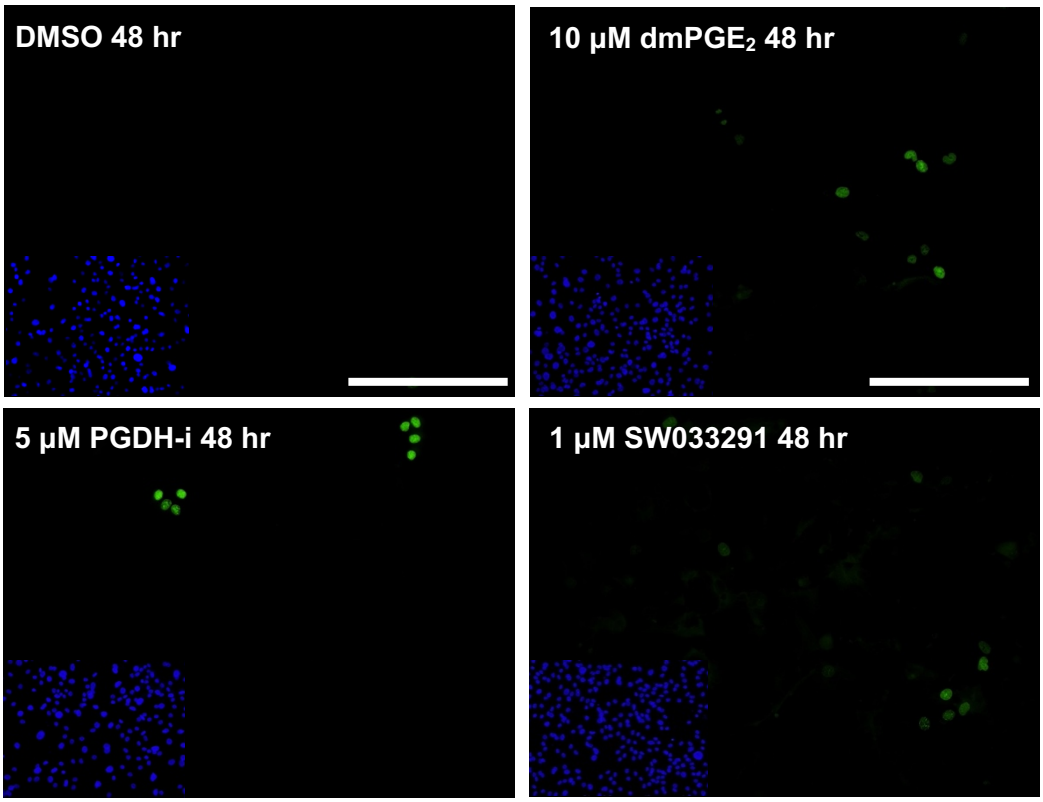
DMSO 48 hr
10 μM dmPGE2 48 hr
5 μM PGDH-i 48 hr
1 μM SW033291 48 hr

g)

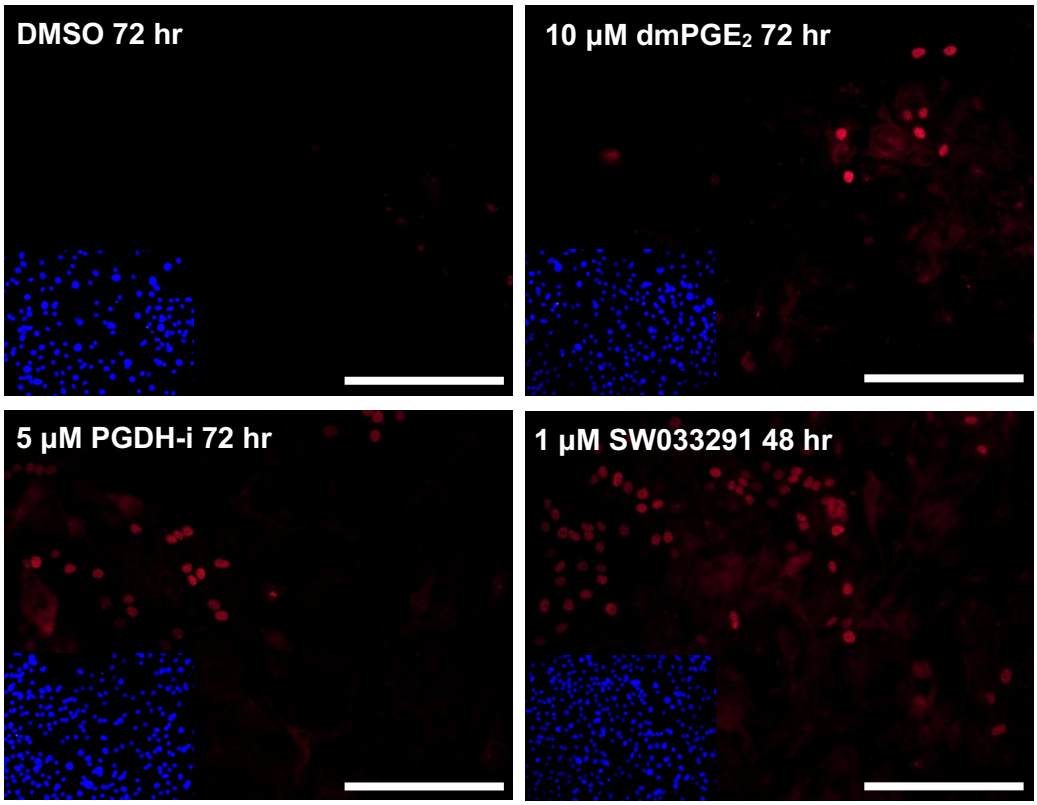
DMSO 72 hr
10 μM dmPGE2 72 hr
5 μM PGDH-i 72 hr
1 μM SW033291 48 hr

h)

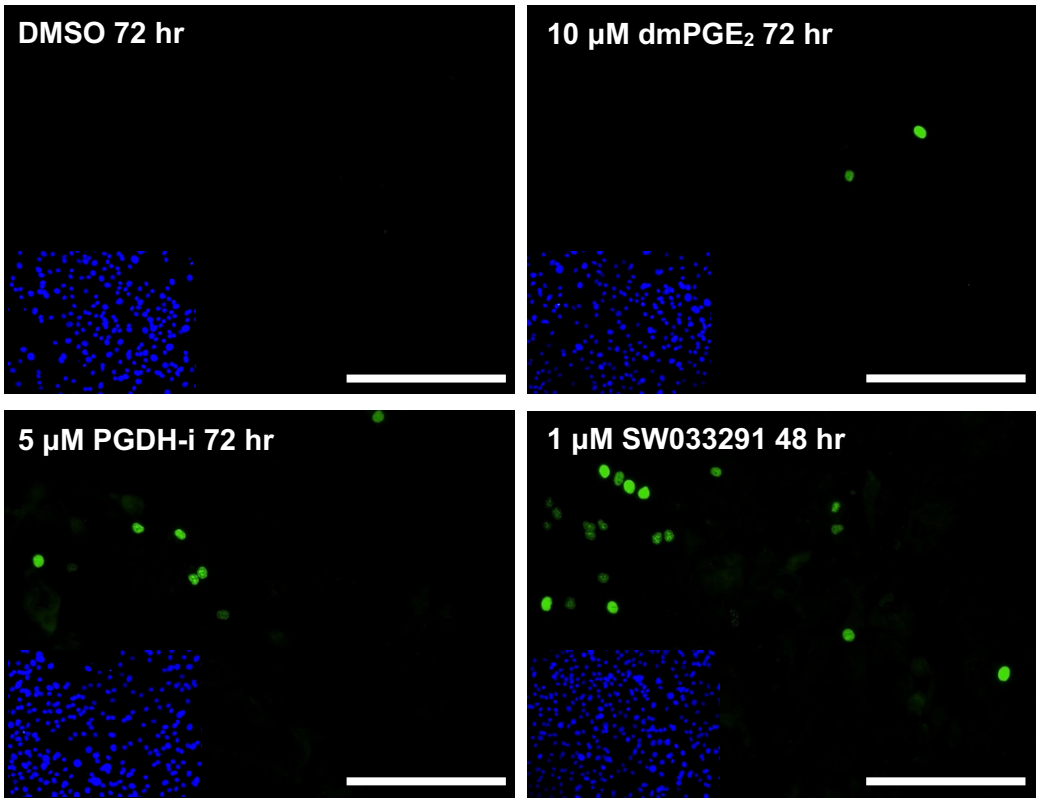
DMSO 72 hr
10 μM dmPGE2 72 hr
5 μM PGDH-i 72 hr
1 μM SW033291 48 hr

Figure 3.16. Effect of PGDH inhibition on cell cycle activity in unwounded NHU cultures

NHU cells (Y2089) were differentiated following the ABS/Ca^{2+} method on glass slides and pre-treated with 10 μM $dmPGE_2$, 5 μM PGDH-i or 1 μM SW033291. Slides were fixed after 48 hours with a) MCM2 positive and b) EdU positive cells quantified or after 72 hours with c) MCM2 positive and d) EdU positive cells quantified. The mean MCM2 and EdU positive nuclei (± SD) was calculated for four fields of view (technical repeats). e-h) Representative images of MCM2 and EdU positive nuclei after 48 and 72 hours. DNA stained with Hoechst 33258 (*blue*) displayed in bottom left corner. Scale bar = 200 μm.

In wounded cultures, 48 hours post-scratch, the percentage of MCM2 positive cells was appeared increased in cultures incubated with SW033291 and PGDH-i compared to the DMSO control, but not in cultured incubated with $dmPGE_2$ (**Figure 3.17a**). Similarly, EdU incorporation appeared increased in cultures incubated with SW033291 and PGDH-i compared to the DMSO control, but not in cultures incubated with $dmPGE_2$ (**Figure 3.17b**). 72 hours post-scratch, no large differences in MCM2 positivity or EdU incorporation were observed between cultures treated with either of the PGDH inhibitors and the DMSO control (**Figure 3.17c-d**).

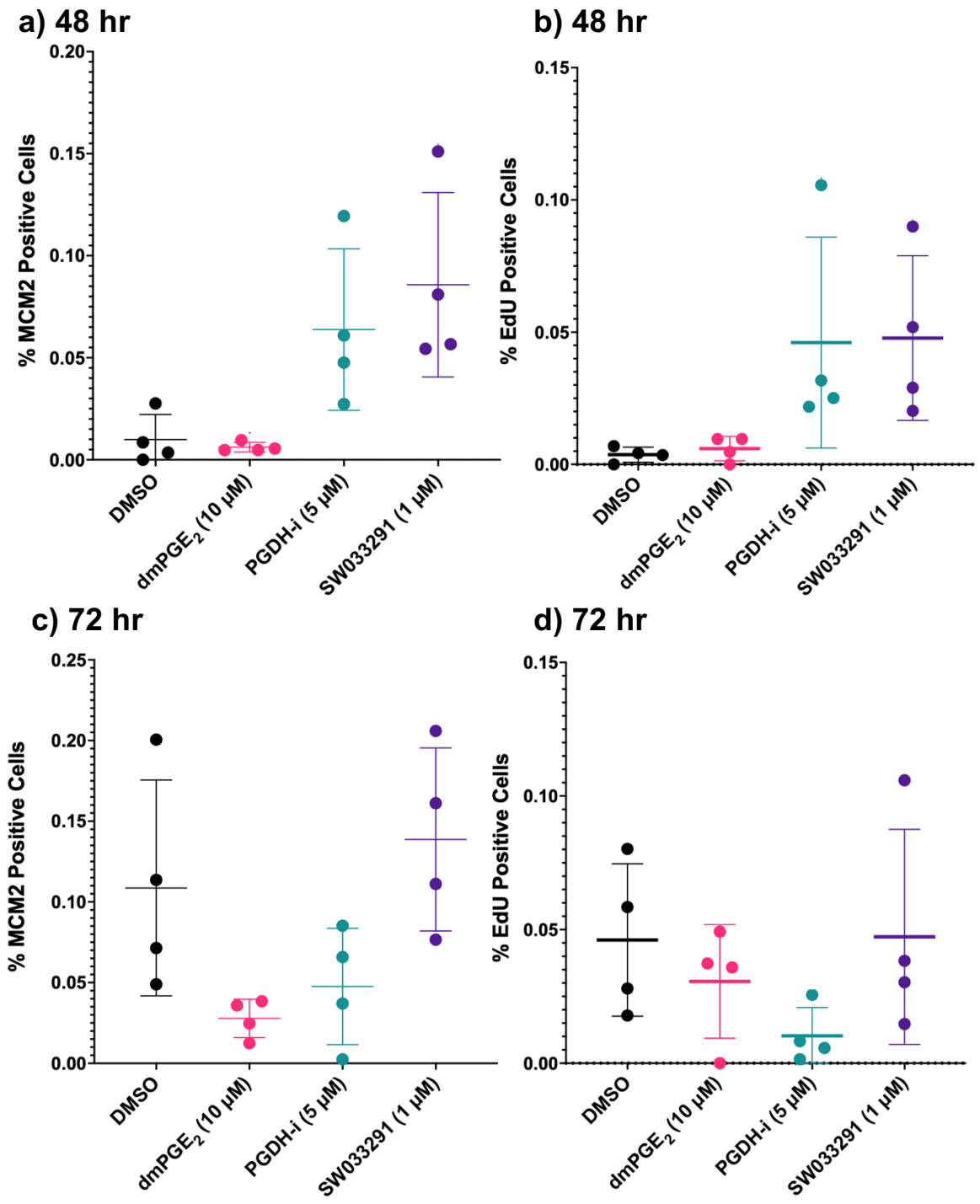
a) 48 hr
% MCM2 Positive Cells
0.20
0.15
0.10
0.05
0.00
DMSO
dmPGE2 (10 μM)
PGDH-i (5 μM)
SW033291 (1 μM)
b) 48 hr
% EdU Positive Cells
0.15
0.10
0.05
0.00
DMSO
dmPGE2 (10 μM)
PGDH-i (5 μM)
SW033291 (1 μM)
c) 72 hr
% MCM2 Positive Cells
0.25
0.20
0.15
0.10
0.05
0.00
DMSO
dmPGE2 (10 μM)
PGDH-i (5 μM)
SW033291 (1 μM)
d) 72 hr
% EdU Positive Cells
0.15
0.10
0.05
0.00
DMSO
dmPGE2 (10 μM)
PGDH-i (5 μM)
SW033291 (1 μM)

e)

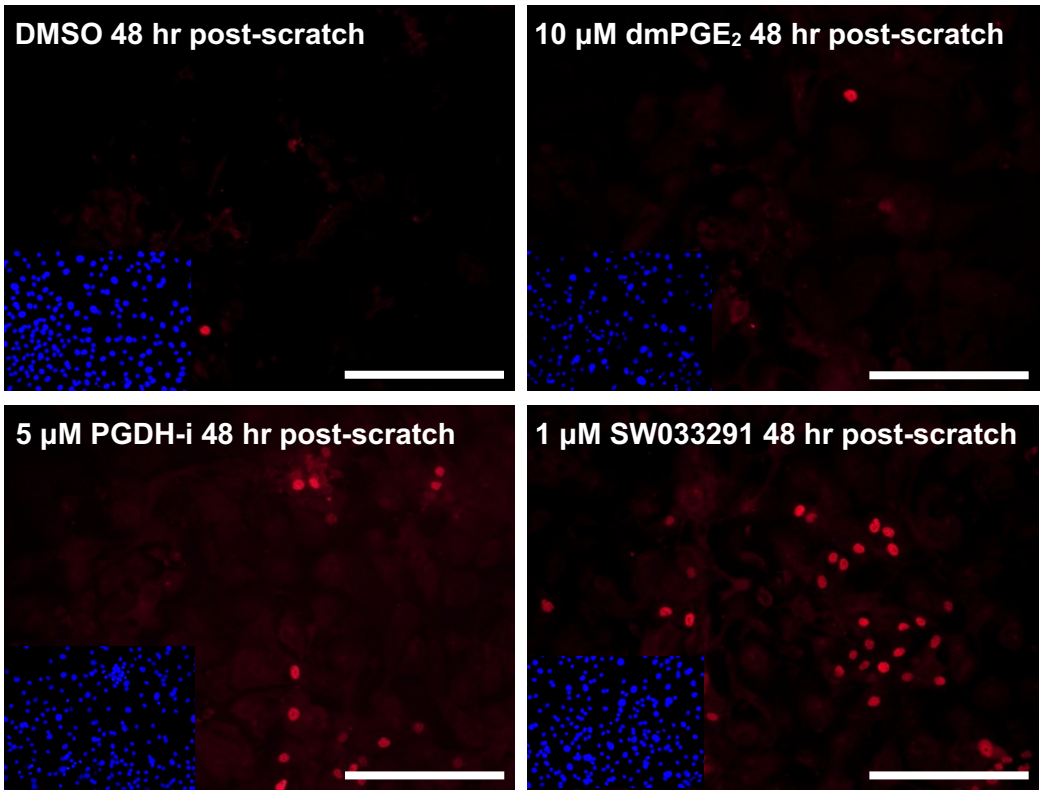
DMSO 48 hr post-scratch
10 μM dmPGE2 48 hr post-scratch
5 μM PGDH-i 48 hr post-scratch
1 μM SW033291 48 hr post-scratch

f)

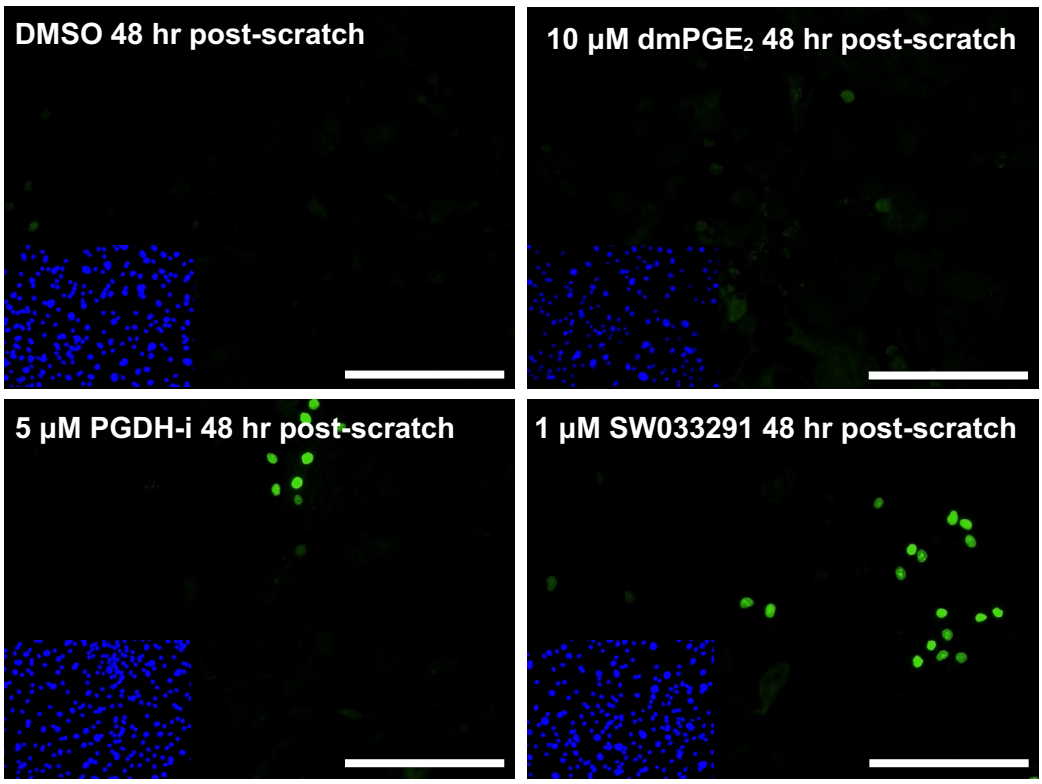
DMSO 48 hr post-scratch
10 μM dmPGE2 48 hr post-scratch
5 μM PGDH-i 48 hr post-scratch
1 μM SW033291 48 hr post-scratch

g)

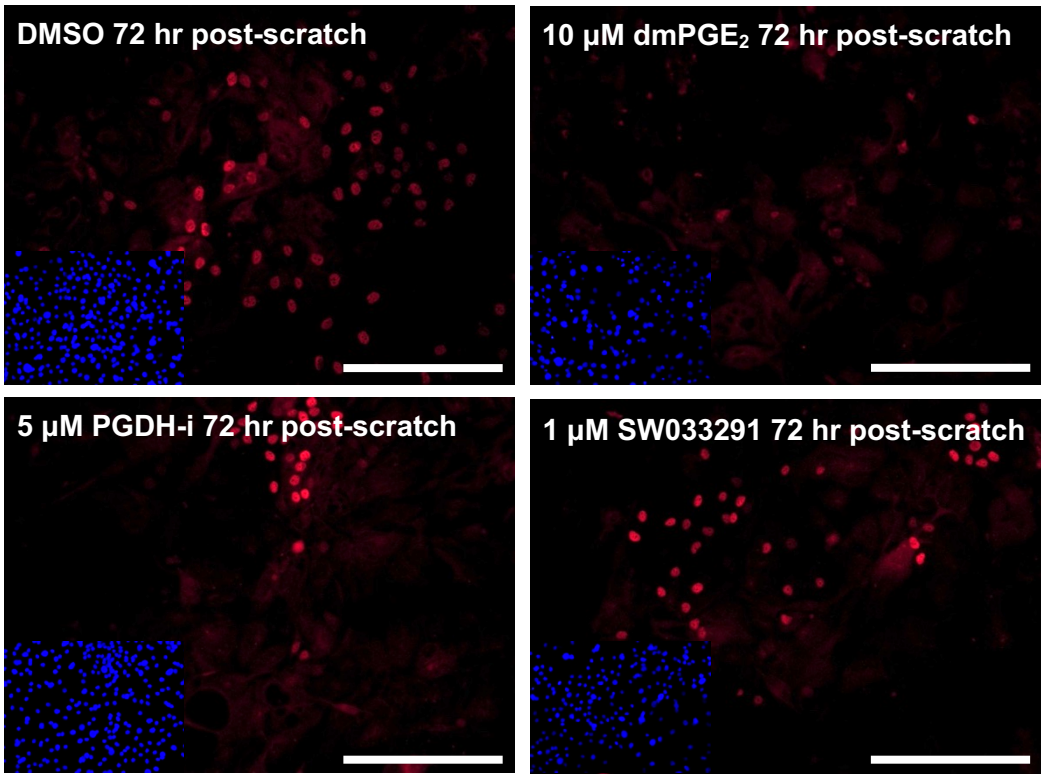
DMSO 72 hr post-scratch
10 μM dmPGE2 72 hr post-scratch
5 μM PGDH-i 72 hr post-scratch
1 μM SW033291 72 hr post-scratch

h)

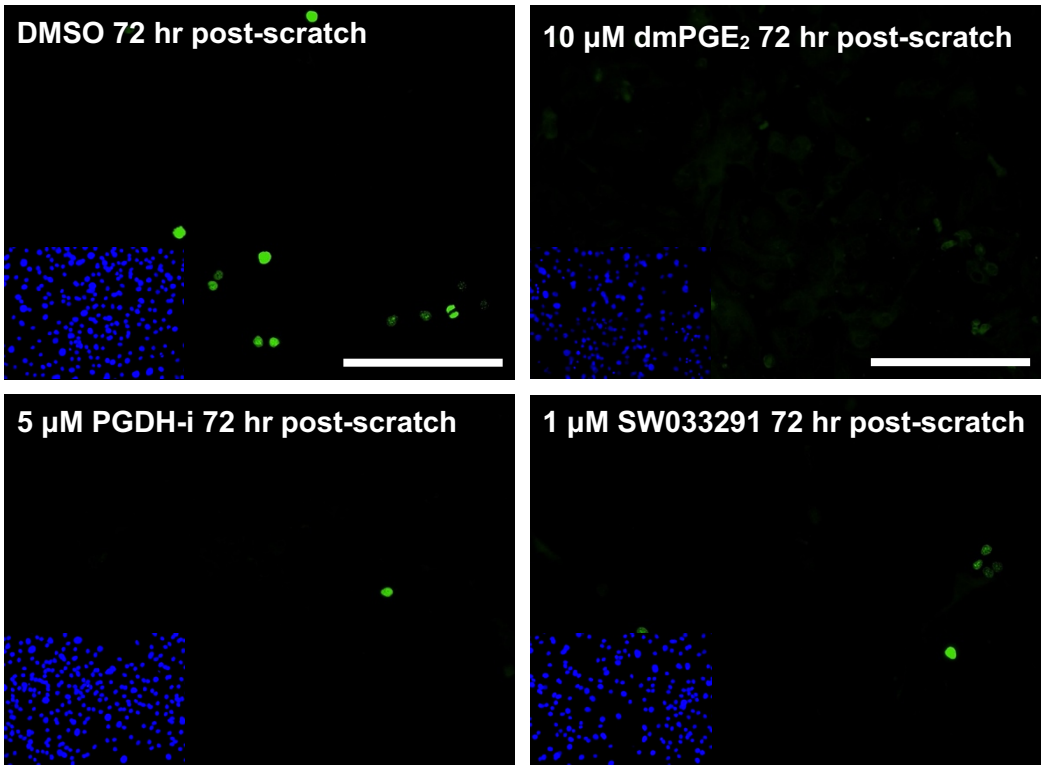
DMSO 72 hr post-scratch
10 μM dmPGE2 72 hr post-scratch
5 μM PGDH-i 72 hr post-scratch
1 μM SW033291 72 hr post-scratch

Figure 3.17. Effect of PGDH inhibition on cell cycle activity during wound repair

NHU cells (Y2089) were differentiated following the ABS/Ca^{2+} method on glass slides and pre-treated with 10 μM $dmPGE_2$, 5 μM PGDH-i or 1 μM SW033291 and scratched with a 200 μl sterile pipette tip. Slides were fixed 48 hours post-scratch with a) MCM2 positive and b) EdU positive cells quantified or 72 hours post-scratch with c) MCM2 positive and d) EdU positive cells quantified. The mean MCM2 and EdU positive nuclei (± SD) was calculated for four fields of view (technical repeats). e-h) Representative images of MCM2 and EdU positive nuclei at 48- and 72-hours post-scratch. DNA stained with Hoechst 33258 (*blue*) displayed in bottom left corner. Scale bar = 200 μm.

ZO-3 staining was used to confirm urothelial differentiation and was imaged after 72 hours in unwounded NHU cultures. ZO-3 was present at cell-to-cell contacts in the DMSO control and in $dmPGE_2$-treated culture (**Figure 3.18**). Cultures incubated with PGDH-i had areas of absent ZO-3 staining and regions where it was present, the labelling was weak. Cultures incubated with SW033291 had weak ZO-3 labelling.

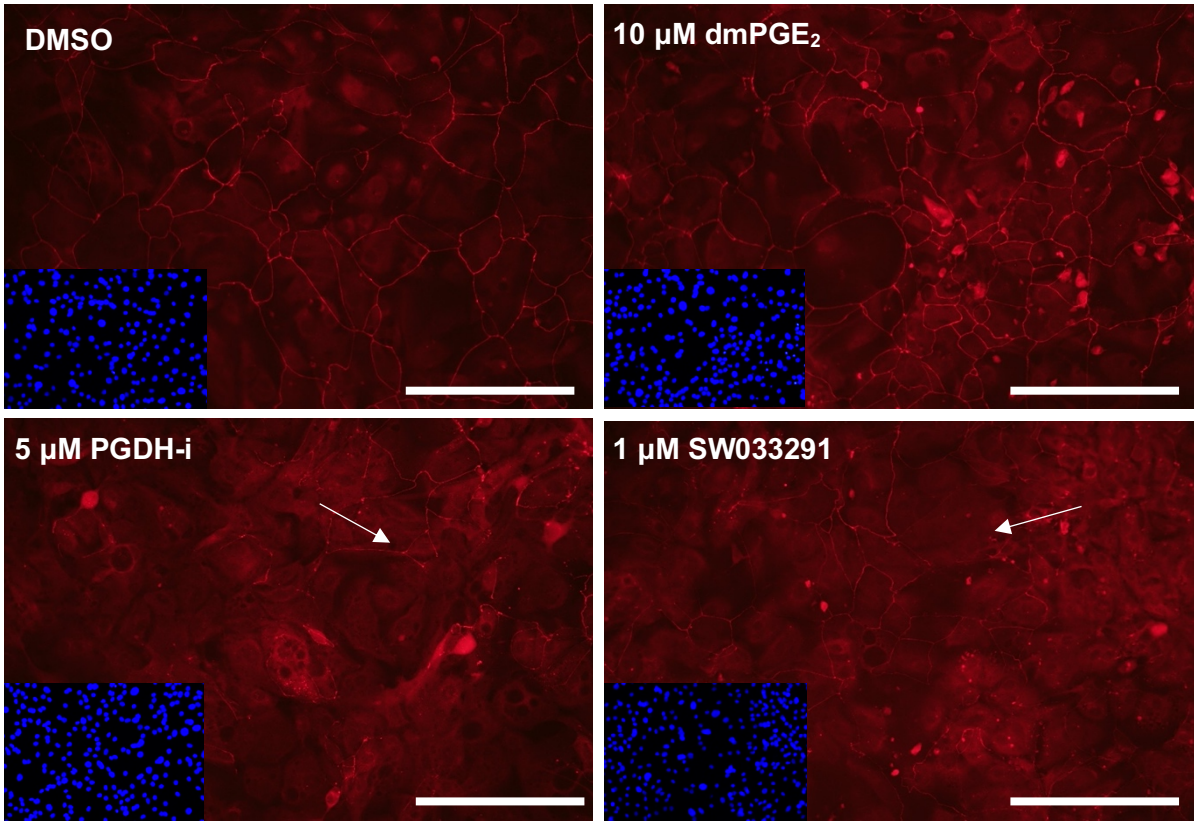

Figure 3.18. Effect of PGDH inhibition on localisation of ZO-3

NHU cells (Y2089) were differentiated following the ABS/Ca^{2+} method on glass slides and pre-treated with 10 µM $dmPGE_2$, 5 µM PGDH-i or 1 µM SW033291. Slides were fixed after 72 hours and labelled for ZO-3. Cultures incubated with PGDI-i and SW033291 has weaker ZO-3 labelling (*white arrows*) compared to the DMSO control and $dmPGE_2$-treated culture. DNA stained with Hoechst 33258 (*blue*) displayed in bottom left corner. Scale bar = 200 µm.

3.5 Discussion

3.5.1 Key findings

The findings of this chapter demonstrate a urothelial differentiation-association for several of the components comprising the PGE_2 metabolic pathway and

importantly, suggest a role for PGDH in maintaining mitotic quiescence, a key characteristic of human urothelium *in situ*. It is important to note the experiments in this chapter have been carried out in a single NHU cell line (derived from a single individual) and interpretation is made with caution. This limitation would need to be addressed in subsequent studies to provide more biological significance.

3.5.2 Expression of PGE_2 metabolic pathway genes in human urothelium

The RNAseq analysis presented in this chapter revealed expression of genes encoding the canonical PGE_2 metabolic pathway by NHU cells *in vitro*. Whilst several genes (*PTGS2*, *PTGES2*, *PTGR1*, *PTGR2*) were expressed in both undifferentiated and ABS/Ca^{2+} differentiated states, others (*PTGES*, *PTGER4*, *HPGD*) were associated solely with a differentiated phenotype. Although transcript expression does not guarantee the presence of functional protein, it does infer the potential for the pathway to play a role in urothelial biology.

Cyclooxygenase 1, encoded by the *PTGS1* gene, considered to play a "housekeeping" role in normal tissue homeostasis by being constitutively expressed in most human tissues (reviewed in Rouzer and Marnett, 2009), was not expressed at the transcript level in either undifferentiated or ABS/Ca^{2+} differentiated NHU cells. By contrast, COX2, canonically associated with inflammation and injury (reviewed in Simon, 1999), was expressed *in vitro* regardless of differentiation status. This data supports *Shirahama, (2000)* who reported that COX1 was not expressed by the bladder epithelial lining. However,

Shirahama, 2000 did not observe COX2 protein expression in the healthy, control, bladder tissue using either immunoblot or immunohistochemistry possibly due to the transcript not being translated into protein. Similarly, COX2 protein is weakly expressed in normal bronchial epithelial cells (Mascaux et al, 2005) but is the dominant, constitutively expressed COX isoform present at the mRNA and protein level in cultured human lung epithelial cells (Asano et al, 1996) exemplifying an *in situ* vs. *in vitro* difference in COX2 expression in another epithelia. Questions over whether COX1 and COX2 are truly 'constitutive' and 'inducible', respectively, have been raised for over a decade, with a study identifying COX2 is expressed under physiological conditions in many human tissues supporting the possibility COX2 may be the dominant COX isoform in human urothelial cells (Zidar et al, 2009). An alternative explanation may be that COX2 expression is mediated by growth factors present in NHU cell culture medium or ABS during serum-induced differentiation. This arises from the observation that COX2 can be induced by growth factors and chemokines produced during inflammation (reviewed in Wang and DuBois, 2010). This may be less likely as the NHU cell culture system would not be associated with a pro-inflammatory environment, however, the effects of EGF in the culture medium on COX2 expression have not been explored. Future studies to explore these possibilities should involve immunolabelling of COX2 in freshly isolated NHU cells to confirm protein expression and to determine whether the subsequent culture time alters its expression.

PTGER4 encodes the PGE_2 receptor, EP4, which was identified previously as having roles in mediating inflammatory responses, angiogenesis, apoptosis, and metastasis (reviewed in Konya et al, 2013). Upregulation of *PTGER4* in ABS/Ca^{2+}

differentiated NHU cells suggest an increase in the ability to respond to PGE_2 in these cells. The EP_4 receptor is reported to stimulate adenylyl cyclase through Gα-stimulatory proteins to elevate intracellular cAMP levels but also activate PI3K, MAPK and canonical Wnt pathways. The specific signalling downstream of the EP_4 receptor appears to be cell-type and context specific making it difficult to predict the outcome of upregulated *PTGER4* in differentiated NHU cells. The lack of phosphorylation of Akt, ERK and GSK3β in differentiated NHU cells treated with $dmPGE_2$ suggest that these pathways may not be the transduction pathway for PGE_2. Gene transcription changes were not investigated in this study directly but in future, RNA from differentiated NHU cells exposed to $dmPGE_2$ for 24 and 48 hours should be harvested to investigate proliferation and anti-apoptotic markers as reported in haematopoietic stem cells treated with $dmPGE_2$ (Goessling et al, 2011).

With PGDH providing the first step of PGE_2 catabolism to a 15-keto derivative with attenuated affinity for the EP receptors, this provides local regulation over activation of the EP receptors by limiting the bioactive PGE_2 locally. *HPGD* was present at the transcript level in ABS/Ca^{2+} differentiated cells with the largest fold change of any component of the PGE_2 metabolic cascade and was in the top 15 most upregulated genes in the entire NHU cell differentiation RNAseq dataset.

3.5.3 Differential-induction of PGDH protein expression

Localisation of PGDH protein to the superficial cells in human ureter supports *Tseng-Rogenski et al, (2008)* who reported PGDH was most abundantly

expressed in the luminal surface of bladder tissue. PGDH protein increased through the ABS/Ca^{2+} method of differentiation which produces a “biomimetic”, barrier-forming epithelium which compares to *Tseng-Rogenski et al, (2008)* who reported mRNA for PGDH in urothelial cells differentiated by incubation with 10% fetal calf serum and 1.8 mM exogenous calcium concentration, although no differentiation control was included. Whilst the localisation of PGDH protein to the cells thought to be “most-differentiated” *in situ* and induction of PGDH protein in the ABS/Ca^{2+} method may suggest a role for PGDH in the development or maintenance of functional urothelial barrier, this may be coincidental and independent.

3.5.4 Effect of PGDH inhibition on differentiated urothelium

Inhibition of PGDH in ABS/Ca^{2+} differentiated NHU cells after 48 hours resulted in increases in cell cycle activity as indicated by the expression of MCM2 and EdU incorporation. This was comparable to ABS/Ca^{2+} differentiated NHU cells incubated with dmPGE_2 suggesting PGDH inhibition increases cell cycle activity through reduced degradation and therefore accumulation of PGE_2. Interestingly, EdU incorporation was only increased after a 48 incubation with PGDH-i, not SW033291 suggestive that the two inhibitors may have distinctive kinetics. ABS/Ca^{2+} differentiated NHU cells treated with SW033291 had increased cell cycle activity after 72 hours whereas those treated with dmPGE_2 and PGDH-i did not providing further evidence for a difference in kinetics of the two PGDH inhibitors. Evidence discussed by *Markowitz et al, (2017)* suggests that SW033291 is a non-competitive and irreversible inhibitor of PGDH whilst *Wu et al, (2011)*

discuss how PGDH-i, a thiazolidinedione derivative, may be a non-competitive and uncompetitive inhibitor with NAD+ and PGE_2, respectively, but the mechanism of action of PGDH-i is not explicitly stated. It can be speculated that the differences seen between PGDH-i and SW033291 on cell cycle activity may be due to a prolonged action of SW033291 due to it not being reversible. Furthermore, repeating this experiment in more individual NHU cell lines is likely to confirm the the effects that PGDH-i and SW033291 have on cell cycle entry in unwounded NHU cell cultures.

Urothelial tight junctions, as indicated by ZO-3 immunolocalisation, appear to be depleted or weakened in ABS/Ca^{2+} differentiated NHU cells treated with PGDH-i and SW033291, but this was not seen in dmPGE_2 treated cultures. PGE_2 has been previously shown to disrupt barrier function in intestinal epithelium mediated by the EP_4 receptor (Rodríguez-Lagunas et al, 2010). Disinhibition of PGE_2 production by PGDH inhibition may cause dissolution of tight junctions in human urothelium but the reasoning behind why the same observation was not made with dmPGE_2 is unclear. It may suggest that PGE_2 only performs one function while inhibition of PGDH results in the release or change in concentration of a different bioactive molecule which performs a separate function. This compares to a study performed in pulmonary endothelial cells in which hypoxia was reported to activate PGDH and the effects seen on proliferation are mediated by a downstream metabolite (Ma et al, 2014).

Incubation of ABS/Ca^{2+} differentiated cells with dmPGE_2 and SW033291 disrupted barrier function, but incubation with PGDH-i did not. Importantly, this observation

was only made in cultures without CT suggestive that cAMP signalling may play a role in mediating this loss in barrier function which is obscured in NHU cell cultures differentiated with CT. The effects of PGDH inhibition on cell cycle activity however were seen in the presence of CT suggestive that this is a cAMP-independent process. Similar observations have been made in myoblasts, in which proliferation is stimulated by PGE_2 via the EP_4 receptor (Mo et al, 2015). Whilst these observations suggest an importance, in part, for cAMP signalling in mediating the effects of PGDH inhibition, no precise mechanism was identified and does not suggest whether cAMP production or movement of intracellular cAMP was altered. The effects of CT on differentiation were also not studied in this set of experiments leaving speculation whether the effects of cAMP were due to changes in urothelial differentiation or if cAMP functions to stimulate signal transduction pathways.

The effects of PGDH inhibition on cell cycle activity during urothelial wound repair were less pronounced with only an effect of PGDH-i and SW033291 being observed after 48 hours. This may result from effects being directly related to positioning to the scratch wound which was not able to be efficiently measured in this experiment as the original scratch area could not be identified. Another possibility is the effect of PGDH inhibition on cell cycle activity is more pronounced in quiescent cultures as opposed to wound repair where after 72 hours cells begin to re-enter the cell cycle irrespective of PGDH inhibition. Importantly, PGDH inhibition did result in decreased recovery rate of urothelial barrier post-scratching. This suggests the importance of PGE_2 in urothelial wound repair may be in barrier recovery and assembly of tight junctions rather than control over cell cycle activity.

An unexpected observation was the observation of small, intensely bright Hoechst 33258 stained nuclei in cultures treated with PGDH-i. Aggregation of heterochromatin and collapse of the nucleus during apoptosis can cause the appearance of condensed apoptotic chromatin (Hendzel et al, 1998) which may explain the appearance of these small nuclei in ABS/Ca^{2+} differentiated NHU cell cultures. Interestingly, PGDH-i is a thiazolidinedione derivative which may act as an agonist for PPARγ, an important driver of urothelial differentiation (Varley et al, 2004). Unpublished data from the Jack Birch Unit suggest prolonged activation of PPARγ with another thiazolidinedione derivative troglitazone (TZ) can cause apoptosis which may explain the appearance of the small nuclei observed in cultures incubated with PGDH-i. Another possibility is that these cells are post-mitotic as some look like daughter cells post cytokinesis. PGDH-i has been discussed earlier in this chapter to increase cell cycle activity which supports the post-mitotic argument but the exact circumstances behind the small nuclei appearance remains unclear.

3.5.5 Overview

Data presented in this chapter suggest a differentially-associated repression of the PGE_2 metabolic pathway caused by upregulation of PGDH protein. Subsequent inactivation of PGE_2 maintains mitotic quiescence by preventing binding of PGE_2 to the EP_4 receptor present in ABS/Ca^{2+} differentiated NHU cells which would promote mitotic activity. PGDH may also play a role in tissue homeostasis by maintenance of urothelial tight junctions to maintain barrier function.

A question which arises from this is why would urothelial differentiation upregulate genes involved in both synthesis and degradation of PGE_2 if ultimately it is important to degrade it to promote mitotic quiescence? As discussed in section 1.2.3, PGE_2 has been reported to signal to underlying detrusor muscle and may play a cytoprotective role in the bladder. It may be possible that the majority of PGE_2 present in the bladder is produced by the urothelium to signal to other bladder structures but not remain inside the urothelium itself. An alternative possibility given the instability of PGE_2 is that PGE_2 can only signal very locally.

Importantly, PGDH expression is confined to the superficial cells of the urothelium and therefore, the PGE_2-degrading activity which suppresses cell cycle activity is contained within these cells. Preferential loss in the context or injury or infection of these PGDH-expressing superficial cells may liberate the urothelium from the suppression it imposes and allow for proliferation and barrier restitution as depicted in figure 3.19.

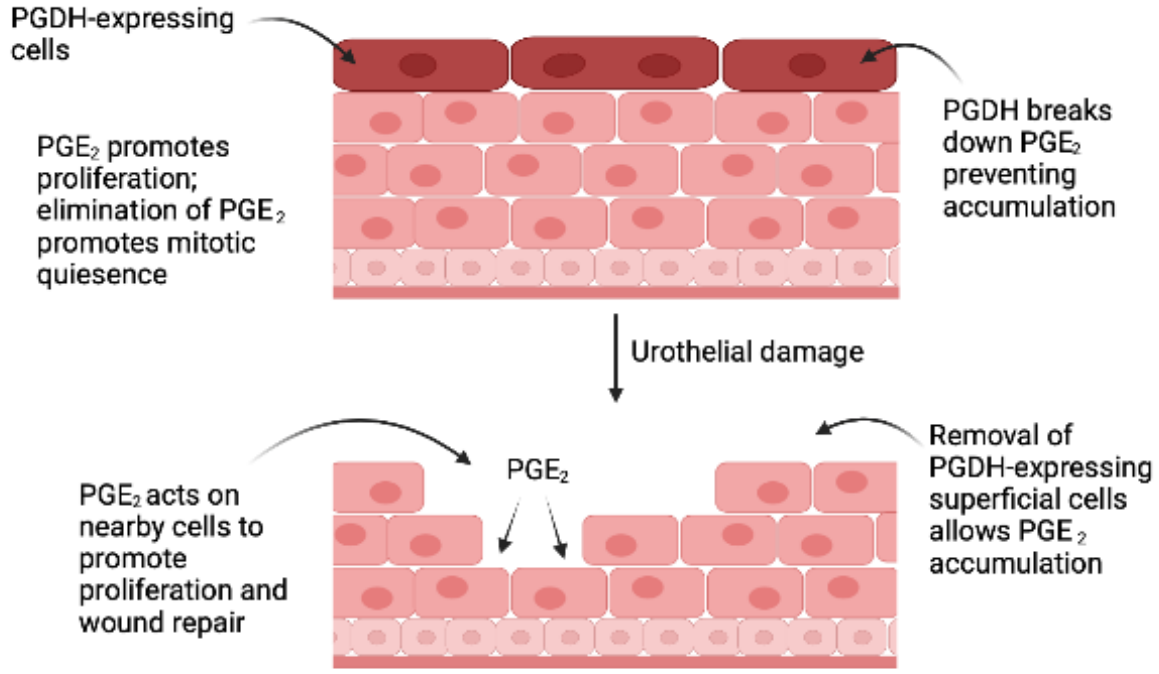

Figure 13.9. Proposed mechanism for PGDH in maintenance of mitotic quiescence and urothelial wound repair

PGDH, whose expression in confined to the luminal, superficial cells, functions to inactive proliferation-promoting eicosanoid PGE_2 allowing the urothelium to form a stable, mitotically-quiescent barrier. Removal of these suppressive superficial cells releases the urothelium into a reparative state for efficient barrier restitution. Created with BioRender.com.

4. Effect of cholera toxin on cell morphology, differentiation, and wound repair in human urothelial cells *in vitro*

4.1 Introduction

The enterotoxin produced by *Vibrio cholerae* has been widely used in the culturing of primary epithelial cells for decades with its structure and mechanism of action being elucidated over the past fifty years (reviewed in Sanchez and Holmgren, 2011). It has commonly been used as a positive control in cyclic adenosine monophosphate (cAMP) experiments because of its activation of AC. Cholera toxin causes constitutive activation of AC through ADP-ribosylation of Gα-stimulatory proteins causing an inactivation of their GTPase activity thus the G protein remains GTP bound and active (reviewed in Bharati and Ganguly, 2011). Downstream activation of protein kinase A (PKA) can alter a multitude of cellular proteins with effects being cell-type specific (Sassone-Corsi, 2012). Initially included in the culture medium for NHU cells to promote plating efficiency, CT can alter multiple signalling pathways simultaneously through production of cAMP and as discussed in chapter 3, may need to be excluded from the culture medium to study the effects of other cAMP-producing molecules. Interestingly, cAMP signalling has been identified as crucial in promoting early stages of adipogenesis, a process with similarities to urothelial differentiation (Petersen et al, 2008). This raises the possibility cAMP signalling may function in urothelial differentiation, such this chapter focuses on exploring any role for CT in urothelial differentiation and wound repair.

4.2 Aims and Hypothesis

The hypothesis is that CT in NHU cell culture media promotes urothelial differentiation during the ABS/Ca^{2+} differentiation protocol via constitutive production of cAMP. To investigate this hypothesis, the aim of this chapter was to evaluate the role of cholera toxin in urothelial differentiation and wound repair in human urothelial cells. Specific objectives were:

- To determine whether cholera toxin has a role in urothelial differentiation by analysing cell morphology and expression of differentiation-associated markers.
- To determine whether cholera toxin alters urothelial wound repair.

4.3 Experimental Approach

To determine whether CT plays a role in urothelial differentiation, micrograph images were taken periodically during ABS/Ca^{2+} differentiation of NHU cell cultures differentiated in the presence and absence of CT from the point of ABS addition. As PGE_2 has been previously shown to modulate TGFβ signalling (Lenicov et al, 2018), differentiated NHU cells were pre-treated with PGE_2 for 4 hours followed by an incubation with TGFβ1 for 1 hour to investigate whether PGE_2 can modulate TGFβ signalling in NHU cells. Previously reported markers of differentiation PPARγ and KRT13 were included as positive differentiation controls (Varley et al, 2004; Varley et al, 2004). cAMP signalling has previously been

reported to modulate TGFβ signalling (Shiller et al, 2010) and with TGFβ signalling previously shown to be important in urothelial wound repair (Fleming et al, 2012), wound repair was investigated in ABS/Ca^{2+} differentiated NHU cells in the presence and absence of CT by indirect immunofluorescence and time-lapse microscopy.

4.4 Results

4.4.1 Effect of cholera toxin on markers associated with urothelial differentiation and migration

Micrograph images taken of NHU cell cultures during ABS/Ca^{2+} differentiation demonstrated morphological differences induced by ABS and physiological 2 mM calcium concentration both in cultures differentiated in the presence and absence of CT (**Figure 4.1**). Addition of ABS causes distinct changes in cell morphology which is unaffected by addition of CT (**Figure 4.1C-D**). However, increasing the Ca^{2+} concentration to 2 mM induces formation of visible islands of stratification but these are reduced in NHU cells differentiated without CT (**Figure 4.1E-F**).

Western blot analysis and densitometry revealed NHU cell cultures differentiated with CT display increased protein expression of markers of differentiation KRT13 and PPARγ (**Figure 4.2A-C**). KRT13 expression was also increased by TGFβ in the presence of CT (**Figure 4.2B**). Whilst PGE_2 did not alter the phosphorylation of SMAD3, an unexpected result was the reduction of SMAD3 phosphorylation in NHU cell cultures differentiated with CT (**Figure 4.2A, 4.2D**). Expression of

SMAD3 protein was increased in cells differentiated with CT, suggesting the reduction in SMAD3 phosphorylation was not due to decreases in SMAD3 protein expression. Phosphorylation of SMAD3 was shown to be between 2 and 3 times higher in cultures differentiated without CT compared to those with CT (**Figure 4.2D**).

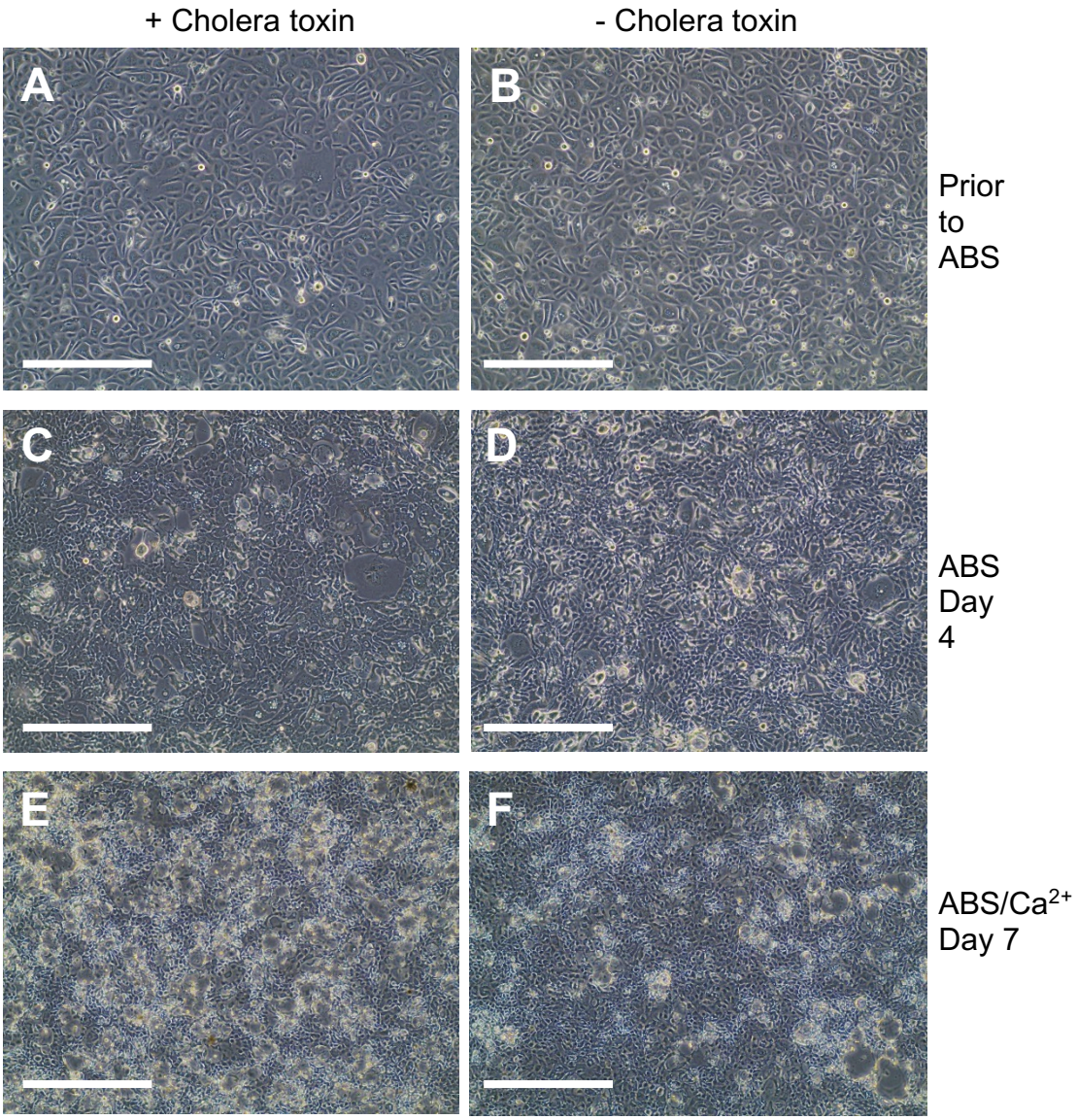

Figure 4.1 Effect of cholera toxin on NHU cell morphology during ABS/Ca^{2+} differentiation

NHU cells (Y2797) were differentiated following the ABS/Ca^{2+} method (+/- cholera toxin) with micrographs taken at sequential time points. Scale bar = 500 μm.

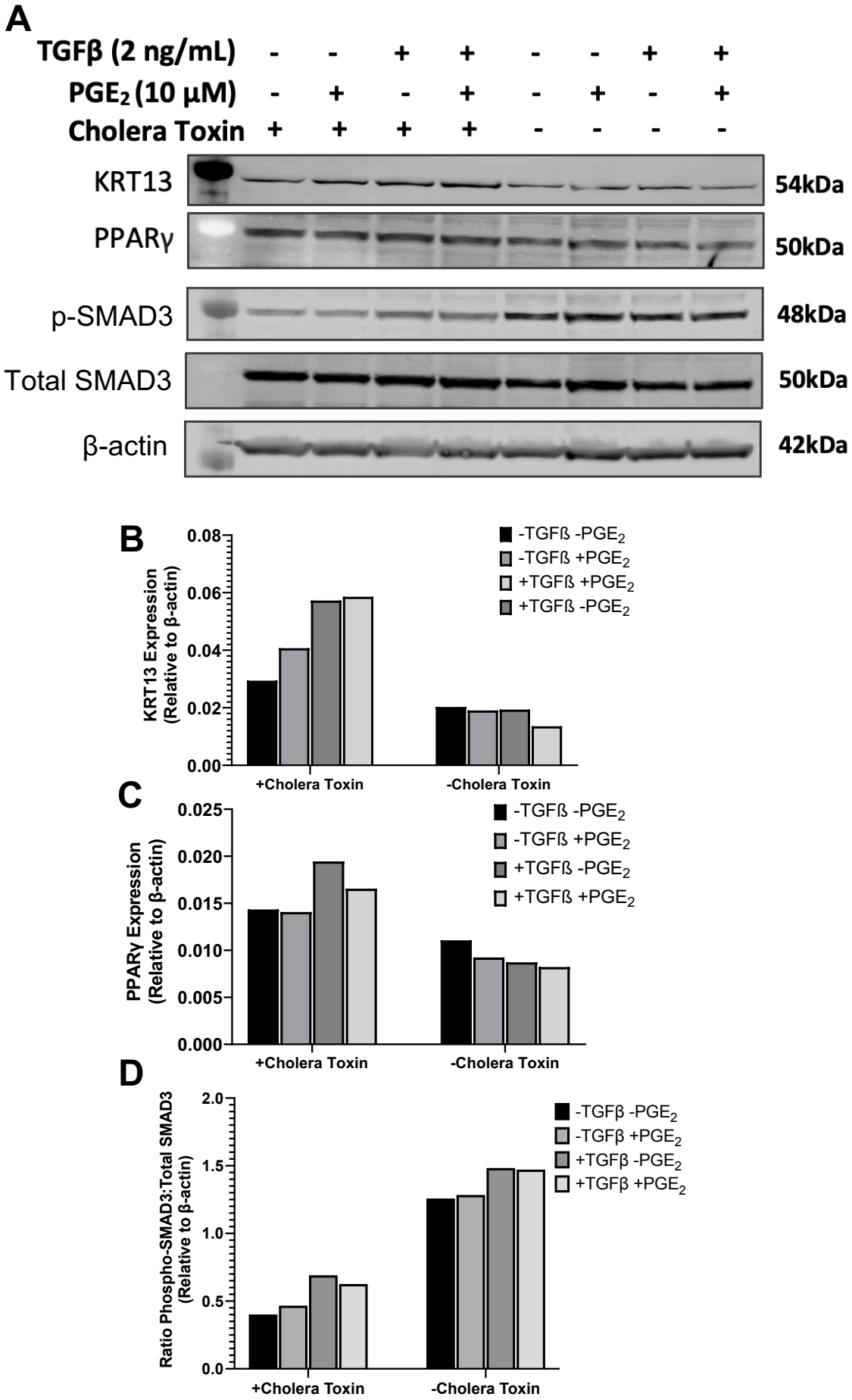
A
TGFβ (2 ng/mL) - - + + - - + +
PGE2 (10 µM) - + - + - + - +
Cholera Toxin + + + + - - - -
KRT13
PPARγ
p-SMAD3
Total SMAD3
β-actin
54kDa
50kDa
48kDa
50kDa
42kDa
B
KRT13 Expression (Relative to β-actin)
0.08
0.06
0.04
0.02
0.00
-TGFß -PGE2
-TGFß +PGE2
+TGFß +PGE2
+TGFß -PGE2
+Cholera Toxin
-Cholera Toxin
C
PPARγ Expression (Relative to β-actin)
0.025
0.020
0.015
0.010
0.005
0.000
-TGFß -PGE2
-TGFß +PGE2
+TGFß -PGE2
+TGFß +PGE2
+Cholera Toxin
-Cholera Toxin
D
Ratio Phospho-SMAD3:Total SMAD3 (Relative to β-actin)
2.0
1.5
1.0
0.5
0.0
-TGFβ -PGE2
-TGFβ +PGE2
+TGFβ -PGE2
+TGFβ +PGE2
+Cholera Toxin
-Cholera Toxin

Figure 4.2. Effect of exogenous PGE_2 and cholera toxin on urothelial differentiation, mitotic quiescence and TGFβ signalling

NHU cells (Y2797) were differentiated following the ABS/Ca^{2+} method (+/- cholera toxin). Once differentiated, cell cultures were pre-treated for 4 hrs with PGE_2 (10 μM) then treated with TGFβ (2 ng/mL) for 1 hr to stimulate phosphorylation of SMAD3 and subsequently lysed in SDS sample buffer. A) Immunoblotting analysis of KRT13, PPARγ, phospho-SMAD3 and Total SMAD3 (n=1). Quantification of band density by densitometry revealed a stronger band of differentiation markers B) KRT13 and C) PPARγ in the presence of cholera toxin. D) Phosphorylation of SMAD3 was standardised to Total SMAD3 and demonstrated a reduction in the presence of cholera toxin. β-actin was included as a loading control.

4.4.2 Effect of cholera toxin on wound repair rate in differentiated NHU cell cultures

As discussed in section 1.1.4.1, TGFβ receptor signalling is important in mediating migration of urothelial cells in wound repair with SMAD3 becoming activated by phosphorylation to promote tissue repair. The increase in phosphorylation of SMAD3 in NHU cultures differentiated without CT suggests these cells may possess a more migratory phenotype compared to NHU cells differentiated with CT. Time-lapse microscopy analysis revealed NHU cultures differentiated with CT took longer to heal than NHU cultures differentiated without CT. NHU cultures differentiated with CT took 36-44 h to fully repair, whilst NHU cultures differentiated without CT took 28-32 hr (**Figure 3.4A**). The time taken to heal 50% of the initial wound was calculated (WC50) for each replicate (**Figure 3.4B**). The time taken to heal 50% of the initial wound for the 12 replicates differentiated with

CT (*M* = 25.54, *SD* = 3.12) compared to the 12 replicates differentiated without CT (*M* = 18.5, *SD* = 4.11) was found to be significantly higher (p = 0.0001) (**Figure 3.4C**). Representative images at interval times through wound repair are illustrated in figure 3.4C.

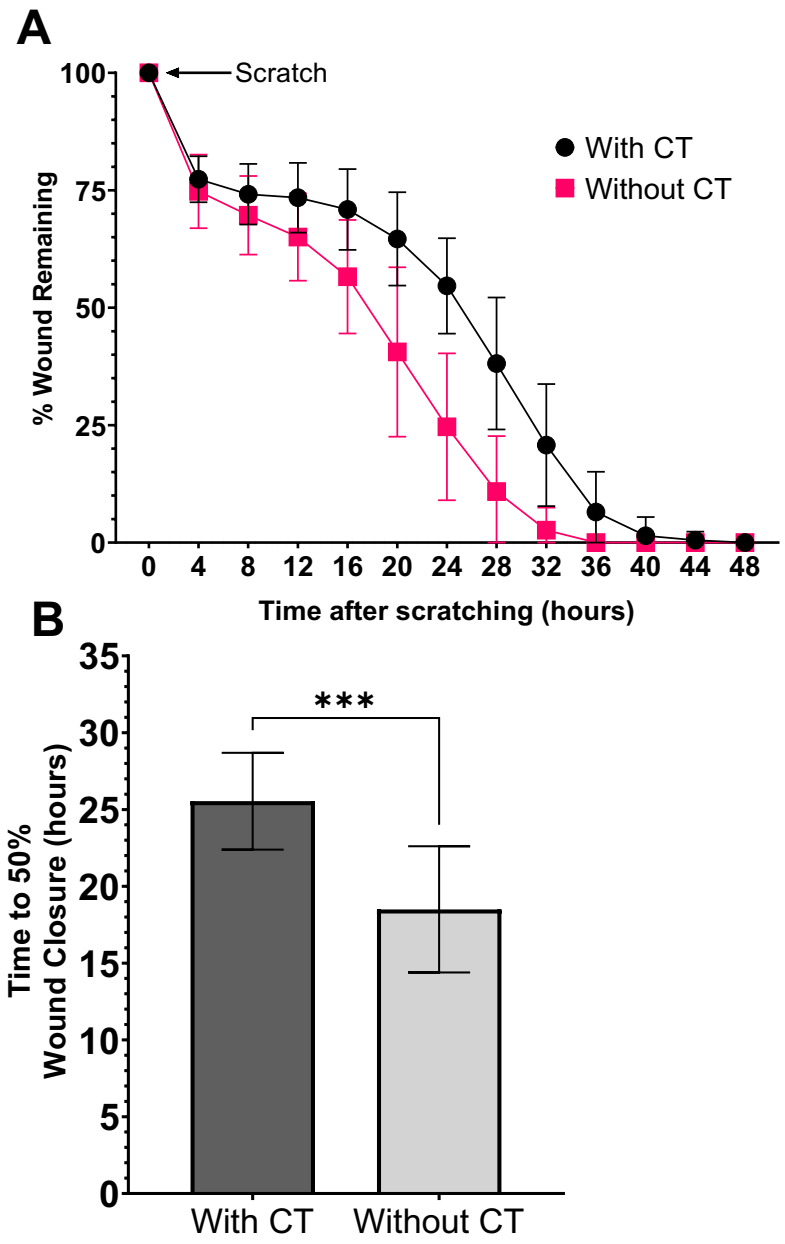

C

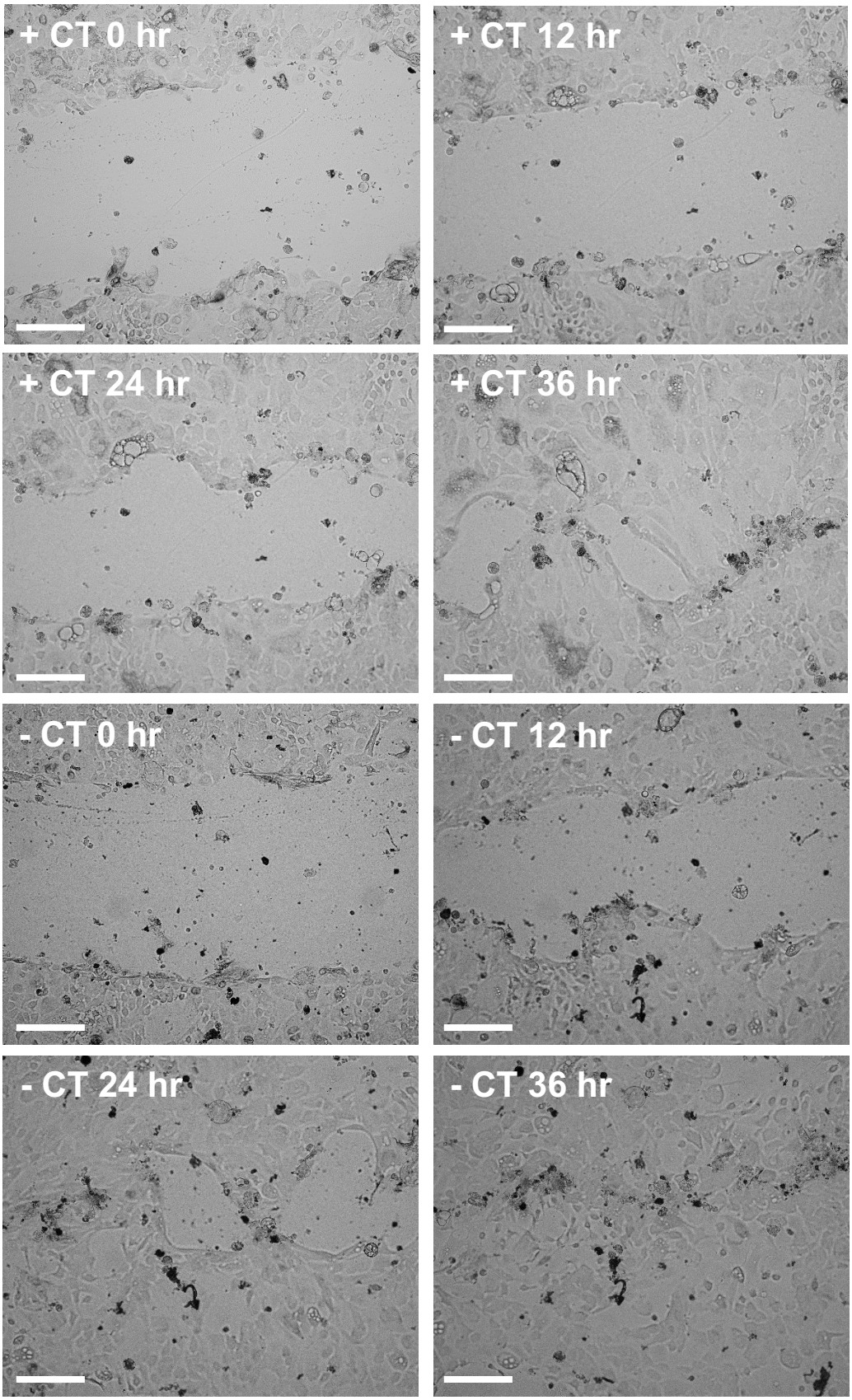

Figure 4.3 Effect of cholera toxin on wound repair rate in differentiated NHU cell cultures

NHU cells (Y929A) were differentiated following the ABS/Ca^{2+} method (+/- cholera toxin). A) Cultures (n=6) were then scratched with a sterile 200 µl pipette tip as indicated with an arrow and repair monitored by videomicroscopy. Percentage wound remaining was plotted against time. B) The mean time to heal 50% of the initial scratch wound was calculated (± SD). An unpaired t-test was used to calculate significance. *** = $p \leq 0.001$. C) Representative images of NHU cells (+/- cholera toxin) showing the initial scratch wound or 12-, 24- or 36-hours post-scratch. Scale bar = 200 µm.

4.4.3 Effect of cholera toxin on TGFβ signalling components and tight junction proteins in wounded differentiated NHU cell cultures

Indirect immunofluorescence analysis identified that 4.5 hours post-scratch, NHU cultures with CT had a greater wound area remaining compared to cultures without CT (p = 0.022) (**Figure 4.4**).

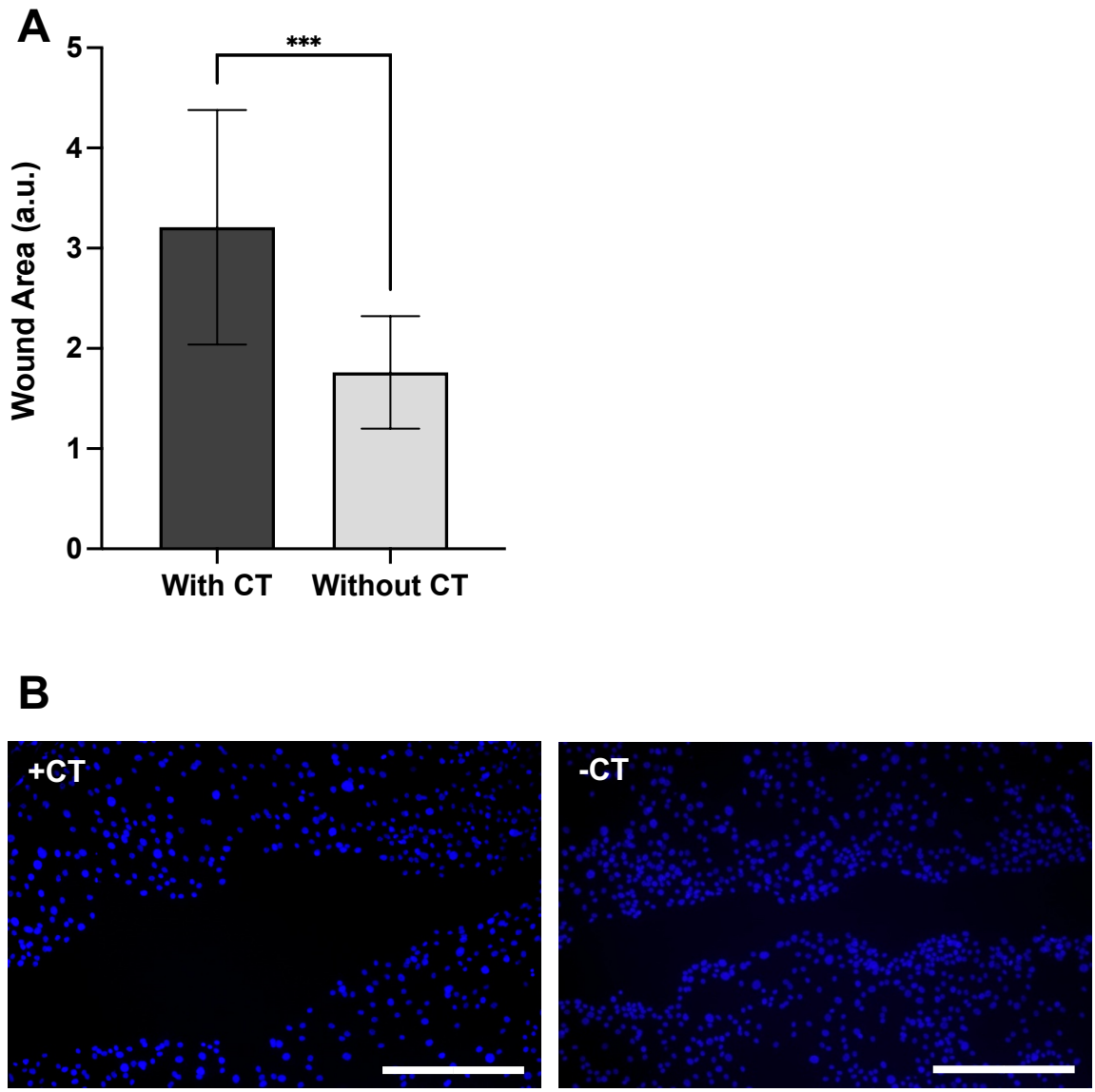

Figure 4.4. Effect of cholera toxin on migration during wound repair in differentiated NHU cell cultures

NHU cells (Y929A) were differentiated following the ABS/Ca^{2+} method (+/- cholera toxin) on glass slides and scratched with a sterile 200 µl pipette tip and fixed mid-migration, 4.5 hours post-scratch (n=1). A) The mean wound area was calculated (± SD) and an unpaired t-test was used to calculate significance. *** = $p \leq 0.001$. B) Representative images of NHU cells (+/- cholera toxin) 5 hours post-scratch. DNA stained with Hoechst 33258 (*blue*) displayed in bottom left corner. Scale bar = 200 µm. No primary antibody control was negative (not shown).

SMAD3 phosphorylation was weaker at both the wound edge and further back in cultures differentiated with CT (**Figure 3.5A**). Similarly, in unwounded cultures, SMAD3 phosphorylation was weaker in cultures with CT. Total SMAD3 protein expression was stronger in cultures differentiated with CT at the wound edge compared to cultures without CT, however, further back from the wound edge and in unwounded cultures, this difference was less distinct (**Figure 3.5B**). ZO-3 staining was weaker in cultures differentiated without CT at both the wound edge and further back but in unwounded cultures, ZO-3 staining was comparable between cultures differentiated in the presence and absence of CT (**Figure 3.6**).

A

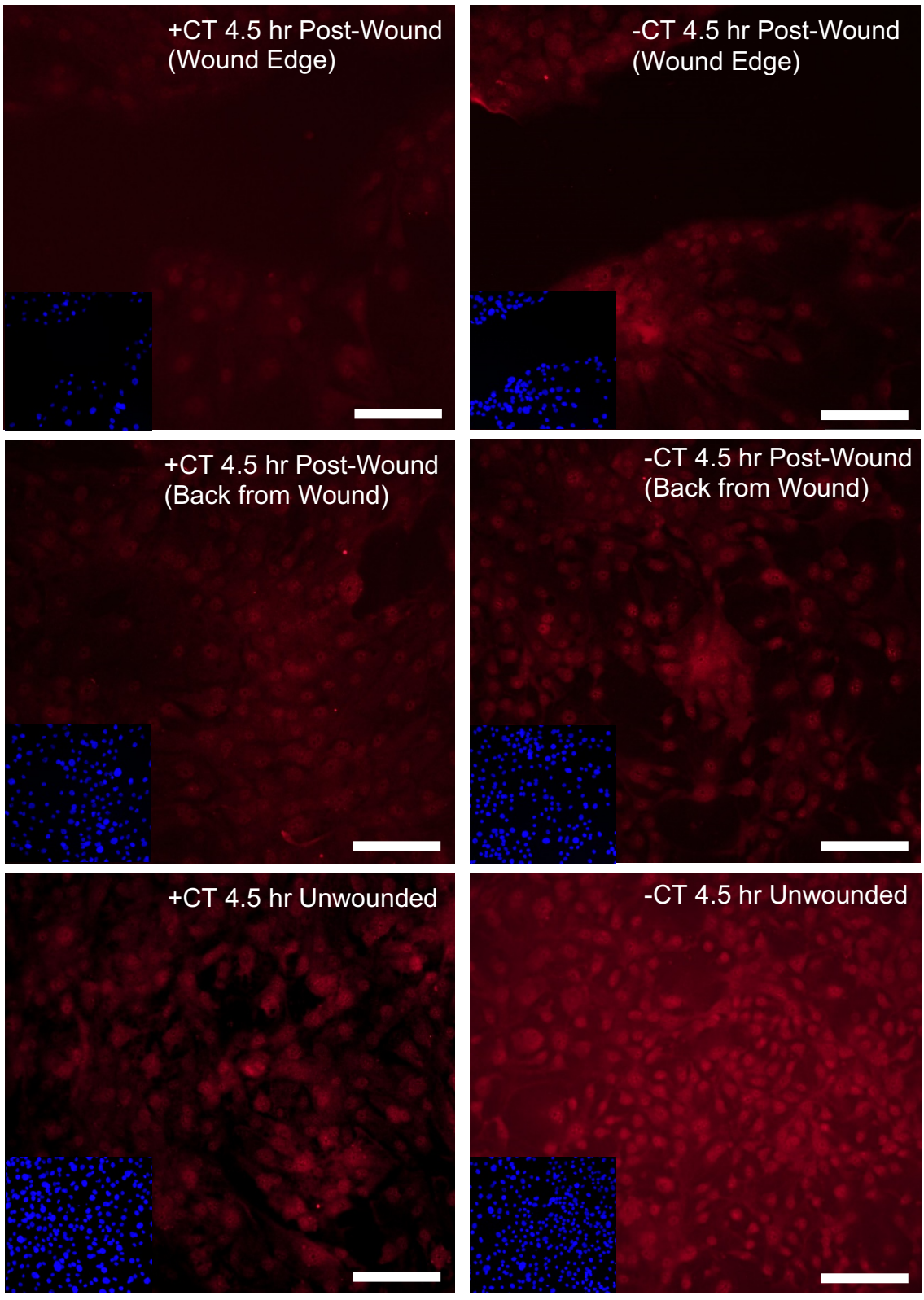
+CT 4.5 hr Post-Wound
(Wound Edge)
-CT 4.5 hr Post-Wound
(Wound Edge)
+CT 4.5 hr Post-Wound
(Back from Wound)
-CT 4.5 hr Post-Wound
(Back from Wound)
+CT 4.5 hr Unwounded
-CT 4.5 hr Unwounded

B

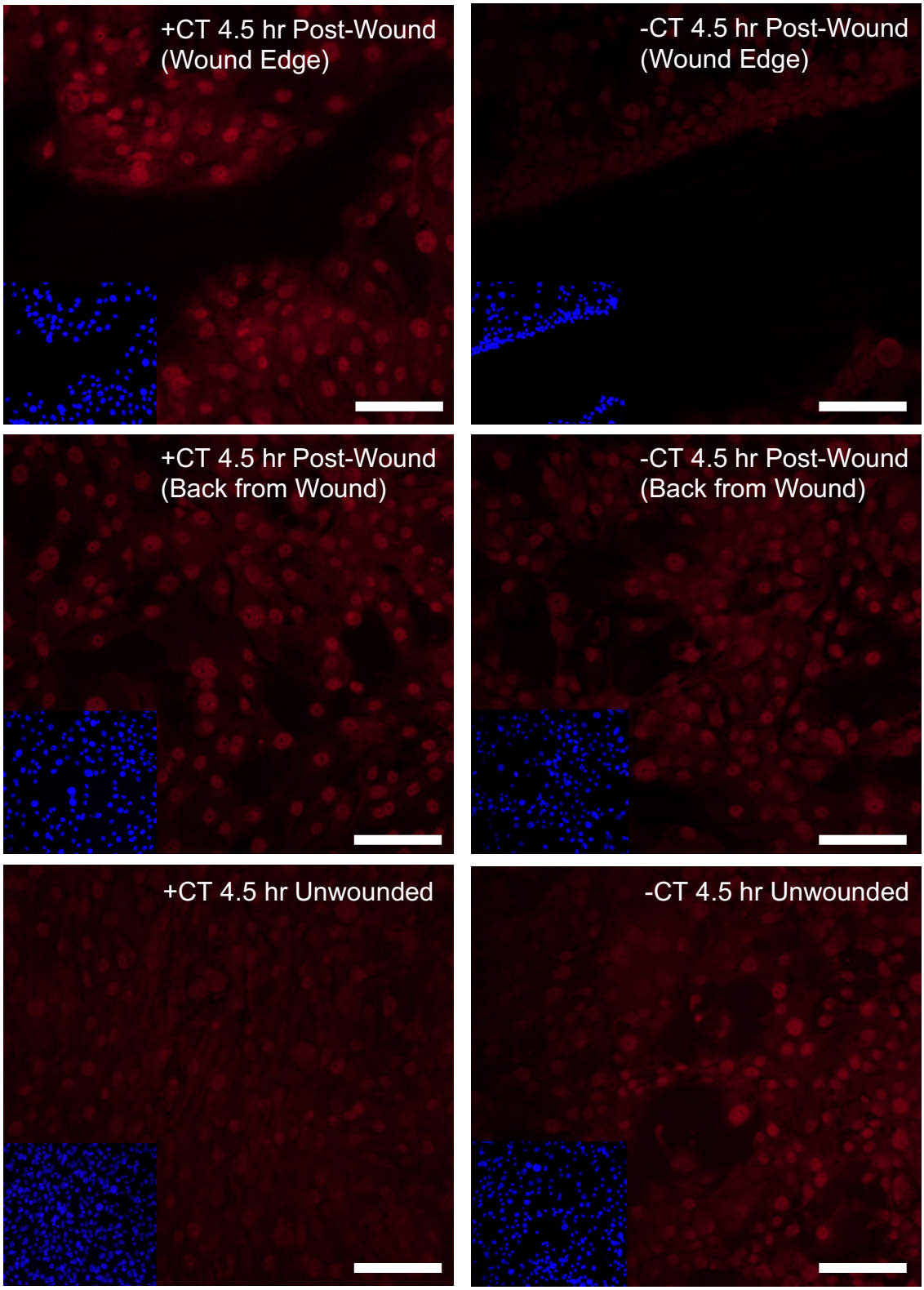
+CT 4.5 hr Post-Wound
(Wound Edge)
-CT 4.5 hr Post-Wound
(Wound Edge)
+CT 4.5 hr Post-Wound
(Back from Wound)
-CT 4.5 hr Post-Wound
(Back from Wound)
+CT 4.5 hr Unwounded
-CT 4.5 hr Unwounded

Figure 4.5. Effect of cholera toxin on TGFβ signalling components during wound repair in differentiated NHU cultures

NHU cells (Y929A) were differentiated following the ABS/Ca^{2+} method (+/- cholera toxin) on glass slides and scratched with a sterile 200 µl pipette tip and fixed mid-migration, 4.5 hours post-scratch (n=1). Representative images of expression of A) p-SMAD3 and B) Total SMAD3. DNA stained with Hoechst 33258 (*blue*) displayed in bottom left corner. Scale bar = 100 µm

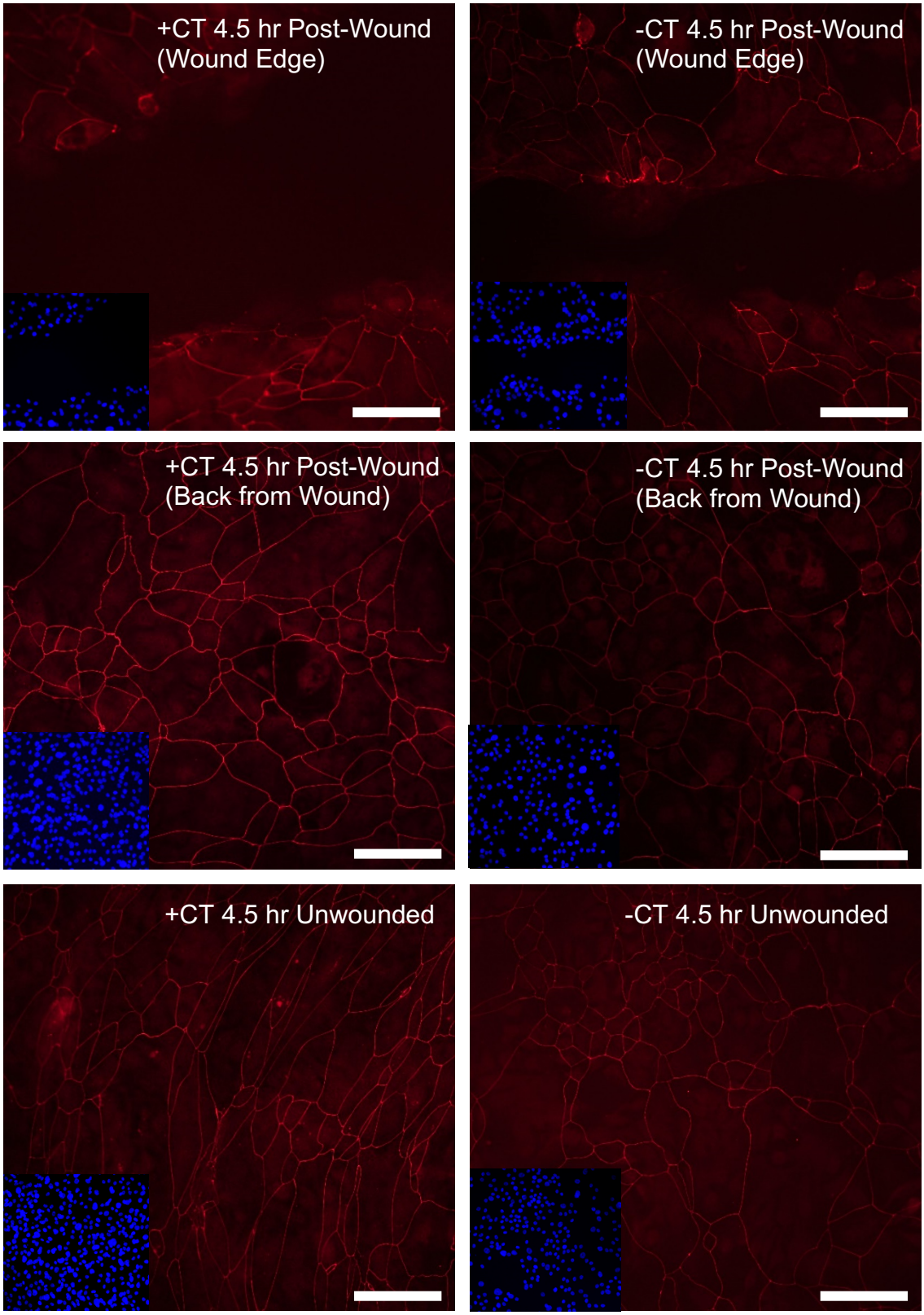
+CT 4.5 hr Post-Wound
(Wound Edge)
-CT 4.5 hr Post-Wound
(Wound Edge)
+CT 4.5 hr Post-Wound
(Back from Wound)
-CT 4.5 hr Post-Wound
(Back from Wound)
+CT 4.5 hr Unwounded
-CT 4.5 hr Unwounded

Figure 4.6. Effect of cholera toxin on ZO-3 expression during wound repair in differentiated NHU cultures

NHU cells (Y929A) were differentiated following the ABS/Ca^{2+} method (+/- cholera toxin) on glass slides and scratched with a sterile 200 µl pipette tip and fixed mid-migration, 4.5 hours post-scratch (n=1). Representative images of ZO-3 staining. DNA stained with Hoechst 33258 (*blue*) displayed in bottom left corner. Scale bar = 100 µm

4.5 Discussion

4.5.1 Key findings

The findings of this chapter revealed an unexpected promotion of urothelial differentiation by CT in NHU cell culture medium and importantly, suggest a role for cAMP signalling in urothelial wound repair by modulation of TGFβ signalling. It is important to note that all experiments in chapter 4 have only been carried out in a single NHU cell line (derived from a single individual) and require repeating in two further independent NHU cell lines to consolidate the evidence and as such, the evidence interpreted here is only preliminary.

4.5.2 Effect of CT on urothelial differentiation

Removal of CT from the culture medium during ABS/Ca^{2+} differentiation resulted in reduced expression of differentiation markers PPARγ, KRT13 and SMAD3. Microscopically, NHU cells differentiated without CT appear less stratified, but this may be coincidental. Regardless of these changes to differentiation-associated proteins, as evaluated in chapter 3, ABS/Ca^{2+} differentiated NHU cells without CT form functional barrier comparable to cultures differentiated with CT. The reason behind this is unclear however, may be due to tight junction protein assembly as ZO-3 immunolocalisation in unwounded cultures was comparable regardless of whether CT was present in the culture medium. Terminal differentiation of keratinocytes compares to urothelial differentiation in that the final product is the

formation of a barrier epithelium and studies have previously reported cAMP signalling increases protein expression of keratins K1 and K10 (Mammone et al, 1998). It is widely understood that cAMP-dependent signalling is crucial for adipogenesis through the induction of early transcription factor C/EBPβ which converges with other factors to drive expression of PPARγ and the mature differentiated adipocyte phenotype (reviewed in Farmer, 2006). Interestingly, C/EBPβ motifs have been shown to be enriched in FAIREseq analysis in differentiation-specific FAIRE peaks within 25 kb of genes upregulated during urothelial differentiation at 24 and 144 hrs (Fishwick et al, 2017). This may suggest the role of CT in urothelial differentiation may lie in the upregulation of C/EBP transcription factors in a similar manner to adipogenesis and may explain the reduction of PPARγ protein expression in ABS/Ca^{2+} differentiated NHU cells without CT. This could be tested in future experiments by evaluating expression of C/EBP transcription factors by rtPCR in cultures differentiated with and without CT.

4.5.3 Effect of CT on urothelial wound repair

An unexpected observation in ABS/Ca^{2+} differentiated cells without CT was an increase in the phosphorylation of SMAD3 distinct to cultures differentiated with CT. Removal of CT from the culture medium resulted in cultures that took significantly less time to migrate and heal the scratch wound. Phosphorylation of SMAD3 was shown to be increased at the wound edge and further back from the wound in ABS/Ca^{2+} differentiated cells without CT illustrative of a culture possessing a more migratory phenotype and thus suggests this is the mechanism behind the increased wound healing observed. cAMP signalling has been reported

previously to modulate TGFβ signalling in fibroblasts, however, SMAD phosphorylation was unaffected, and the effect was a result of the abolishment of SMAD3 binding to cAMP-response element-binding protein (CREB)-binding protein (CBP), a transcriptional co-activator (Schiller et al, 2010). Interestingly, ZO-3 immunolocalisation suggested a dissolution of tight junctions at the wound edge and further back in cultures differentiated without CT suggestive that an early response to cAMP signalling may be tight junction degradation and release into a migratory phenotype. These results begin to illustrate a role for CT in wound repair, but the exact mechanism remains elusive. Subsequent experiments should aim to visualise cAMP in live cells as its effects have been reported to be mediated in distinct intracellular compartments and may be a result of localised signalling (Dikolayev et al, 2019). Multiple types of cAMP biosensor have been developed but a challenge in NHU cells differentiated *in vitro* is the multi-layered epithelium posing difficultly in visualising these biosensors. Inhibition of PKA may also provide a valuable experiment to elucidate whether it mediates the effects of cAMP.

4.5.4 Overview

Data presented in this chapter demonstrate an association between CT and urothelial differentiation although questions remain over the mechanism behind this although there have been previous suggestions that induction of C/EBP transcription factors, evaluated for their orchestral role in adipogenesis, may converge to drive PPARγ expression. The result of ABS/Ca^{2+} differentiated in the

absence of CT is a culture with a more migratory, less-differentiated phenotype which take less time to regenerate post-scratch wounding.

A question which arises from these observations is what is the *in situ* relevance? Initially investigated as a potential cell culture artifact has identified an important role for CT in promoting urothelial differentiation *in vitro* but whether cAMP signalling plays a role in urothelial differentiation *in situ* is unclear. The exact mechanism as to how CT affects TGFβ signalling also remains elusive. The stark inhibition of SMAD3 phosphorylation by CT suggests either an alteration to TGFβ receptor expression or activity but this was not studied in these experiments and requires further study.

5. Conclusions

The bioactive eicosanoid PGE_2 has been previously implicated in promoting of proliferation, angiogenesis and modulating wound repair in several epithelia. PGDH, whose activity catalyses the inactivation of PGE_2 localises to the “most-differentiated” superficial cells of the human urothelium, a barrier epithelium which functions to maintain a high-resistance barrier to urine in the bladder and ureters. Whilst previous studies have identified PGDH is differentiation-associated in urothelial cells isolated *in vitro* and that knockdown disrupts urothelial differentiation, the function of PGDH had not been fully explored.

This thesis aimed to explore both the expression and function of the PGE_2 metabolic cascade with a focus on PGDH activity as this was identified as the most upregulated gene in the pathway.

Inhibition of PGDH caused dysregulation of mitotic quiescence assessed by expression of DNA-replicating initiation factor MCM2 and incorporation of a labelled DNA analogue, EdU. PGDH inhibition also reduced barrier recovery during urothelial wound repair and this process was cAMP-dependent as exogenous stimulation with cholera toxin diminished these effects. These results illustrate a role for PGDH in mediating urothelial tissue homeostasis but the wider effects of other components of the PGE_2 metabolic pathway, especially synthesis enzyme cyclooxygenase-2 (COX-2) were not studied. From the results presented in this thesis, a more detailed analysis of COX-2 expression and activity in normal human urothelium cells would be informative given the association of COX2 and

carcinogenesis. More detailed examination of the mode of action of both PGDH-i and SW033291 would also be useful including quantification of PGE_2 production in the presence of these inhibitors. Finally, whilst PGE_2 is suggested to be important in promoting proliferation when PGDH is inhibited and this is likely through the EP_4 receptor, the precise mechanism was not elucidated in this study and examination of NHU cells stimulated with a specific EP_4 receptor agonist may aid in this.

In addition, a limitation in this study was that each experiment was only carried out in a single NHU cell line and thus the data presented here are only preliminary in nature. Repeating each experiment in a further two individual NHU cell lines would strengthen the arguments proposed in this thesis by providing more biological replicates.

Appendix 1: Suppliers

Company Name	Web Address
Abcam	www.abcam.com
Cayman	www.caymanchem.com
Cell Signalling	www.cellsignal.com
Fisher Scientific	www.fisher.co.uk
Li-Cor	www.licor.com
Merck-Millipore	www.merckmillipore.com
Olympus	www.olympus.co.uk
Origene	www.origene.com
Pierce	www.piercenet.com
R&D Systems	www.rndsystems.com
Rockland	www.rockland-inc.com
Sarstedt	www.sarstedt.com
Sigma-Aldrich Ltd	www.sigmaaldrich.com
Solent Scientific	www.solentsci.com
Thermo Scientific	www.thermoscientific.com

Appendix 2: Stock Solutions

General Solutions

Phosphate-buffered saline (PBS)

137 mM NaCl, 2.7 mM KCl, 3.2 mM Na_2HPO_4, pH 7.2 in dH_2O. Tablets (sigma) were used to prepare PBS.

Tris-buffered saline (TBS)

50 mM Tris-HCl (pH 7.6) and 150 mM NaCl in dH_2O.

Cell Culture Solutions

Cholera Toxin

Cholera toxin (Sigma) made up to 30 ng/ml in KSFM, aliquoted in 5 ml.

EDTA

0.1 or 1% (w/v) EDTA (Fisher) stock solution made up in PBS.

Trypsin in Versene (TV)

20 ml Trypsin (Sigma), 4 ml 1% EDTA, 176ml Hank's balanced salt solution, aliquoted in 5 ml.

Trypsin Inhibitor (TI)

100 mg Trypsin Inhibitor (Sigma) dissolved in 5 ml PBS, aliquoted in 100 µl.

Immunoblotting Solutions

SDS Electrophoresis Sample Buffer (2x)

125 mM Tris-HCl (pH 6.8), 20% glycerol (w/v), 200 mM sodium fluoride, 2 mM sodium orthovanadate, 40 mM tetra-sodium pyrophosphate, *d*H_2O to 50 ml, aliquoted in 1 ml.

Western Blot Transfer Buffer

20 mM Tris, 150 mM glycine, 20% methanol (v/v), *d*H_2O to 1 L.

Appendix 3: Titration of PGDH inhibitors

a)

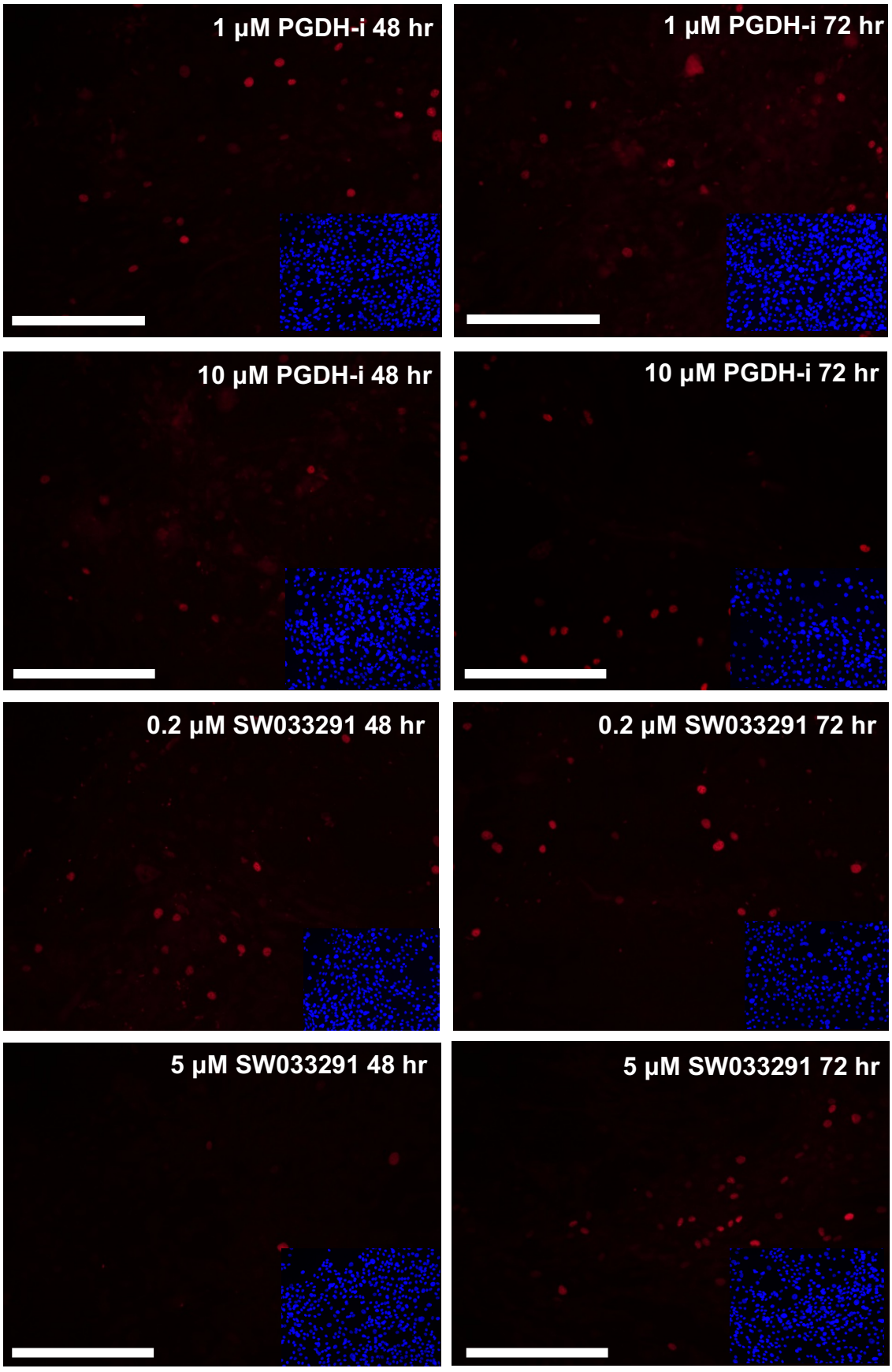

b)

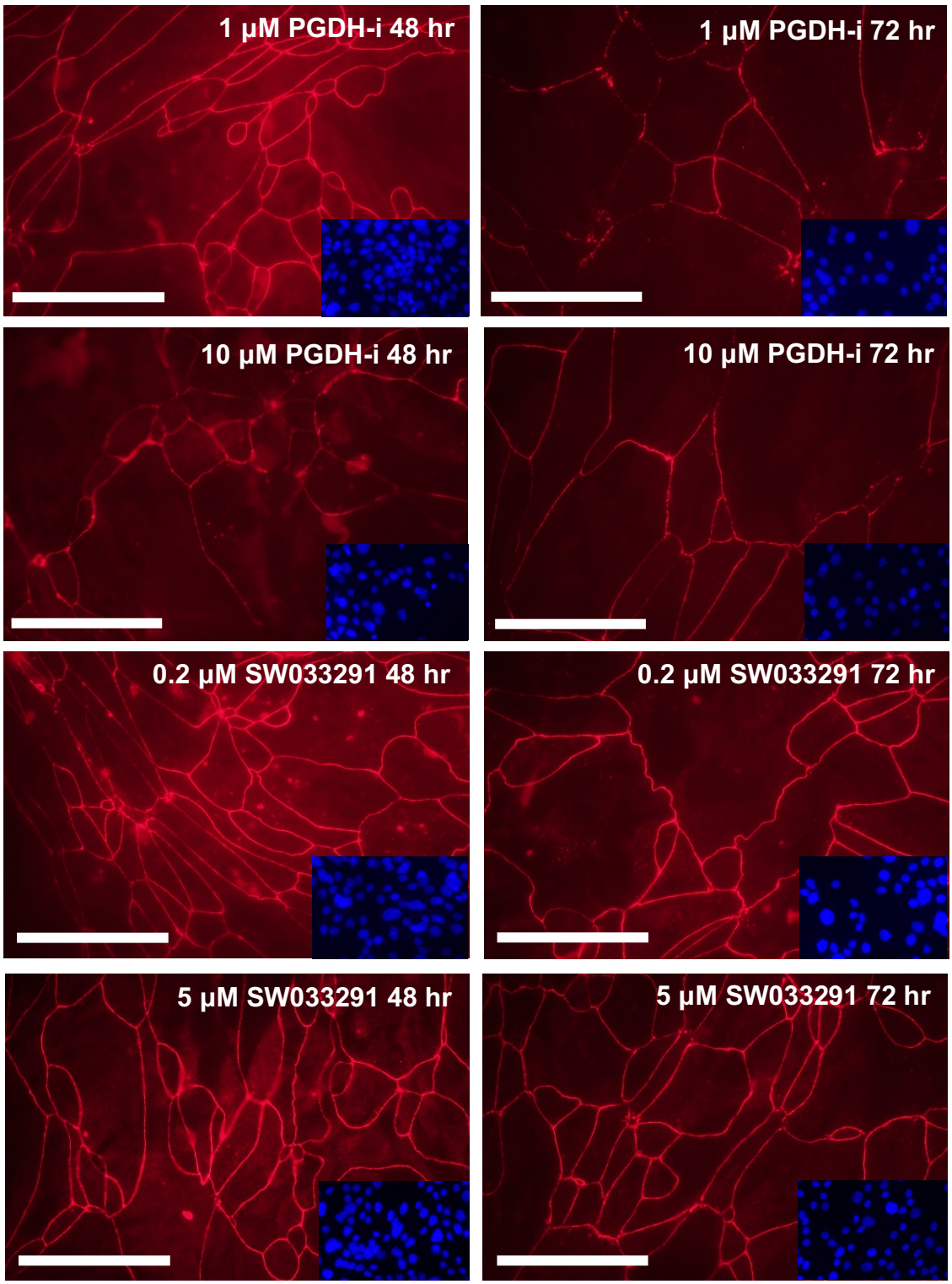
1 µM PGDH-i 48 hr
1 µM PGDH-i 72 hr
10 µM PGDH-i 48 hr
10 µM PGDH-i 72 hr
0.2 µM SW033291 48 hr
0.2 µM SW033291 72 hr
5 µM SW033291 48 hr
5 µM SW033291 72 hr

Figure 6.1. Titration of PGDH inhibitors on cell cycle activity

NHU cells (Y929A) were differentiated following the ABS/Ca^{2+} method on glass slides and fixed 48 and 72 hours after treatment with 1-10 μM PGDH-inhibitor or 0.2-5 μM SW033291. Representative images of a) MCM2 positive NHU cells and b) ZO-3 staining after treatment with concentrations chosen not optimum 1 and 10 μM PGDH-inhibitor or 0.2 and 5 μM SW033291 after 48 and 72 hours. DNA stained with Hoechst 33258 (*blue*) displayed in bottom left corner. Scale bar = 200 μm for MCM2; Scale bar = 40 μm for ZO-3.

Abbreviations

ABS	Adult bovine serum
AC	Adenylyl cyclase
ATP	Adenosine triphosphate
AUM	Asymmetric unit membrane
BMP	Bone morphogenetic protein
BPE	Bovine pituitary extract
BSA	Bovine serum albumin
cAMP	Cyclic adenosine monophosphate
cPGES	Cytosolic prostaglandin E synthase
CT	Cholera toxin
COX	Cyclooxygenase
CK	Cytokeratin
***d*H2O**	De-ionised water
DMSO	Dimethyl sulfoxide
EDTA	Ethylenediaminetetraacetic acid
EdU	5-ethynyl-2'-deoxyuridine
EGFR	Epidermal growth factor receptor
ERK	Extracellular signal-regulated kinase
EVOM	Electronic volt-ohmmeter
GPRC	G-protein coupled receptor
GSK3β	Glycogen synthase kinase 3β
HPGD	*Hydroxyprostaglandin dehydrogenase*
IC	Interstitial cystitis
KSFM	Keratinocyte serum-free medium

KSFMc	KSFM supplemented with BPE, recombinant EGF and cholera toxin
MIBC	Muscle-invasive bladder cancer
mPGES	Microsomal prostaglandin E synthase
NMIBC	Non-muscle invasive bladder cancer
NHU	Normal human urothelium
NSAID	Non-steroidal anti-inflammatory drug
PBS	Phosphate buffered saline
PGDH	Prostaglandin dehydrogenase
PKA	Protein kinase A
PPAR	Peroxisome proliferator activated receptor
RZ	Rosiglitazone
TBS	Tris-buffered saline
TCF/LEF	T cell-factor/lymphoid enhancer factor
TER	Trans-epithelial electrical resistance
TGFβ	Transforming growth factor beta
TPM	Transcripts per million
TZ	Troglitazone
UPK	Uroplakin
ZO	Zonula occludens

References

Abrams, P. H., Sykes, J. A., Rose, A. J and Rogers, A. F. (1979). The synthesis and release of prostaglandins by human urinary bladder muscle in vitro, *Investigative urology*, 16(5), pp. 346–348.

Apodaca, G. (2004). The uroepithelium: not just a passive barrier, *Traffic*, 5(3), pp. 117–128.

Asano, K., Lilly, C. M. and Drazen, J. M. (1996). Prostaglandin G/H synthase-2 is the constitutive and dominant isoform in cultured human lung epithelial cells, *The American journal of physiology*, 271(1 Pt 1), pp. L126–31.

Balda, M. S. and Matter, K. (2016). Tight junctions as regulators of tissue remodelling, *Current opinion in cell biology*, 42, pp. 94–101.

Bharati, K. and Ganguly, N. K. (2011). Cholera toxin: a paradigm of a multifunctional protein, *The Indian journal of medical research*, 133, pp. 179–187.

Bharati, K. and Ganguly, N. K. (2011). Cholera toxin: a paradigm of a multifunctional protein. *Indian Journal of Medical Research, 133*, 179–187.

Birder, L. A. (2010). Urothelial signaling, *Autonomic neuroscience: basic & clinical*, 153(1-2), pp. 33–40.

Birder, L. A. and de Groat, W. C. (2007). Mechanisms of disease: involvement of the urothelium in bladder dysfunction, *Nature clinical practice. Urology*, 4(1), pp. 46–54.

Bryan, R. T. (2015). Cell adhesion and urothelial bladder cancer: the role of cadherin switching and related phenomena, *Philosophical transactions of the Royal Society of London. Series B, Biological sciences*, 370(1661), p. 20140042.

Bygdeman, M. (2003). Pharmacokinetics of prostaglandins, *Best practice & research. Clinical obstetrics & gynaecology*, 17(5), pp. 707–716.

Cancer Research UK. (2017). Bladder cancer statistics. *Https://www.cancerresearchuk.org/health-professional/cancer-statistics/*statistics-by-cancer-type/bladder-cancer

Carattino, M. D., Prakasam, H. S., Ruiz, W. G., Clayton, D. R., McGuire, M., Gallo, L. I. and Apodaca, G. (2013). Bladder filling and voiding affect umbrella cell tight junction organization and function, *American journal of physiology. Renal physiology*, 305(8), pp. F1158–68.

Celis, J. E., Ostergaard, M., Basse, B., Celis, A., Lauridsen, J. B., Ratz, G. P., Andersen, I., Hein, B., Wolf, H., Orntoft, T. F. and Rasmussen, H. H. (1996). Loss of adipocyte-type fatty acid binding protein and other protein biomarkers is

associated with progression of human bladder transitional cell carcinomas, *Cancer research*, 56(20), pp. 4782–4790.

Chang, E. Y., Chang, Y. C., Shun, C. T., Tien, Y. W., Tsai, S. H., Hee, S. W., Chen, I. J. and Chuang, L. M. (2016). Inhibition of prostaglandin reductase 2, a putative oncogene overexpressed in human pancreatic adenocarcinoma, induces oxidative stress-mediated cell death involving xCT and CTH gene expressions through 15-keto-PGE2, *PloS one*, 11(1), p. e0147390.

Cheung, G., Sahai, A., Billia, M., Dasgupta, P. and Khan, M. S. (2013). Recent advances in the diagnosis and treatment of bladder cancer, *BMC medicine*, 11, p. 13.

Chopra, B., Hinley, J., Oleksiewicz, M. B. and Southgate, J. (2008). Trans-species comparison of PPAR and RXR expression by rat and human urothelial tissues, *Toxicologic pathology*, 36(3), pp. 485–495.

Cross, W.R., Eardley, I., Leese, H.J. and Southgate, J. (2005). A biomimetic tissue from cultured normal human urothelial cells: analysis of physiological function, *American journal of physiology. Renal physiology*, 289(2), pp. F459–68.

Daugherty, S. E., Pfeiffer, R. M., Sigurdson, A. J., Hayes, R. B., Leitzmann, M., Schatzkin, A., Hollenback, A. R. and Silverman, D. T. (2011). Nonsteroidal antiinflammatory drugs and bladder cancer: a pooled analysis, *American journal of epidemiology*, 173(7), pp. 721–730.

DeGraff, D. J., Cates, J. M., Mauney, J. R., Clark, P. E., Matusik, R. J. and Adam, R. M. (2013). When urothelial differentiation pathways go wrong: implications for bladder cancer development and progression, *Urologic oncology*, 31(6), pp. 802–811.

Dikolayev, V., Tuganbekov, T. and Nikolaev, V. O. (2019). Visualizing Cyclic Adenosine Monophosphate in Cardiac Microdomains Involved in Ion Homeostasis, *Frontiers in physiology*, 10, p. 1406.

Ding, Y., Tong, M., Liu, S., Moscow, J. A. and Tai, H. H. (2005). NAD + -linked 15-hydroxyprostaglandin dehydrogenase (15-PGDH) behaves as a tumor suppressor in lung cancer, *Carcinogenesis*, 26(1), pp. 65–72.

Endo, S., Suganami, A., Fukushima, K., Senoo, K., Araki, Y., Regan, J. W., Mashimo, M., Tamura, Y. and Fujino, H. (2020). 15-Keto-PGE2 acts as a biased/partial agonist to terminate PGE2-evoked signaling, *The Journal of biological chemistry*, 295(38), pp. 13338–13352.

Fan, Y., Wang, Y. and Wang, K. (2015). Prostaglandin E2 stimulates normal bronchial epithelial cell growth through induction of c-Jun and PDK1, a kinase implicated in oncogenesis, *Respiratory research*, 16, p. 149.

Farmer, S. R. (2006). Transcriptional control of adipocyte formation, *Cell metabolism*, 4(4), pp. 263–273.

Fishwick, C., Higgins, J., Percival-Alwyn, L., Hustler, A., Pearson, J., Bastkowski, S., Moxon, S., Swarbreck, D., Greenman, C. D. and Southgate, J. (2017). Heterarchy of transcription factors driving basal and luminal cell phenotypes in human urothelium, *Cell death and differentiation*, 24(5), pp. 809–818.

Fleming, J. M., Shabir, S., Varley, C. L., Kirkwood, L. A., White, A., Holder, J., Trejdosiewicz, L. K. and Southgate, J. (2012). Differentiation-associated reprogramming of the transforming growth factor β receptor pathway establishes the circuitry for epithelial autocrine/paracrine repair, *PloS one*, 7(12), p. e51404.

Fujino, H., West, K. A. and Regan, J. W. (2002). Phosphorylation of Glycogen Synthase Kinase-3 and Stimulation of T-cell Factor Signaling following Activation of EP2 and EP4 Prostanoid Receptors by Prostaglandin E2*, *The Journal of biological chemistry*, 277(4), pp. 2614–2619.

Funk, C. D. (2001). Prostaglandins and leukotrienes: advances in eicosanoid biology, *Science*, 294(5548), pp. 1871–1875.

Gobeil, F., Fortier, A., Zhu, T., Bossolasco, M., Leduc, M., Grandbois, M., Heveker, N., Bkaily, G., Chemtob, S. and Barbaz, D. (2006). G-protein-coupled receptors signalling at the cell nucleus: an emerging paradigm, *Canadian journal of physiology and pharmacology*, 84(3-4), pp. 287–297.

Goessling, W. *et al.* (2011). Prostaglandin E2 enhances engraftment of human cord blood stem cells and shows long-term safety in preclinical non-human primate transplant models, *Cell Stem Cell*, 8(4), pp. 445–458.

Haque, S. and Morris, J. C. (2017). Transforming growth factor-β: A therapeutic target for cancer, *Human vaccines & immunotherapeutics*, 13(8), pp. 1741–1750.

Hendzel, M. J., Nishioka, W. K., Raymond, Y., Allis, C. D., Bazett-Jones, D. P. and Th'ng J. P. (1998). Chromatin condensation is not associated with apoptosis, *The Journal of biological chemistry*, 273(38), pp. 24470–24478.

Hicks, R. M. (1975). The mammalian urinary bladder: an accommodating organ, *Biological reviews of the Cambridge Philosophical Society*, 50(2), pp. 215–246.

Jabbour, H. N. and Boddy, S. C. (2003). Prostaglandin E2 induces proliferation of glandular epithelial cells of the human endometrium via extracellular regulated kinase 1/2-mediated pathway, *The Journal of clinical endocrinology and metabolism*, 88(9), pp. 4481–4487.

Kalinski, P. (2012). Regulation of immune responses by prostaglandin E2, *Journal of immunology,* 188(1), pp. 21–28.

Kashiwagi, E., Inoue, S., Mizushima, T., Chen, J., Ide, H., Kawahara, T., Reis, L. O., Baras, A. S., Netto, G. J and Miyamoto, H. (2018). Prostaglandin receptors induce urothelial tumourigenesis as well as bladder cancer progression and

cisplatin resistance presumably via modulating PTEN expression, *British Journal of Cancer*, 118, pp. 213–223.

Khan, M. A., Thompson, C. S., Mumtaz, F. H., Jeremy, J. Y., Morgan R. J. and Mikhailidis, D. P. (1998). Role of prostaglandins in the urinary bladder: an update, *Prostaglandins, leukotrienes, and essential fatty acids*, 59(6), pp. 415–422.

Khandelwal, P., Abraham, S. N. and Apodaca, G. (2009). Cell biology and physiology of the uroepithelium, *American journal of physiology. Renal physiology*, 297(6), pp. F1477–501.

Konya, V., Marsche, G., Schuligoi, R. and Heinemann, A. (2013). E-type prostanoid receptor 4 (EP4) in disease and therapy, *Pharmacology & therapeutics*, 138(3), pp. 485–502.

Kozak, K. R., Crews, B. C., Ray, J. L., Tai, H. H., Morrow, J. D. and Marnett, L. J. (2001). Metabolism of prostaglandin glycerol esters and prostaglandin ethanolamides in vitro and in vivo, *The Journal of biological chemistry*, 276(40), pp. 36993–36998.

Krause, G., Winkler, L., Mueller., S. L., Haseloff, R. F., Piontek, J. and Blasig, I. E. (2008). Structure and function of claudins, *Biochimica et biophysica acta*, 1778(3), pp. 631–645.

Kreft, M. E., Sterle, M., Veranic, P. and Jezernik, K. (2005). Urothelial injuries and the early wound healing response: tight junctions and urothelial cytodifferentiation, *Histochemistry and cell biology*, 123(4-5), pp. 529–539.

Kurtova, A. V., Xiao, J., Mo, Q., Pazhanisamy, S., Krasnow, R., Lerner, S. P., Chen, F., Roh, T. T., Lay, E., Ho, P. L. and Chan, K. S. (2015). Blocking PGE2-induced tumour repopulation abrogates bladder cancer chemoresistance, *Nature*, 517, pp. 209–213.

Larsson, P., Ibel Chamorro, C. and Fossum, M. (2016). A review on bladder wound healing after mechanical injury, *Journal of tissue science & engineering*, 7(2).

Lenicov, F. R., Paletta, A. L., Prinz, M. G., Varese, A., Pavillet, C. E., Malizia, Á. L., Sabetté, J., Geffner, J. R. and Ceballos, A. (2018). Prostaglandin E2 Antagonizes TGF-β Actions During the Differentiation of Monocytes Into Dendritic Cells, *Frontiers in Immunology*.

Ma, C., Liu, Y., Wang, Y., Zhang, C., Yao, H., Ma, J., Zhang, L., Zhang, D., Shen, T. and Zhu, D. (2014). Hypoxia activates 15-PGDH and its metabolite 15-KETE to promote pulmonary artery endothelial cells proliferation via ERK1/2 signalling, *British Journal of Pharmacology*, pp. 3352–3363.

Mammone, T., Marenus, K., Maes, D. and Lockshin, R. A. (1998). The Induction of Terminal Differentiation Markers by the cAMP Pathway in Human HaCaT Keratinocytes, *Skin Pharmacology and Physiology*, *11*, pp. 152–160.

Markowitz, S., Willson, J. K. V., Posner, B. A., Ready, J., Zhang, Y., Tai, H.-H., Antczak, M., Gerson, S., Bae, K., Yang, S. Y. and Desai, A. (2017). Compositions and Methods of Modulating 15-PGDH Activity, *Pharmaceutical Sciences Faculty Patents.* 170.

Mascaux, C., Martin, B., Verdebout, J. M., Ninane, C. and Scullier, J. P. (2005). COX-2 expression during early lung squamous cell carcinoma oncogenesis, *European respiratory journal: official journal of the European Society for Clinical Respiratory Physiology*, 26(4), pp. 753–753.

Matsumoto, Y., Nakanishi, Y., Yoshioka, T., Yamaga, Y., Masuda, T., Fukunaga, Y., Sono, M., Yoshikawa, T., Nagao, M., Araki, O., Ogawa, S., Goto, N., Hiramatsu, Y., Breyer, R. M., Fukuda, A. and Seno, H. 2019. Epithelial EP4 plays an essential role in maintaining homeostasis in colon, *Scientific reports*, 9(1), p. 15244.

Miyazono, K. (2000). Positive and negative regulation of TGF-beta signaling, *Journal of cell science*, 113 (Pt 7), pp. 1101–1109.

Miyoshi, H., VanDussen, K. L., Malvin, N. P., Ryu, S. H., Wang, Y., Sonnek, N, M., Lai, C. W. and Stappenbeck, T. S. (2017). Prostaglandin E2 promotes intestinal repair through an adaptive cellular response of the epithelium, *The EMBO journal*, 36(1), pp. 5–24.

Mo, C., Zhao, R., Vallejo, J., Igwe, O., Bonewald, L., Wetmore, L. and Brotto, M. (2015). Prostaglandin E2 promotes proliferation of skeletal muscle myoblasts via EP4 receptor activation, *Cell cycle*, 14(10), pp. 1507–1516.

Mysorekar, I. U., Mulvey, M. A., Multgren, S. J. and Gordon, J. I. (2002). Molecular Regulation of Urothelial Renewal and Host Defenses during Infection with Uropathogenic Escherichia coli* 210, *The Journal of biological chemistry*, 277(9), pp. 7412–7419.

Nakahara, T., Kubota, Y., Mitani, A., Maruko, T., Sakamoto, K. and Ishii, K. (2003). Protease-activated receptor-2-mediated contraction in the rat urinary bladder: the role of urinary bladder mucosa, *Naunyn-Schmiedeberg's archives of pharmacology*, 367(2), pp. 211–213.

Nosjean, O. and Boutin, J. A. (2002). Natural ligands of PPARγ: Are prostaglandin J2 derivatives really playing the part?, *Cellular signalling*, 14(7), pp. 573–583.

Oll, M., Baumann, C., Behbahani, T. E., von Ruecker, A., Müller, S. C. and Ellinger, J. (2012). Identification of prostaglandin receptors in human ureters, *BMC urology*, 12, p. 35.

Pai, R., Soreghan, B., Szabo, I. L., Pavelka, M., Baatar, D. and Tarnawski, A. S. (2002). Prostaglandin E2 transactivates EGF receptor: a novel mechanism for promoting colon cancer growth and gastrointestinal hypertrophy, *Nature medicine*, 8(3), pp. 289–293.

Park, J. Y., Pillinger, M. H. and Abramson, S. B. (2006). Prostaglandin E2 synthesis and secretion: the role of PGE2 synthases, *Clinical immunology,* 119(3), pp. 229–240.

Pastar, I., Stojadinociv, O., Yin, N. C., Ramirez, H., Nusbaum, A. G., Sawaya, A., Patel, S. B., Khalid, L., Isseroff, R. R. and Tomic-Canic, M. (2014). Epithelialization in Wound Healing: A Comprehensive Review, *Advances in wound care: the journal for prevention and healing*, 3(7), pp. 445–464.

Petersen, R. K., Madsen, L. and Pedersen, L. M. (2008). Cyclic AMP (cAMP)-mediated stimulation of adipocyte differentiation requires the synergistic action of Epac-and cAMP-dependent protein kinase-dependent processes, *Molecular and cellular biology*. 28(11), 3804–3816.

Rastogi, P., Rickard, A., Dorokhov, N., Klumpp, D. and McHowat, J. (2008). Loss of prostaglandin E2 release from immortalized urothelial cells obtained from interstitial cystitis patient bladders, *American journal of physiology. Renal physiology*, 294(5), pp. F1129–35.

Reader, J., Holt, D. and Fulton, A. (2011). Prostaglandin E2 EP receptors as therapeutic targets in breast cancer, *Cancer metastasis reviews*, 30(3-4), pp. 449–463.

Rodríguez-Lagunas, M. J., Martín-Venegas, R., Moreno, J. J. and Ferrer, R. (2010). PGE2 promotes Ca2+-mediated epithelial barrier disruption through EP1 and EP4 receptors in Caco-2 cell monolayers, *American journal of physiology. Cell physiology*, 299(2), pp. C324–34.

Rouzer, C. A. and Marnett, L. J. (2009). Cyclooxygenases: structural and functional insights, *Journal of lipid research*, 50 Suppl, pp. S29–34.

Rouzer, C. A. and Marnett, L. J. (2009). Cyclooxygenases: structural and functional insights, *Journal of lipid research*, 50 Suppl, pp. S29–34.

Rubenwolf, P. and Southgate, J. (2011). Permeability of differentiated human urothelium in vitro, *Methods in molecular biology,* 763, pp. 207–222.

Saginala, K., Barsouk, A., Aluru, J. S., Rawla, P., Padala, S. A. and Barsouk, A. (2020). Epidemiology of Bladder Cancer, *Medical Sciences*, p. 15.

Sanchez, J., and Holmgren, J. (2011). Cholera toxin - a foe & a friend. *Indian Journal of Medical Research, 133*, 153–163.

Sassone-Corsi, P. (2012). The cyclic AMP pathway, *Cold Spring Harbor perspectives in biology*, 4(12).

Savla, U., Appel, H. J., Sporn, P. H. and Waters, C. M. (2001). Prostaglandin E2 regulates wound closure in airway epithelium, *American Journal of Physiology-Lung Cellular and Molecular Physiology*, 280(3), pp. L421–L431.

Schiller, M., Dennler, S., Anderegg, U., Kokot, A., Simon, J. C., Luger, T. A., Mauviel, A. and Böhm, M. (2010). Increased cAMP levels modulate transforming growth factor-β/smad-induced expression of extracellular matrix components and other key fibroblast effector functions, *Journal of Biological Chemistry*, 285(1), pp. 409–421.

Sellers, D., Chess-Williams, R. and Michel, M. C. (2018). Modulation of lower urinary tract smooth muscle contraction and relaxation by the urothelium, *Naunyn-Schmiedeberg's archives of pharmacology*, 391(7), pp. 675–694.
Shin, K., Lee, J., Guo, N., Kim, J., Lim, A., Qu, L., Mysorekar, I. U. and Beachy, P. A. (2011). Hedgehog/Wnt feedback supports regenerative proliferation of epithelial stem cells in bladder, *Nature*, 472(7341), pp. 110–114.

Shirahama, T. (2000). Cyclooxygenase-2 expression is up-regulated in transitional cell carcinoma and its preneoplastic lesions in the human urinary bladder, *Clinical cancer research: an official journal of the American Association for Cancer Research*, 6(6), pp. 2424–2430.

Simon, L. S. (1999). Role and regulation of cyclooxygenase-2 during inflammation, *The American journal of medicine*, 106(5B), p. 37S–42S.

Smith, N. J., Hinley, J., Varley, C. L., Eardley, I., Trejdosiewicz, L. K. and Southgate J. (2015). The human urothelial tight junction: claudin 3 and the ZO-1α+ switch, *Bladder*, 2(1), p. e9.

Southgate, J., Hutton, K. A., Thomas, D. F. and Trejdosiewicz, L. K. (1994). Normal human urothelial cells in vitro: proliferation and induction of stratification, *Laboratory investigation; a journal of technical methods and pathology*, 71(4), pp. 583–594.

Southgate, J., Masters, J.R.W. and Trejdosiewicz, L.K. (2002). Culture of Human Urothelium, *Culture of Specialized Cells*, pp.381–399.

Stahlschmidt, J., Varley, C. L., Toogood, G., Selby, P. J. and Southgate, J. (2005). Urothelial differentiation in chronically urine-deprived bladders of patients with end-stage renal disease, *Kidney international*, 68(3), pp. 1032–1040.

Sun, T. T., Zhao, H., Provet, J., Aebi, U. and Wu, X. R. (1996). Formation of asymmetric unit membrane during urothelial differentiation, *Molecular biology reports*, 23(1), pp. 3–11.

Tai, H. -H. (2011). Prostaglandin catabolic enzymes as tumor suppressors, *Cancer metastasis reviews*, 30(3-4), pp. 409–417.

Tanikawa, N., Ohmiya, Y., Ohkubo, H., Hashimoto, K., Kangawa, K., Kojima, M., Ito, S. and Watanabe, K. (2002). Identification and characterization of a novel type of membrane-associated prostaglandin E synthase, *Biochemical and biophysical research communications*, 291(4), pp. 884–889.

Tanioka, T., Nakatani, Y., Semmyo, N., Murakami, M. and Kudo, I. (2000). Molecular identification of cytosolic prostaglandin E2 synthase that is functionally coupled with cyclooxygenase-1 in immediate prostaglandin E2 biosynthesis, *The Journal of biological chemistry*, 275(42), pp. 32775–32782.

Thomas, P. E., Peters-Golden, M., White, E. S., Thannickal, V. J. and Moore, B. B. (2007). PGE2 inhibition of TGF-β1-induced myofibroblast differentiation is Smad-independent but involves cell shape and adhesion-dependent signaling, *American Journal of Physiology-Lung Cellular and Molecular Physiology*, 293(2), pp. L417–L428.

Tran, L., Xiao, J. F., Agarwal, N., Duex, J. E. and Theodorescu, D. (2021). Advances in bladder cancer biology and therapy, *Nature reviews. Cancer*, 21(2), pp. 104–121.

Tseng-Rogenski, S., Gee, J., Ignatoski, K. W., Kunju, L. P., Bucheit, A., Kintner, H. J., Morris, D., Tallman, C., Evron, J., Wood, C. G., Grossman, H. B., Lee, C. T. and Liebert, M. (2010). Loss of 15-hydroxyprostaglandin dehydrogenase expression contributes to bladder cancer progression, *The American journal of pathology*, 176(3), pp. 1462–1468.

Tseng-Rogenski, S., Lee, I. L., Gebhardt, D., Fischer, S. M., Wood, C., Park, J. M. and Liebert, M. (2008). Loss of 15-hydroxyprostaglandin dehydrogenase expression disrupts urothelial differentiation, *Urology*, 71(2), pp. 346–350.

Varley, C. L., Garthwaite, M. A., Cross, W., Hinley, J., Trejdosiewicz, L. K. and Southgate J. (2006). PPARγ-regulated tight junction development during human urothelial cytodifferentiation, *Journal of Cellular Physiology*, pp. 407–417.

Varley, C. L., Stahlschmidt, J., Lee, W. C., Holder, J., Diggle, C., Selby, P. J., Trejdosiewicz, L. K. and Southgate J. (2004). Role of PPAR γ and EGFR signalling in the urothelial terminal differentiation programme, *Journal of cell science*, 117(10), pp. 2029–2036.

Varley, C. L., Stahlschmidt, J., Smith, B., Stower, M., and Southgate, J. (2004). Activation of Peroxisome Proliferator-Activated Receptor-γ Reverses Squamous Metaplasia and Induces Transitional Differentiation in Normal Human Urothelial Cells. *The American Journal of Pathology*, *164*, 1789–1798.

Volpato, M., Cummings, M., Shaaban, A. M., Abderrahman, B., Hull, M. A., Maximov, P. Y., Broom, B. M., Hoppe, R. Fan, P., Brauch, H., Jordan, V. C. and Speirs, V. (2020). Downregulation of 15-hydroxyprostaglandin dehydrogenase during acquired tamoxifen resistance and association with poor prognosis in ERα-positive breast cancer, *Exploration of Targeted Anti-tumor Therapy*.

Wang, D. and DuBois, R. N. (2010). Eicosanoids and cancer, *Nature Reviews Cancer*, pp. 181–193.

Wezel, F., Pearson, J. and Southgate, J. (2014). Plasticity of in vitro-generated urothelial cells for functional tissue formation, *Tissue engineering. Part A*, 20(9-10), pp. 1358–1368.

Wolf, I., O'Kelly, J., Rubinek, T., Tong, M., Nguyen, A., Lin, B. T., Tai, H. H., Karlan, B. Y. and Koeffler, H. P. (2006). 15-hydroxyprostaglandin dehydrogenase is a tumor suppressor of human breast cancer, *Cancer research*, 66(15), pp. 7818–7823.

Woolbright, B. L., Pilbeam, C. C. and Taylor, J. A., 3rd (2020). Prostaglandin E2 as a therapeutic target in bladder cancer: From basic science to clinical trials, *Prostaglandins & other lipid mediators*, 148, p. 106409.

Wu, X. R., Kong, X. P., Pellicer, A., Kreibich, G. and Sun, T. T. (2009). Uroplakins in urothelial biology, function, and disease, *Kidney international*, 75(11), pp. 1153–1165.

Wu, Y., Karna, S., Choi, C.H., Tong, M., Tai, H.-H., Na, D.H., Jang, C.H., and Cho, H. (2011). Synthesis and biological evaluation of novel thiazolidinedione analogues as 15-hydroxyprostaglandin dehydrogenase inhibitors, *Journal of medicinal chemistry*, 54(14), pp. 5260–5264.

Zhang, Y., Desai A., Yang, S. Y., Bae, K. B., Antczak, M. I., Fink, S. P., Tiwari, S., Willis, J. E., Williams, N. S., Dawson, D. M., Wald, D., Chen, W. D., Wang, Z., Kasturi, L., Larusch, G. A., He, L., Cominelli, F., Di Martino, L., Djuric, Z., Milne, G. L., Chance, M., Sanabria, J., Dealwis, C., Mikkola, D., Naidoo, J., Wei, S., Tai, H. H., Gerson, S. L., Ready, J. M., Posner, B., Willson, J. K. and Markowitz, S. D. (2015). TISSUE REGENERATION. Inhibition of the prostaglandin-degrading enzyme 15-PGDH potentiates tissue regeneration, *Science*, 348(6240), p. aaa2340.

Zidar, N., Odar, K., Glavac, D., Jerse, M., Zupanc, T. and Stajer, D. (2009). Cyclooxygenase in normal human tissues - is COX-1 really a constitutive isoform, and COX-2 an inducible isoform?, *Journal of Cellular and Molecular Medicine*, pp. 3753–3763.